

Brandteknik
Lunds Tekniska Högskola
Lunds Universitet



Department of Fire Safety Engineering
Lund Institute of Technology
Lund University

Report 5025

Fire Modelling Using CFD

-An introduction for Fire Safety Engineers

Jörgen Carlsson

Lund 1999

Report 5025

Fire Modelling Using CFD

-An introduction for Fire Safety Engineers

Jörgen Carlsson

Lund 1999



Department of Fire Safety Engineering

Lund Institute of Science and Technology
Lund University

Title: Fire Modelling Using CFD- An introduction for Fire Safety Engineers.

Author: Jörgen Carlsson

Keywords: Field modelling, CFD, Computational Fluid Dynamics, computer models, numerical models, SOFIE, simulation of fire.

Abstract

Fundamental laws of nature used in field modelling using Computational Fluid Dynamics are discussed and explained. Extensions and models used to complement these basic laws of physics in fire specific scenarios are also discussed. The field model SOFIE, Simulation Of Fires In Enclosures, has been used and predictions of gas-temperature, gas-velocity and presence of combustion gases are compared to experimental results from three different experimental series.

**© Copyright Department of Fire Safety Engineering and Jörgen Carlsson
Lund Institute of Science and Technology, Lund University, Lund 1999.**

Cover/Layout: Jörgen Carlsson

Summary

Computer modelling of fire has increased significantly during the last decades. Two-zone models such as CFAST, DSLAYV etceteras, are extensively employed in building fire safety design. It is no secret though, that the two-zone model is frequently used also in situations where its reliability and accurateness are indeed questionable. Thus, the fire safety community really does require a more general and more accurate method to make use of in its work. It is probable that the zone model in time will be replaced with the field model. To what extent and exactly when in time is of course not predictable. However, the two-zone model will surely last also beyond the first decade of the new millennium.

The report deals with field modelling using computational fluid dynamics techniques and is divided into two separate parts. The purpose of the first part is to introduce the general theory in CFD modelling of fires. Governing equations used in describing fluid flow are discussed as well as some of the fire specific models used. The second part summarises present results from three different experiment series compared to CFD calculations using the CFD code SOFIE (Simulation Of Fires In Enclosures).

The theoretical part has been written mainly to satisfy a fire safety engineer. The importance of understanding the general features of the code is indeed very essential for a successful usage of a CFD package. The main effort in Part 1 is put on the general fluid dynamics area. It is important to recognise that this part can not lay claim on being a real comprehensive review of the subject and further reading may be necessary in order to fully understand how simulations are done.

From the CFD simulations, performed using the CFD code SOFIE, some general conclusions can be drawn. The results presented in this work indicate the level of development of CFD modelling of compartment fires today. However, they do not give the reader any hint of the amount of time spent to obtain them. The numerical results are basically within the margin of error and larger discrepancies can mostly be explained to have their origin in the particular experiment. As the aim of this work is not to evaluate the computer code SOFIE, but rather to give the fire safety engineer an introduction to the subject, the specific problems involved using SOFIE have not been issued in this report. Nevertheless, the first general conclusion of Part 2 is that a successful use of a field model requires a lot in terms of computer power (speed and memory). The second conclusion is that CFD modelling is still very much an issue for researchers and not yet a tool for the fire safety engineer. The author hopes that this will not be the case for much longer. Concerning user friendliness, probably the most subjective word in today's computer realm, CFD codes tend to require rather a lot from their users in terms of knowledge and patience. However, with the coming of graphical pre-processors life will probably become a bit brighter to the engineers in question. Knowledge about specific models, numerical techniques and uncertainties in calculations will always be of absolute necessity for a successful use of CFD modelling techniques in fire safety calculations. It is no doubt that field models offer a powerful tool in fire safety engineering and its breakthrough is as much a matter of time, knowledge and computer power as of actual programming. It is also the authors opinion that before CFD modelling is fully accepted in the fire safety engineering community it has to prove its superiority in a manner that is not done today. However, considering the different activities scheduled in the recent development of SOFIE, for example development of flamelet combustion data for different fuels, fire spread models, two-phase flow model, more accurate turbulence and radiation models, parallelisation etc this should not be so difficult.

Sammanfattning (Summary in Swedish)

Under det senaste decenniet har användningen av datorstödd modellering av brand och dess konsekvenser fått en särställning vid projektering av byggnaders brandsäkerhet. Detta har varit på gott och ont, resultat från datorsimuleringar tas ofta för att vara den absoluta sanningen, relativt enkla tvåzonsmodeller har en monopolställning och det är ingen hemlighet att dessa modeller används även i situationer där deras tillförlitlighet är tvivelaktig. I dessa sammanhang har man under det senaste decenniet då och då hört talas om termer som fältmodeller, CFD etc. Det har blivit mer och mer uppenbart att brandkonsulter är i behov av ett mer tillförlitligt och allmängiltigt verktyg i sitt arbete. Det är troligt att zonmodellen med lite tid kommer att ersättas med den mer allmänna fältmodellen. På vilket sätt detta kommer att ske och när i tiden kan givetvis inte förutspås, likväl kommer zonmodellen med stor sannolikhet att bestå ytterligare ett flertal år in i det nya millenniet.

Föreliggande rapport behandlar brandmodellering med fältmodeller och numeriska CFD, Computational Fluid Dynamics, tekniker. Rapporten är indelad i två separata delar. Den första delen avser att introducera allmän teori om CFD och speciella modeller använda speciellt för brandmodellering. I den andra delen presenteras tre experimentserier, ett fullskaleförsök och två småskaleförsök, ett experiment från varje serie jämförs med simuleringsresultat från fältmodellen SOFIE, Simulation Of Fires In Enclosures.

Den teoretiska delen, Part 1, har skrivits för att i stort sett kunna läsas av en brandingenjör med examen från Lunds tekniska högskola. Huvudvikten är lagd på allmän fluidodynamik och presenterar fundamentala ekvationer samt modeller använda för att komplettera dessa i specialfall med brandmodellering. Det skall betonas att denna rapport inte gör anspråk på att ge en fullständig täckning av den teoretiska bakgrunden till fältmodellering och att praktisk användning av en fältmodell kan kräva ytterligare bakgrundskunskap på området.

Utifrån de CFD simuleringar som utförts med CFD koden SOFIE, kan ett antal allmänna slutsatser dras. De resultat som presenteras i rapporten visar i stort sett var i utvecklingen fältmodellering av rumsbrand befinner sig idag. Dessa resultat ger emellertid inte läsaren någon information om den långa tid det tagit att erhålla dem. De numeriska siffrorna håller sig i stort sett inom ramen för vad som får kallas felmarginal och större avvikelser kan härledas till och förklaras med den experimentella datan. Eftersom det inte är rapportens avsikt att utvärdera fältmodellen SOFIE, utan mer att ge läsaren en övergripande introduktion till fältmodellernas värld, har de specifika problem som författaren stött på under arbetet med koden inte behandlats. Den första allmänna slutsatsen är emellertid att en fältmodell ställer höga krav på använd hårdvara (hög klockfrekvens och stor minneskapacitet). Den andra slutsatsen är att CFD modellering än idag är till för forskare och inte är anpassat såsom ett verktyg till brandingenjörer. Förhoppningsvis kommer detta faktum inte vara sant inom en snar framtid. Ifråga om det mest subjektiva fenomenet i datorvärlden nämligen användarvänlighet kan tilläggas att användning av en CFD kod tenderar att kräva en hel del av sin användare i termer av både kunskap och tålamod. Med hjälp av grafiska indatabehandlare kommer livet bli åtminstone lite mer uthärdligt för användarna. Det skall framhållas att kunskap om använda modeller, numeriska lösningsmetoder och osäkerheter i beräkningar alltid kommer att vara av största betydelse för att datormodellering skall kunna fylla sitt syfte, detta oavsett om modellen kallas fältmodell eller zonmodell. Det råder inget tvivel om att fältmodeller erbjuder ett kraftfullt verktyg att användas i brandskyddsprojektering och deras genomslag är lika mycket fråga om tid, kunskap och datorkraft som programmering. Det är vidare författarens åsikt att innan fältmodellen accepteras av brandkonsulter måste den på ett övertygande sätt visa sin överlägsenhet. Detta är inte fallet idag men med tanke på de aktiviteter som schemalagts för SOFIEs utveckling exempelvis framtagande av flamelet data för olika bränslen, brandspridningsmodeller, förbättrade strålnings- och turbulensmodeller, en omskrivning av koden för att tillåta parallella processorer etc så borde detta inte vara särskilt svårt.

Nomenclature

c_p	specific heat capacity at constant pressure,
f	mixture fraction,
h_{total}	total enthalpy,
k	turbulent kinetic energy,
k_a	gas absorption coefficient,
k_s	scattering coefficient,
m	mass,
\mathbf{n}	normalised vector,
p	pressure,
\dot{q}_j^R	heat flux due to thermal radiation,
s	stoichiometric fuel to oxidant ratio,
t	time,
u, v, w	gas velocity in x - y - and z - direction respectively,
u_{char}	characteristic velocity,
u_i	gas velocity in x_i direction,
\bar{u}	Reynolds averaged velocity,
\tilde{u}	Favre averaged velocity,
u_i'	fluctuating part of gas velocity in i direction,
u_i''	fluctuating part of gas velocity i direction,
x, y, z	room co-ordinates,
x_{char}	characteristic length scale of flow,
A	Arrhenius pre-exponential factor for a chemical reaction,
B_i	body forces in the x_i direction,
C_R, C'_R	empirical constants in equation 3.2,
$C_{\epsilon 1}$	empirical constant in the k - ϵ turbulence model,
$C_{\epsilon 2}$	empirical constant in the k - ϵ turbulence model,
$C_{\epsilon 3}$	empirical constant in the k - ϵ turbulence model,
C_μ	empirical constant in the k - ϵ turbulence model,
D	mass diffusion coefficient,
D	diffusion conductance per unit area (chapter 5),
E	total emissive power,
E_a	activation energy,
E_g	emissive power for a gas with temperature T_g ,
F	force,
F	convective mass flux through a unit area (chapter 5),
G_B	buoyancy term in equation 2.21,
G_K	shear stress term in equation 2.21,
H_r	heat of reaction,
I	radiant intensity,
L	turbulent mixing length,
M_i	chemical symbol for species i ,
N	number of chemical species in a reaction,
P	probability,
R	ideal gas constant,
Re	Reynolds number,
R_f	flux Richardson number,
R_{fu}	rate of reaction,

S_α	source term in the chemical species conservation equation,
S	sectional area,
T	temperature,
Y_α	mole fraction of species α ,
β	thermal expansion coefficient in the k- ϵ turbulence model,
Γ_ϕ	turbulent diffusivity for scalar ϕ ,
δ	Kronecker's delta,
ϵ	viscous dissipation rate of turbulent kinetic energy,
ϵ	emissivity,
λ	heat conductivity,
μ	dynamic viscosity,
μ'	bulk viscosity,
μ_t	turbulent kinematic viscosity,
ν	kinematic viscosity,
ν_i'	stoichiometric coefficient for reactant i ,
ν_i''	stoichiometric coefficient for product i ,
ρ	density,
σ	Stefan Boltzmann constant,
σ_ϵ	turbulent Prandtl number for turbulent kinetic energy,
σ_k	turbulent Prandtl number for dissipation of turbulent kinetic energy,
σ_t	turbulent Prandtl number,
τ_{ij}	stress tensor,
ϕ	symbolises an arbitrarily scalar,
Ω	arbitrarily volume in space,

Superscripts

a, b, c	model constants in the Arrhenius expression for the rate of reaction,
'	Reynolds averaged fluctuating variable,
"	Favre averaged fluctuating variable,
·	time derivate,
–	Reynolds, or time, average,
~	Favre, or density weighted, average.

Subscripts

α	chemical species,
fu	fuel or fuel stream,
i, j, k	Cartesian co-ordinator directions,
Nb	neighbouring control volume,
ox	oxidant or oxidant stream,
pr	products,
t	turbulent,

Co-ordinate system

e, w, n, s, t, b denotes east, west, north, south, top and bottom cell face respectively, where

e	positive x - direction,
w	negative x - direction,
n	positive y - direction,
s	negative y - direction,
t	positive z - direction,
b	negative z - direction.

Table of contents

SUMMARY	1
SAMMANFATTNING (SUMMARY IN SWEDISH).....	3
NOMENCLATURE	5
TABLE OF CONTENTS	9
ACKNOWLEDGEMENTS	11
INTRODUCTION: PREDICTING THE COURSE OF FIRE	13
ZONE MODELS	13
FIELD MODELLING USING CFD.....	14
PART 1: BASIC FLUID DYNAMICS AND FUNDAMENTALS ON COMBUSTION MODELLING	17
1. GOVERNING EQUATIONS	19
1.1 THE DIFFERENTIAL EQUATIONS	19
1.2 CONSERVATION OF MASS	20
1.3 CONSERVATION OF MOMENTUM.....	21
1.4 CONSERVATION OF ENERGY	23
1.5 CONSERVATION OF CHEMICAL SPECIES	24
1.6 EQUATION OF STATE	25
1.7 SUMMARY	25
2. TURBULENCE	27
2.1 THE PHENOMENA	27
2.2 INTRODUCTION TO TURBULENCE MODELLING	28
2.3 AVERAGING TECHNIQUES.....	28
2.3.1 <i>Reynolds averaging</i>	29
2.3.2 <i>Favre averaging</i>	33
2.4 THE BOUSSINESQ EDDY VISCOSITY CONCEPT.....	35
2.5 THE K- ϵ TURBULENCE MODEL	36
2.5.1 <i>The high Reynolds number k-ϵ model</i>	36
2.5.2 <i>The low Reynolds k-ϵ turbulence model</i>	38
2.5.3 <i>Documented disadvantages in the k-ϵ model</i>	38
2.6 SUMMARY	39
3. MODELLING COMBUSTION	41
3.1 THE EDDY BREAK UP MODEL	41
3.2 THE LAMINAR FLAMELET COMBUSTION MODEL	43
3.3 SUMMARY	44
4. THERMAL RADIATION	45
4.1 GENERAL	45
4.2 MODELLING THERMAL RADIATION.....	46

4.3 SUMMARY	48
5. NUMERICAL SOLUTION OF THE GOVERNING EQUATIONS.....	51
5.1 INTRODUCTION	51
5.2 AN INTRODUCTION TO THE FINITE VOLUME METHOD	53
5.2.1 <i>An illustrative example</i>	54
5.2.2 <i>Finite volume method on a steady one-dimensional convection-diffusion problem</i> 57	
5.2.3 <i>The upwind differencing scheme</i>	59
5.3 SOLVING THE EQUATIONS	60
5.4 SUMMARY	60
REFERENCES	63
PART 2: EXPERIMENTAL RESULTS AND FIELD MODEL SIMULATIONS.....	65
1. THE METHANE SMALL-SCALE EXPERIMENTS.....	67
1.1 THE EXPERIMENTAL SETUP	67
2. THE HEPTANE SMALL-SCALE EXPERIMENTS	71
2.1 SHORT DESCRIPTION OF THE EXPERIMENTAL SET-UP.....	71
3. THE CARDINGTON LARGE-SCALE EXPERIMENTS.....	73
3.1 SHORT DESCRIPTION OF THE EXPERIMENTAL SETUP	73
4. THE FIELD-MODEL SOFIE	77
4.1 PRE-PROCESSOR.....	77
4.1.1 <i>Special models under development</i>	78
4.2 SOLVER.....	78
4.3 OUTPUT AND POST-PROCESSOR POSSIBILITIES.....	79
5. RESULTS FROM SIMULATIONS	81
5.1 GENERAL REMARKS	81
5.2 THE METHANE EXPERIMENTS	81
5.2.1 <i>Input fundamentals</i>	81
5.2.2 <i>Steady state mode</i>	82
5.2.3 <i>Transient mode</i>	83
5.3 THE HEPTANE EXPERIMENTS	85
5.3.1 <i>Input fundamentals</i>	85
5.3.2 <i>Results from transient simulation</i>	86
5.4 THE CARDINGTON EXPERIMENTS	87
5.4.1 <i>Input fundamentals</i>	87
5.4.2 <i>Results from transient simulation; 270 seconds</i>	87
5.4.3 <i>Results from transient simulation; 750 seconds</i>	90
REFERENCES	93
APPENDIX.....	95
APPENDIX A METHOD FOR CALCULATING THE RATE OF HEAT RELEASE	97
<i>References</i>	99
APPENDIX B METHANE SIMULATION SCRIPTFILE.....	101
APPENDIX C HEPTANE SIMULATION SCRIPTFILE	107
APPENDIX D CARDINGTON SIMULATION SCRIPTFILE	113

Acknowledgements

This report is the result of the work carried out in the course “Problembaserad Brandteknisk Riskhantering”, VBR 135, the final course for Fire Safety Engineers at Lund Institute of Science and Technology, Lund University.

As the author reflect upon the time spent working on this report he must thank his supervisor Dr Björn Karlsson who also have had the onerous task of helping him with the English language. Tekn Lic Lars-Göran Bengtsson acted as assistant supervisor, the author would like to thank him for providing his experimental results and for patiently helping the author with whatever problem he encountered. Also thanks to Prof Göran Holmstedt for valuable discussions and encouragement. Dr Philip Rubini and Dr Heimo Tuovinen have helped me to a better understanding of the computer code SOFIE and for this the author is very grateful; thank you. Finally, the author acknowledges those very special people who in different ways have contributed to this work and to his life.

*Is it thy will that I should wax and wane,
Barter my cloth of gold for hidden grey,
And at thy pleasure weave that web of pain
Whose brightest threads are each a wasted day?*

Oscar Fingal O’Flahertie Wills Wilde

Introduction: Predicting the course of fire

In modern society, the everyday safety is more or less taken for granted. Without spending too much thought on it, we largely depend on correct safety designs as well as the professional skill of the rescue or fire brigades. As civilisation grows, becoming increasingly complex, methods for protection and preserving will inevitably have to develop continuously. In order to understand, predict and describe the course of a fire and its influence on its environment different scientific methods are employed, including practical experiments and mathematical modelling.

Performing full-scale experiments is expensive and requires considerable work. Of course experiments are not used in ordinary building design but are more used as a tool for the scientists. Often small-scale experiments are performed in which the geometry is scaled to more convenient proportions, for example to 1/3 of the true scale. Using the results from these experiments mathematical models, hand-calculation methods and computer-based models can be derived and/or evaluated. It should however be kept in mind that experimental results are not necessarily entirely accurate. There are always measuring errors present, sometimes more and sometimes less significant but as a rule of thumb one can say that measuring errors can be approximately 30 percent.

Mathematical models in fire science concern different ways of describing fire-related phenomena using analytical and numerical techniques. Due to rapidly growing knowledge and understanding of fire-related phenomena and a widespread access to powerful computers at reasonable cost, great progress has been made when predicting phenomena such as smoke spread, presence and concentration of combustible and toxic gases, calculation of pressure and temperature fields in enclosures due to fire, et cetera. There are primarily two approaches in mathematical fire modelling, the deterministic and the non-deterministic /1,2/.

The non-deterministic approach uses statistics to include fire frequencies, barrier failures, fire growth et cetera. Different methods are incorporated to take account for uncertainties and in the literature, one sometimes encounters the division into probabilistic and stochastic models.

The deterministic approach is today the most widespread and it clearly dominates all other methods. The deterministic models are based on chemical and physical relationships, empirical or analytically derived. A specific scenario is studied and outputs are provided as discrete numbers. Unlike the non-deterministic modes a limited number of design-fires are considered in order to cover relevant scenarios. Mathematical models used today, hand-calculation models as well as computer models, are based on this way of thinking.

In computer modelling of fires in enclosures one distinguishes between zone modelling and field modelling using CFD. Below is a very short presentation of these two modelling approaches. The latter technique is essentially the issue for the rest of this report.

Zone models

Zone models /3,4/ describe the influence of fire in an enclosed room by using a limited number of zones or control volumes. The most common model is the so-called two-zone model, which divides the room into two distinct control volumes; one upper control volume near the ceiling called upper layer, consisting of burnt and entrained hot gases and one cold lower layer which contains fresh air. *Figure 1* illustrates the zone model concept. Semi-empirical equations for mass, momentum, energy and chemical species are solved separately for upper and lower layer respectively and transition of mass and energy between the zones is accounted for by the use of a plume model. In some models, the plume appears as a third "layer" though in other models the influence of the plume is ignored implying that transient plume effects, for example the temporal build up of the plume and the time for the hot

gases to move from the core of the fire in the lower layer to the upper layer, are left without consideration. Both layers, or control volumes, are assumed homogenous and temperature, density, pressure et cetera can be considered to represent average values over the zones.

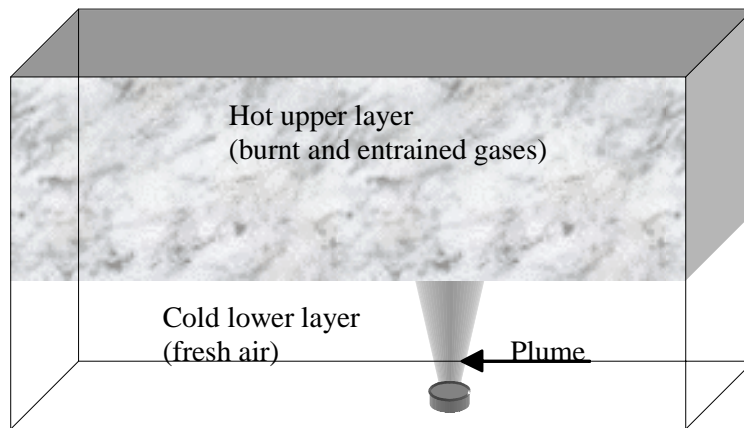


Figure 1. Illustration of the zone model concept

The approximations made in zone models are well documented and information on this is readily available in the literature, for example references /4/ and /5/.

A large number of experiments have been performed in order to verify and evaluate the validity of zone models and to identify the uncertainties. It is a matter of course that there are uncertainties embodied in these models and that in some cases the errors are of a magnitude that clearly makes the zone model inapplicable /6, 7, 8/. The zone-models are mainly developed in order to present approximate values on gas layer temperature and location of the smoke interface. In large spaces, for example in high atria, the zone model should be used with extra care. Consequently, it should be in the professional users own interest that he or she is aware of and kept updated on the limits of the models used.

Field modelling using CFD

Using field modelling, a domain in space is first defined. This domain is the actual world for the simulation to be carried through and its proportions are determined by the size of the object that is to be simulated. The domain is divided into a large number of small control volumes, which in addition can be defined as being walls or obstacles of some kind, or simply to consist of fluid space or air. In this way, the actual geometry that is to be simulated is built up inside the computational world, the domain, defined earlier and relevant boundary conditions can be predetermined including restrictions and limitations on the solution. CFD technique, Computational Fluid Dynamics, is then applied in order to solve a set of non-linear partial differential equations derived from basic laws of nature. Now, most flows encountered in real life are very complex. This indicates that one has to incorporate various models in order to make simulations possible. In the case of fire, a combustion model is used to simulate the course of combustion, a turbulence model has to be included for the prediction of the buoyancy driven turbulent flow as well as a radiation model to simulate the thermal radiation. Of course, there are many additional sub-models that can be included such as fire-spread models, soot models et cetera.

In computational fluid dynamics, one often talks about the use of a pre-processor, a solver and a post-processor. The pre-processor is used to define the actual problem and includes grid generation, boundary conditions, selection of calculation models to be used and what output is required etc. As the name implies, the solver uses the input data to find a solution to the problem. Now, as the conservation

equations are non-linear partial differential equations they have no simple analytical solutions. Instead, field models use different kinds of numerical techniques to find the solutions. The solutions obtained are then examined and presented using some post processor software. A sample result from the procedure outlined above is illustrated in *Figure 2*.

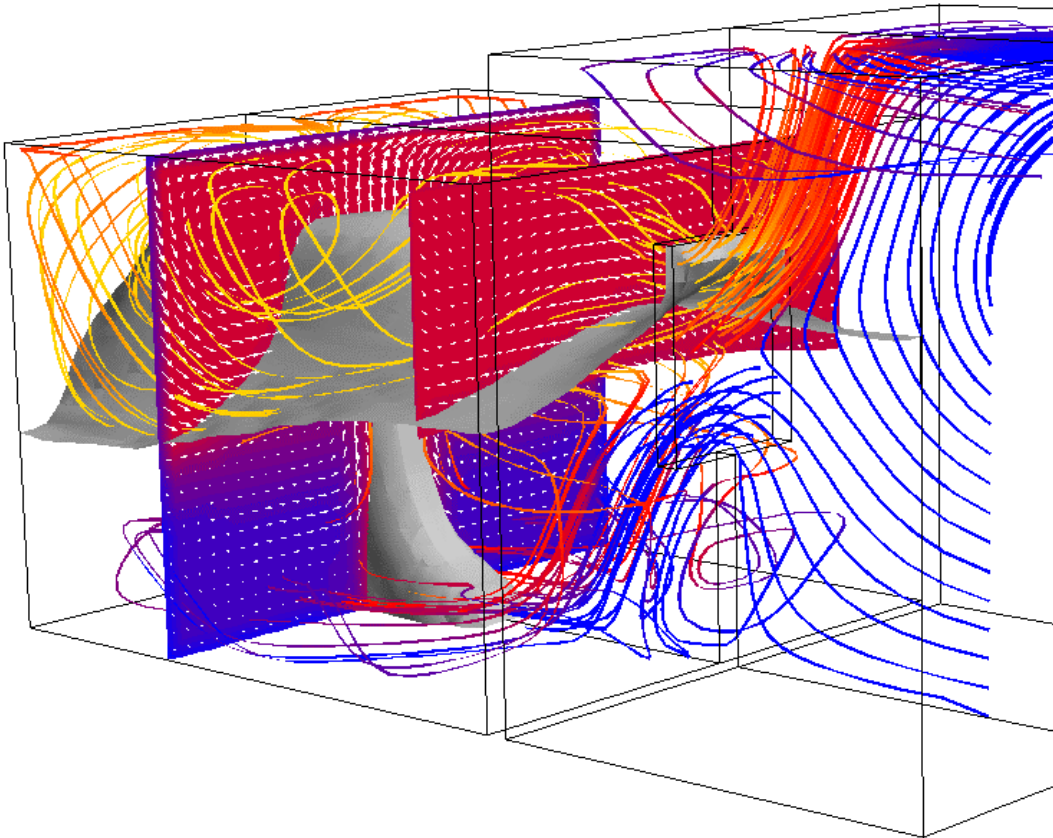


Figure 2. Visualisation of a completed CFD simulation. /9/

Given the rapid progress in computer power and the availability of this to a low cost, field models are not only a tool for the fire researchers but also applicable in conventional fire safety engineering to optimise the fire safety in buildings et cetera.

The accuracy of a simulation depends for example on factors such as the grid resolution and the specific models being used. Indeed field modelling can be a powerful tool but again the engineer has an ethic and moral responsibility to learn and to be aware of limitations and uncertainties in his or hers software /10/.

Part 1: Basic fluid dynamics and fundamentals on combustion modelling

Today, the use of computers is very much part of our every day life, and consequently we do not spend much time nor pains to meditate upon questions such as how our software works and which principles it is governed by. Whilst this might be perfectly normal from a general point of view, for an engineer, for example a fire safety engineer using computer based calculation models to analyse and predict the course of fire in a building, this can be a decisive mistake. It should be of interest for every professional user to recognise the fundamental features as well as the limitations of his or her computational tools. The models, whether they are programmed as part of a computer code or not, are not reality but merely a description, usually a simplification, of a real process or phenomenon. Nevertheless, once the difference between reality and the models has been understood and accepted the user should feel free to play the game of modelling.

The objective of this part is to provide the reader with the fundamentals in modelling fluid flow and combustion using computational fluid dynamics, CFD. Some basic concepts are introduced and explained, and hopefully some of the mysteries of field modelling using CFD technique will be revealed. It should be pointed out that the presentation made here cannot lay claim to be a comprehensive study on the subject, however it should give the reader some idea of the underlying physical laws, major principles and assumptions made in CFD modelling. The interested reader is referred to his favourite source.

1. Governing equations

The purpose of this chapter is to introduce and develop an understanding for the equations used to describe the flow of fluids, heat transfer and other related processes involved in a normal flow situation, and also in a fire. Once equations like these have been expressed in mathematical form, it might seem a straightforward procedure to obtain the numerical solution for a specified problem. However, due to a number of reasons, for example the mathematical nature of the governing equations, the presence of turbulence et cetera, this proves not to be the case. Instead, specific numerical calculation methods must be employed to attain the correct solutions.

The governing equations are derived from the basic laws of physics. These laws are the so-called laws of conservation according to which nature remains constant with the passage of time. Mathematically the laws of conservation are usually expressed in terms of differential equations.

1.1 The differential equations

Each of the conservation equations uses a physical quantity as its dependent variable. These dependent variables are usually expressed on a unit mass basis, for example specific heat and velocity (momentum). Note that temperature, which is a frequently used dependent variable, is not a specific property, however it arises from equations that are more basic, using specific internal energy or specific enthalpy as the dependent variable.

Consider an arbitrary domain in space divided into a large number of small control volumes as in *Figure 1.1* below.

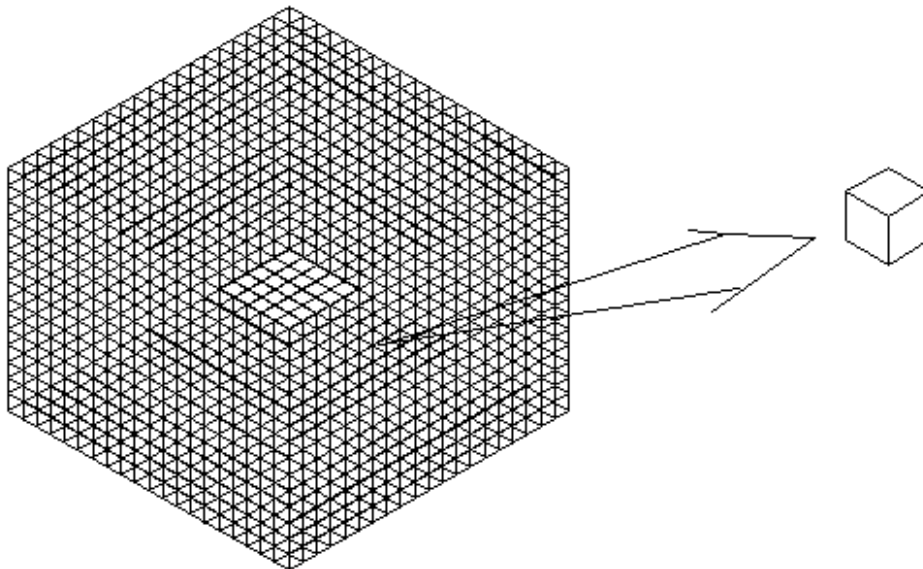


Figure 1.1 Illustration of an arbitrary grid representing a computational domain.

Now using the laws of physics declaring that nature remains constant in time, mathematically expressed by means of conservation equations, a kind of budget can be conducted, keeping record of the flow of mass, momentum, energy and chemical species for each of the control volumes in the domain. Knowing this one would be inclined to write the equations on a unit volume basis instead of mass basis. The true benefit of this will be obvious later, in chapter five where a balance over a control volume will be used in translating the partial differential equation into a numerical solution.

1.2 Conservation of mass

The mass conservation equation, also called the mass continuity equation or simply the continuity equation, implies that matter can be neither created nor destroyed and that the total mass in an isolated system is left unchanged regardless of the changes in physical and chemical properties of substances within the system. Some might argue that this is not entirely true, that mass is not absolute and that mass and energy are equivalent. Indeed in both chemical and nuclear reactions some conversions between mass and energy occur, however, in our case the difference in mass is so slight that the effects of Einstein's theory of relativity may be safely ignored and we will not take account of this throughout the present work.

In *Figure 1.2* mass flow through a control volume in the x direction is shown. According to the law of mass conservation, the rate of increase of mass in the control volume must equal the net rate of inflow across its faces.

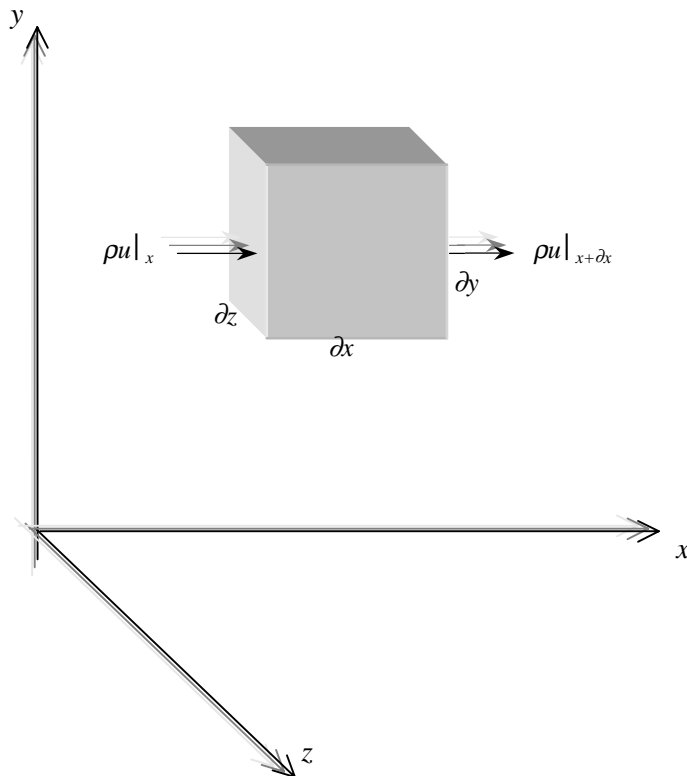


Figure 1.2 Mass flow through a control volume in x-direction

Thus in mathematical terms we can write

$$\frac{\partial \rho}{\partial t} + \frac{\partial}{\partial x}(\rho u) + \frac{\partial}{\partial y}(\rho v) + \frac{\partial}{\partial z}(\rho w) = 0 \quad (\text{Eq. 1.1})$$

Or in a more compact form

$$\frac{\partial \rho}{\partial t} + \frac{\partial}{\partial x_j}(\rho u_j) = 0 \quad (\text{Eq. 1.2})$$

I II

Here

I is the rate of change of density, or mass per unit volume, accumulation in the control volume due to density variations, and

II is the net rate of flow through the control volume due to convection

This equation, Equation 1.2, is the so-called unsteady mass conservation equation for a compressible fluid.

1.3 Conservation of momentum

Momentum is a quantity equal to the mass of an object, for example a control volume of a fluid, multiplied by its velocity and thus momentum is a vector quantity. According to Newton's second law of motion the sum of all forces acting on an object equals the time rate of change of momentum, or:

$$\sum F = \frac{d}{dt}(mv) \quad (\text{Eq. 1.3})$$

Here $\sum F$ is the sum of all forces acting on the object, m is the mass and v is the velocity vector. In deriving the equation for momentum conservation one always starts from this relationship.

The total force on a fluid volume is a combination of forces due to normal stresses and tangential stresses acting on each side of the control volume. One may differentiate between two kinds of forces acting on a fluid:

- **Surface forces**, for example pressure fields and viscosity.
- **Body forces**, for example gravitational- and electromagnetic fields.

In the momentum equation, surface forces are frequently presented as separate terms and body forces as source terms /10/.

The law of momentum conservation implies that, in an isolated system, motion never changes so that the total momentum remains constant in time. The derivation of the equation describing momentum conservation can be done in various ways, for the x-direction one obtains:

$$\frac{\partial}{\partial t}(\rho u_x) + \frac{\partial}{\partial x}(\rho u_x u_x) + \frac{\partial}{\partial y}(\rho u_y u_x) + \frac{\partial}{\partial z}(\rho u_z u_x) = -\frac{\partial p}{\partial x} + \frac{\partial \tau_{xx}}{\partial x} + \frac{\partial \tau_{yx}}{\partial y} + \frac{\partial \tau_{zx}}{\partial z} + \rho B_x \quad (\text{Eq. 1.4})$$

The equations for y and z directions can easily be shown to have the same structure and so, using the notation of Cartesian tensors, the complete equation becomes:

$$\frac{\partial}{\partial t}(\rho u_i) + \frac{\partial}{\partial x_j}(\rho u_j u_i) = -\frac{\partial p}{\partial x_i} + \frac{\partial \tau_{ij}}{\partial x_j} + \rho B_i \quad (\text{Eq. 1.5})$$

I II III IV V

As discussed earlier all terms are written on a unit volume basis and it can be seen that the left hand side represents the total change of momentum for the fluid and the right hand side include all forces acting on the fluid, this can be compared to Equation 1.3.

- I is the local rate of change of momentum in time for a control volume,
- II is the rate of change of momentum due to motion through an unsteady flow field,
- III represents pressure forces acting on the fluid,
- IV are viscous shearing forces and
- V represents body forces, such as gravitational forces.

Equation 1.5 gives the partial differential equation for all three spatial dimensions in a nice and simple way and as such the Cartesian tensor notation will be used from now on. This was also used in equation 1.2 but was not mentioned by name. The nomenclature used mainly follows that found in Cox, reference /11/.

The stress tensor, τ_{ij} , in matrix form expressed as

$$\tau_{ij} = \begin{bmatrix} \tau_{11} & \tau_{12} & \tau_{13} \\ \tau_{21} & \tau_{22} & \tau_{23} \\ \tau_{31} & \tau_{32} & \tau_{33} \end{bmatrix}$$

is given by the relationship

$$\tau_{ij} = \left(\mu' - \frac{2}{3} \mu \right) \frac{\partial u_k}{\partial x_k} \delta_{ij} + \mu \left(\frac{\partial u_i}{\partial x_j} + \frac{\partial u_j}{\partial x_i} \right) \quad (\text{Eq. 1.6})$$

Here μ is the dynamic viscosity, also called first viscosity, and μ' expresses the bulk viscosity of the fluid. The bulk viscosity has been shown to be negligible for monatomic gas mixtures and in common practise it is always set equal to zero /12/. δ_{ij} is the so-called Kronecker's delta defined as

$$\delta_{ij} = \begin{bmatrix} 1 & 0 & 0 \\ 0 & 1 & 0 \\ 0 & 0 & 1 \end{bmatrix}$$

Sometimes the stress tensor also includes the pressure term. The relationship is then written as

$$\sigma_{ij} = \begin{bmatrix} \sigma_{11} & \tau_{12} & \tau_{13} \\ \tau_{21} & \sigma_{22} & \tau_{23} \\ \tau_{31} & \tau_{32} & \sigma_{33} \end{bmatrix} = -p\delta_{ij} + \tau_{ij} \quad (\text{Eq. 1.7})$$

The momentum conservation equations are also known as the Navier- Stoke equations.

1.4 Conservation of energy

The law of energy conservation is virtually identical to the first law of thermodynamics and it implies that energy can be neither created nor destroyed. Nevertheless, it can be changed from one form to another, including for example chemical energy, kinetic energy, potential energy et cetera.

In a multi-component reacting system, there are several mechanisms that contribute to the total heat flux, the most common known as conduction, convection and radiation. Mainly two additional effects are encountered in the literature; these are the effect of mechanical work done on the system due to buoyancy and the so-called Dufor effect. The latter describes the heat flux in a system due to concentration gradients and in general, this term can be neglected. Due to the low velocities involved in a fire the mechanical work term can be ignored as well /12/.

The energy equation can be written in different ways depending on which quantity is used as the dependent variable. Using the total enthalpy, $h_{total} = c_p T + \sum Y_\alpha H_r$ where H_r is the component heat of reaction, as dependent variable, the conservation of energy equation becomes:

$$\begin{array}{cccc} \frac{\partial}{\partial t}(\rho h) & + & \frac{\partial}{\partial x_j}(\rho u_j h) & = & \frac{\partial p}{\partial t} + \frac{\partial}{\partial x_j} \left(\frac{\lambda}{c_p} \frac{\partial h}{\partial x_j} - \dot{q}_j^R \right) \\ \text{I} & & \text{II} & & \text{III} \quad \text{IV} \end{array} \quad (\text{Eq. 1.8})$$

where h is the static enthalpy of the mixture and

- I is the time rate of change of storage of enthalpy in a fluid,
- II is the net rate of influx of enthalpy due to convection,
- III represents the work done on the fluid due to pressure and
- IV includes terms for the net flux of heat due to conduction and thermal radiation respectively.

1.5 Conservation of chemical species

In an ordinary fluid-flow situation the equations above can be used to describe the motion of fluids and, if relevant, the transport of heat. However, in dealing with combustion an additional conservation equation arises, that for conservation of chemical species. This is used as a supplement to the mass continuity equation and it simply states that species in a reacting system are conserved. This implies that the time rate of accumulation of a specific species α in a control volume must equal the net rate of flow through the volume and the net rate of production within the volume.

Consider the generalised single chemical reaction

$$\sum_{i=1}^N v_i' M_i \leftrightarrow \sum_{i=1}^N v_i'' M_i \quad (\text{Eq. 1.9})$$

Here

- v_i' is the stoichiometric coefficient of the reactants,
- v_i'' is the stoichiometric coefficient of the products,
- M_i is the chemical symbol for species i , and
- N is the number of species present in the reaction.

Now because of the law of conservation of chemical species, once a value of v_i' has been set there is a constraint on the values of v_i'' , that is v_i'' cannot be arbitrary. In terms of partial differential equations the conservation of species α can be written as

$$\frac{\partial}{\partial t}(\rho Y_\alpha) + \frac{\partial}{\partial x_j}(\rho u_j Y_\alpha) = \frac{\partial}{\partial x_j} \left(\rho D \frac{\partial Y_\alpha}{\partial x_j} \right) + S_\alpha \quad (\text{Eq. 1.10})$$

I
II
III
IV

Here

- I is the rate of change of α , or the accumulation of α within the control volume,
- II is the net rate of influx of species α due to convection,
- III is the net rate of change of α due to molecular diffusion, and
- IV is the rate of change of species α due to different sources within the control volume, i.e. the net change of α from production and consumption in the control volume.

1.6 Equation of state

In order to close the above set of equations an equation of state is required, that is an additional equation relating relevant variables to each other is needed in order to obtain as many equations as there are unknown quantities.

For example, using ρ and T as state variables and assuming ideal gas we have:

$$P = \rho RT \quad (\text{Eq. 1.11})$$

This is the ideal-gas equation.

1.7 Summary

To sum up Chapter 1 we have discussed a fundamental feature of nature, namely the principle of conservation. In mathematical terms, this was described using partial differential equations. As these conservation equations involve fluid motion, they are sometimes referred to as transport equations. Now, if these transport equations are compared to each other, it soon becomes evident that there are several similarities in the structure of the equations. They all contain one term for the time rate of change of the dependent variable, one term describing property change due to macroscopic movement in space (or convection) and one term representing transport due to microscopic movement (or diffusion). Thus for an arbitrary dependent variable ϕ a generalised conservation equation can be written as

$$\frac{\partial}{\partial t}(\rho\phi) + \frac{\partial}{\partial x_i}(\rho u_j \phi) = \frac{\partial}{\partial x_i} \left(\Gamma_{ij} \frac{\partial \phi}{\partial x_j} \right) + S_\phi \quad (\text{Eq. 1.12})$$

I II III IV

where

- I is the time rate of change of ϕ in the control volume,
- II is the change of ϕ due to convection,
- III is the change of ϕ due to diffusion and
- IV is a source term.

2. Turbulence

The purpose of this chapter is to introduce the art of turbulence modelling and the difficulties that have to be dealt with. This will lead to questions such as: why turbulence has to be modelled, what is modelled and how and of course if these models are reliable.

2.1 The phenomena

The conservation equations as presented in Chapter 1 are only applicable in the case of laminar flow, i.e. in a flow characterised by a smooth and orderly motion. However, it is no secret that in practice this is generally not the case in fluid flow. Instead, most flows encountered in real life seems to be more or less irregular and random in both time and space, or to put it in other words: fluid motion is most often turbulent.

Turbulence can be characterised by the use of Reynolds number, named after one of the pioneers in the study of turbulent motion, Osborne Reynolds. The Reynolds number, Re , is a dimensionless number defined as the ratio of inertia forces to viscous forces.

$$Re = \frac{u_{char} x_{char} \rho}{\mu} = \frac{u_{char} x_{char}}{\nu} = \frac{\textit{inertia forces}}{\textit{viscous forces}} \quad (\text{Eq. 2.1})$$

Here

u_{char} is the characteristic velocity, usually taken as the mean velocity of the flow,

x_{char} denotes the characteristic length scale of the mean flow,

ρ is the density, and

μ and ν are the dynamic and kinematic viscosity respectively.

For a low Reynolds number fluid motion is essentially steady and smooth and the flow is said to be laminar. Increasing the Reynolds number a transition stage will be reached where the inertia forces dominate over viscosity to an extent where flow becomes unstable and oscillation of the flow parameters about a mean value can be observed. At high Re flow will be turbulent containing eddies, or vortices in a very large spectrum of sizes; in a fire typically ranging from sizes about the magnitude of the plume diameter to extremely small lengths where viscosity dominates over inertia. /13 /

The large scale eddies are created by whatever process driving the flow. In a fire, for example, the driving force and so the process behind the generation of large eddies, is the buoyancy force. The interaction between the large scale eddies cause them to break down forming smaller eddies, and so starting a process that continues ultimately to eddy-sizes where the flow is dominated by viscosity. The energy in these smallest eddies will be dissipated into heat and what is called “the turbulent cascade” ends. The transition of turbulent kinetic energy through mechanical energy into thermal energy (heat) is illustrated below in *Figure 2.1.* /14/. This will be further discussed in the chapter on combustion modelling, Section 3.1.

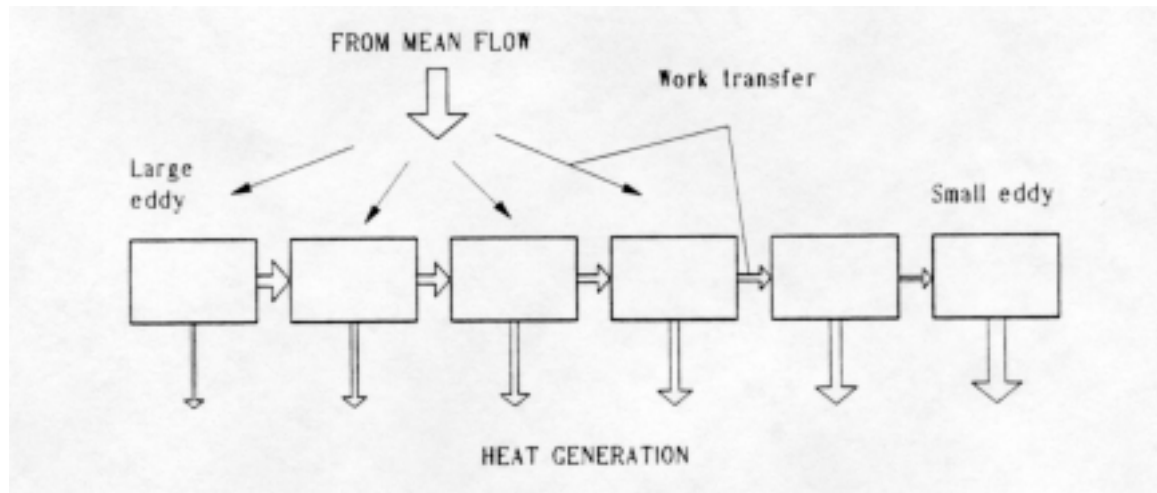


Figure 2.1 Turbulence energy transfer. /13/

2.2 Introduction to turbulence modelling

Although turbulence is characterised by spatial and temporal irregularity and randomness, the turbulent motion must follow the fundamental laws of nature, the laws of conservation. However, due to these characteristic features of turbulence the computational results will necessarily be random in both time and space. This is sometimes referred to as an example of deterministic chaos. One result of this deterministic chaos is that the course of two fires will develop in two different ways even though they take place under identical conditions. /15/

Thus, one logical way to take account for turbulence is to solve the conservation equations in such a manner that the rapid fluctuations of variables followed by turbulence can be determined. Such an approach is classified as a *Direct Numerical Simulation* (DNS) method. Using this approach in predicting turbulence the size of the control volumes needs to be consistent with the size of the smallest eddies making this method rather useless in fire modelling and other engineering usage for the time being and in a near future.

A similar technique to Direct Numerical Simulation is the *Large Eddy Simulation* (LES) method, in which the spatial resolution is made small enough to cover the largest eddies whilst a turbulence model is incorporated in order to take account for the smaller eddies. Analogous to the DNS approach, this method is very demanding in terms of computational power and it is of limited value for the engineer. However, it becomes increasingly attractive as computer power increases, although its use in fire safety design does not belong to the near future.

From this short presentation and discussion on Direct Numerical Simulation and Large Eddy Simulation it is apparent that a simple but stable and relatively non-demanding way of modelling turbulence is desirable, particularly for engineering purposes. Nevertheless, it is interesting to note that the possibility of solving the conservation equations exactly exists. The problem is more a question of computational hardware. /16, 17/

2.3 Averaging techniques

Again, the characteristic features of turbulent motion are its irregularity and randomness in time and space. Now instead of wasting time and effort on the exact (or almost exact) solutions of the governing conservation equations the fluctuating motion can be conveniently simplified by the introduction of averaged quantities. In the averaging procedure, the instantaneous quantities are written as the sum of

the mean value and a value representing the random fluctuations. Substituting these relationships into the conservation equations, a new set of governing equations arises, in which the presence of turbulence is introduced. There are two different averaging techniques. /12/

1. Conventional time averaging also called Reynolds averaging.
2. Mass or density weighted averages also known as Favre averages.

2.3.1 Reynolds averaging

Consider *Figure 2.2*, representing the variable ϕ as a function of time at a fixed point in a turbulent flow field.

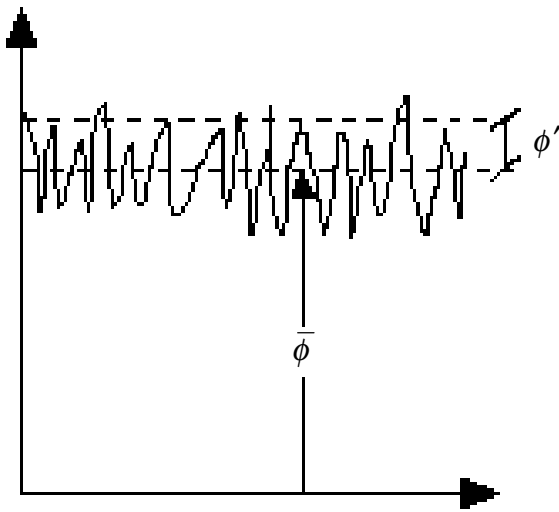


Figure 2.2 Illustration of the concept of fluctuation about a mean value

Using velocity as dependent variables, the mathematical expression for the instantaneous velocity field can be modelled as:

$$u_j(x_j, t) = \bar{u}(x_j) + u'_j(x_j, t) \quad (\text{Eq. 2.2})$$

where

\bar{u} is the mean velocity defined by the expression

$$\bar{u}_j = \lim_{\Delta t \rightarrow \infty} \frac{1}{\Delta t} \int_{t_0}^{t_0 + \Delta t} u_j(t) dt \quad (\text{Eq. 2.3})$$

and u'_j represents the random fluctuations in the flow. The average of the fluctuating quantities will by definition be equal to zero, that is

$$\overline{u'} \equiv 0 \quad (\text{Eq. 2.4})$$

Now, in order to obtain a set of time averaged conservation equations one can follow the simple procedure outlined below.

1. Consider the equations for the instantaneous quantities, i.e. in the same form as in Chapter 1.
2. Write all relevant physical quantities, such as velocity components, enthalpy, density, pressure et cetera in terms of a mean and a fluctuating part.
3. Take the average on both sides.
4. Substitute the instantaneous quantities for the relationships obtained in step 2.
5. Simplify the equation.

Example

Write the continuity equation in Reynolds form!

Solution

Step 1. The continuity equation (eq 1.2) using instantaneous quantities is written

$$\frac{\partial \rho}{\partial t} + \frac{\partial}{\partial x_j}(\rho u_j) = 0$$

Because of the law of conservation, this equation is valid in all flow fields, laminar as well as for turbulent.

Step 2. The turbulent flow is modelled using the assumption that the instantaneous quantities can be written as the sum of a mean and a fluctuating term. In this case, velocity and density need to be considered resulting in:

$$u_i = \bar{u}_i + u'_i \quad \rho = \bar{\rho} + \rho'$$

Step 3. The time average is taken on both sides

$$\overline{\frac{\partial \rho}{\partial t} + \frac{\partial}{\partial x_j}(\rho u_j)} = 0$$

Step 4. The relationships from step 2 are substituted into the equation.

$$\overline{\frac{\partial}{\partial t}(\bar{\rho} - \rho') + \frac{\partial}{\partial x_j}((\bar{\rho} + \rho')(\bar{u}_j + u'_j))} = 0$$

Step 5. In simplifying some operations called “Reynolds rules of averaging”, are found useful. Given f and g as quantities composed of a mean and a fluctuating component and c as a constant, the following will hold:

$$\overline{fg} = \bar{f}\bar{g} \quad \overline{f+g} = \bar{f} + \bar{g} \quad \overline{cf} = c\bar{f} \quad \overline{fg} = \bar{f}\bar{g} + \overline{f'g'} \quad \overline{\frac{\partial f}{\partial x}} = \frac{\partial \bar{f}}{\partial x}$$

Also by definition,

$$\bar{f}' = 0 \quad (\text{eq 2.4}) \quad \overline{f'g'} = 0 \quad \text{but} \quad \overline{f'f'} \neq 0$$

Using these operations, we obtain

$$\frac{\partial \bar{\rho}}{\partial t} + \frac{\partial}{\partial x_j} (\bar{\rho} \bar{u}_j + \overline{\rho' u'_j}) = 0$$

or,

$$\frac{\partial \bar{\rho}}{\partial t} + \frac{\partial}{\partial x_j} (\bar{\rho} \bar{u}_j) + \frac{\partial}{\partial x_j} (\overline{\rho' u'_j}) = 0$$

This equation does not look too different from the original one. Nevertheless, one additional term has come up, representing mass transport due to density and velocity fluctuations. This term is frequently ignored in the literature, implying no or very small density fluctuations in the flow field. Thus the Reynolds averaged continuity equation is most often written:

$$\frac{\partial \bar{\rho}}{\partial t} + \frac{\partial}{\partial x_j} (\bar{\rho} \bar{u}_j) = 0$$

If the procedure is carried out properly the result should look something like the equations below. Again, the convenient Cartesian tensor notation is put to use.

Mass continuity equation:

$$\frac{\partial \bar{\rho}}{\partial t} + \frac{\partial}{\partial x_j} (\bar{\rho} \bar{u}_j + \overline{\rho' u'_j}) = 0 \quad (\text{Eq. 2.5})$$

or, ignoring density fluctuations

$$\frac{\partial \bar{\rho}}{\partial t} + \frac{\partial}{\partial x_j} (\bar{\rho} \bar{u}_j) = 0$$

Momentum conservation equation:

Following the five steps that were proposed above the total Reynolds averaged momentum equation becomes:

$$\frac{\partial(\overline{\rho u} + \overline{\rho' u'})}{dt} + \frac{\partial}{\partial x_j} (\overline{\rho u_i u_j} + \overline{u_i u'_j \rho'}) = -\frac{\partial \overline{p}}{\partial x_i} + \frac{\partial}{\partial x_j} (\overline{\tau_{ij}} - \overline{\rho u'_i u'_j} - \overline{u_j \rho' u'_i} - \overline{\rho' u'_i u'_j}) + \overline{B}$$

where

$$\overline{\tau_{ij}} = \left(\mu' - \frac{2}{3} \mu \right) \frac{\partial \overline{u}_k}{\partial x_k} \delta_{ij} + \mu \left(\frac{\partial \overline{u}_i}{\partial x_j} + \frac{\partial \overline{u}_j}{\partial x_i} \right)$$

Again, density fluctuations are often ignored in this stage and the equation is then written

$$\frac{\partial \overline{\rho u}_i}{dt} + \frac{\partial}{\partial x_j} (\overline{\rho u_i u_j}) = -\frac{\partial \overline{p}}{\partial x_i} + \frac{\partial}{\partial x_j} (\overline{\tau_{ij}} - \overline{\rho u'_i u'_j}) + \overline{B}_i \quad (\text{Eq. 2.6})$$

Again, we see that an additional term arise as a result of the averaging. This term, representing the turbulent contribution to the momentum equation, is referred to as turbulent stresses or Reynolds stresses. From the appearance in Equation 2.6 and from the name, the Reynolds stresses seem to be some kind of turbulent stress tensor. However, this is not entirely true. The term is rather an inertia component and it has its origin in the second term on the left side of Equation 2.6. This can easily be found by carrying out the averaging procedure that was described above, starting from the momentum equation for instantaneous quantities, Equation 1.5.

As the Reynolds stresses are unknown their appearance implies that we again face an unclosed set of equations and that the time averaged conservation equations can not be solved until a relationship for the turbulent stresses has been established. This is the task of a turbulence model.

Energy conservation equation:

The energy equation, using the total enthalpy as dependent variable and ignoring density fluctuations is written

$$\frac{\partial}{\partial t} (\overline{\rho h}) + \frac{\partial}{\partial x_j} (\overline{\rho u_j h}) = \frac{\partial \overline{p}}{\partial t} + \frac{\partial}{\partial x_j} \left(\frac{\lambda}{c_p} \frac{\partial \overline{h}}{\partial x_j} - \overline{\rho u'_j h'} \right) - \frac{\partial \overline{\dot{q}}_j^R}{\partial x_j} \quad (\text{Eq. 2.7})$$

Species conservation equation:

$$\frac{\partial}{\partial t} (\overline{\rho Y_\alpha}) + \frac{\partial}{\partial x_j} (\overline{\rho u_j Y_\alpha}) = \frac{\partial}{\partial x_j} \left(\overline{\rho D} \frac{\partial \overline{Y_\alpha}}{\partial x_j} - \overline{\rho u'_j Y'_\alpha} \right) + \overline{S_\alpha} \quad (\text{Eq. 2.8})$$

Here, again, the effects of density fluctuations have not been included. In the energy and chemical species equations, the terms representing the turbulence contribution, that is the terms made up by variables with prime, are called turbulence scalar fluxes or simply Reynolds fluxes. Like the Reynolds stresses, they are unknowns implying that they inevitably will have to be subject to some kind of turbulence modelling. /16, 18/

2.3.2 Favre averaging

The conventional time averaging procedure is rather easy and straightforward, however, there are some major disadvantages. For example in the equations above, Eq 2.5 – Eq 2.8, we had to make the assumption that all terms involving a density fluctuation term could be ignored, in order to make the equations easier and to avoid introducing too many unknowns. Whilst this may be acceptable in some of the more simple cases, in a turbulent combustion flow field, as in the case of fire, implying significant density variations, this will only be true in the flow far away from the origin of the fire. This indicates that another kind of averaging procedure should be put to use in these and similar cases.

In mass-weighted averaging, often referred to as Favre averaging after the French scientist named Favre who first suggested the method, flow variables, except for pressure and density, are averaged as the sum of a mean and a fluctuating term so that, using velocity as an example

$$u_j(x_j, t) \equiv \tilde{u}_j(t) + u_j''(x_j, t) = \frac{\overline{\rho u_j}}{\bar{\rho}} + u_j'' \quad (\text{Eq. 2.9})$$

The double prime indicates a fluctuation about the Favre averaged mean value. Pressure and density are averaged using conventional time averaging. From the definition of mass-weighted average, Equation 2.9, it is easy to find some characteristic features, most important:

$$\overline{\rho u_j''} = 0 \quad \text{but} \quad (\text{Eq. 2.10})$$

$$\overline{u_j''} = \frac{\overline{\rho' u_j'}}{\bar{\rho}} \neq 0 \quad (\text{Eq. 2.11})$$

In order to obtain the mass-weighted average conservation equations the steps to follow are the very same as those outlined for Reynolds averaging procedure in the last section. The difference will be obvious reading the example below.

Example

Write the continuity equation in Favre averaged form!

Solution

Step 1. The continuity equation using instantaneous quantities is written

$$\frac{\partial \rho}{\partial t} + \frac{\partial}{\partial x_j}(\rho u_j) = 0$$

Step 2. Write all relevant instantaneous quantities as the sum of a mean and a fluctuating term. Here density is averaged using conventional time averaging and the velocity term is mass-weight averaged.

$$u_j = \tilde{u}_j + u_j'' \quad \rho = \bar{\rho} + \rho'$$

Step 3. Taking the time average on both sides of the equation becomes

$$\overline{\frac{\partial \rho}{\partial t} + \frac{\partial}{\partial x_j}(\rho u_j)} = 0$$

Step 4. Substitute the instantaneous quantities for the relationships with a mean term and a term representing the fluctuations about this mean value due to turbulence.

$$\overline{\frac{\partial}{\partial t}(\bar{\rho} - \rho') + \frac{\partial}{\partial x_j}((\bar{\rho} + \rho')(\tilde{u}_j + u_j''))} = 0$$

Step 5. The equation obtained in step 4 looks quite like the one obtained using Reynolds averaging. However, because of the definition of the mass-weighted average and by using simple mathematics the resulting Favre averaged continuity equation results in Equation 2.12. Below, the Favre averaged momentum, energy and chemical species equations follow in that order.

Mass continuity equation:

$$\frac{\partial \bar{\rho}}{\partial t} + \frac{\partial}{\partial x_j}(\bar{\rho} \tilde{u}_j) = 0 \quad (\text{Eq. 2.12})$$

Momentum conservation equation:

$$\frac{\partial \bar{\rho} \tilde{u}_i}{dt} + \frac{\partial}{\partial x_j}(\bar{\rho} \tilde{u}_i \tilde{u}_j) = - \frac{\partial \bar{p}}{\partial x_i} + \frac{\partial}{\partial x_j}(\bar{\tau}_{ij} - \bar{\rho} \overline{u_i'' u_j''}) + \bar{B}_i \quad (\text{Eq. 2.13})$$

It may be interesting to illustrate the practical difference between Reynolds and Favre averaging procedure. An example of this is presented below.

$$\overline{\rho u_i u_j} = \underbrace{\overline{\bar{\rho} \tilde{u}_i \tilde{u}_j} + \overline{\rho u_i u_j}}_{\text{Favre averaging}} = \underbrace{\overline{\bar{\rho} u_i \bar{u}_j} + \bar{\rho} \overline{u_i' u_j'}}_{\text{Reynolds averaging}} + \bar{u}_i \overline{\rho u_j'} + \bar{u}_j \overline{\rho u_i'}$$

Thus, using Favre averaging, the frequent assumption that density fluctuations can be ignored made when using Reynolds averaging becomes nonessential. However, no matter how much easier the mathematical treatment becomes using Favre averaging, the procedure inevitably hides some of the physical interactions that are present in the flow.

Energy conservation equation:

$$\frac{\partial}{\partial t}(\bar{\rho}\tilde{h}) + \frac{\partial}{\partial x_j}(\bar{\rho}\tilde{u}_j\tilde{h}) = \frac{\partial\bar{p}}{\partial t} + \frac{\partial}{\partial x_j}\left(\frac{\lambda}{c_p}\frac{\partial\tilde{h}}{\partial x_j} - \bar{\rho}u_j''h''\right) - \frac{\partial\bar{q}_j^R}{\partial x_j} \quad (\text{Eq. 2.14})$$

Species conservation equation:

$$\frac{\partial}{\partial t}(\bar{\rho}\tilde{Y}_\alpha) + \frac{\partial}{\partial x_j}(\bar{\rho}\tilde{u}_j\tilde{Y}_\alpha) = \frac{\partial}{\partial x_j}\left(\bar{\rho}D\frac{\partial\tilde{Y}_\alpha}{\partial x_j} - \bar{\rho}u_j''Y_\alpha''\right) + \bar{S}_\alpha \quad (\text{Eq. 2.15})$$

Again terms representing turbulence, in this case the terms with double primes, are referred to as Reynolds stresses in the momentum equation and as Reynolds fluxes in the energy and species conservation equation respectively. They are additional unknowns compared to equations for instantaneous quantities; this is however, the only difference. /16, 17, 18/

2.4 The Boussinesq eddy viscosity concept

By carrying out the averaging procedure, we ended up with some additional unknowns in the form of Reynolds stresses and Reynolds fluxes. This implies that the system of equations holds more unknowns than there are equations and the system is unclosed. To close this new set of equations some kind of turbulence model has to be used.

One obvious approach is to try to derive and solve equations for the Reynolds stresses themselves. Two models using this method are the so-called Algebraic Stress Models and the Reynolds Stress Models. Another approach is to deal with the whole system of equations, to find some sort of procedures in order to simplify the influence of turbulence on the conservation equations even further. A common way of simplifying includes the so-called Boussinesq's eddy viscosity concept, first proposed by Boussinesq in 1877, in which the turbulent stresses are assumed proportional to the mean velocity gradient, Equation 2.16. /10, 19/

$$-\bar{\rho}u_i''u_j'' = \mu_t\left(\frac{\partial\tilde{u}_i}{\partial x_j} + \frac{\partial\tilde{u}_j}{\partial x_i}\right) - \frac{2}{3}\delta_{ij}\left(\bar{\rho}\tilde{k} + \mu_t\frac{\partial\tilde{u}_k}{\partial x_k}\right) \quad (\text{Eq. 2.16})$$

Here μ_t is the recently introduced eddy viscosity and k is the turbulent kinematic energy, using Favre averaged quantities, defined as

$$\tilde{k} = \frac{1}{2}\frac{\bar{\rho}u_i''u_i''}{\bar{\rho}} = \frac{1}{2}u_i''^2 \quad (\text{Eq. 2.17})$$

This is analogous to the treatment of the laminar viscous shear stresses (Equation 1.6) with the proportionality constant, the laminar viscosity, replaced for the eddy or turbulent viscosity. Unlike the laminar viscosity, the eddy viscosity is by definition a property of the flow, not of the fluid.

Now, by carrying out this operation, the number of unknowns in the momentum equation, Equation 2.13, has been reduced from six variables, that is the Reynolds stresses, to only one constant and that

is the eddy or turbulent viscosity. However, the assumptions making this simplification possible, also introduce a few additional uncertainties. For example, using the Boussinesq eddy viscosity concept we assume that the turbulent motion is identical in all three spatial dimensions, turbulence is believed to be isotropic. This will not be the case in a fire.

Analogous to the treatment of turbulent momentum transport, turbulent scalar transport, such as energy and chemical species, can be assumed proportional to the relevant mean scalar gradient. For the Favre averaged scalar ϕ , the following is believed to hold

$$-\overline{\rho u_i'' \phi_j''} = \frac{\mu_t}{\sigma_t} \frac{\partial \tilde{\phi}_j}{\partial x_i} = \Gamma_\phi \frac{\partial \tilde{\phi}_j}{\partial x_i} \quad (\text{Eq. 2.18})$$

Here σ_t is an empirical constant called turbulent Prandtl number and

$$\Gamma_\phi = \frac{\mu_t}{\sigma_t} \quad \text{is known as the eddy or turbulent diffusivity for the scalar } \phi.$$

Again, using the Boussinesq eddy viscosity concept, the task of the turbulence model has been reduced to the determination of one single constant: the eddy viscosity μ_t . The most popular and widespread model for predicting the value of μ_t is, today, the k- ϵ model. /12/

2.5 The k- ϵ turbulence model

The k- ϵ turbulence model is a two-equation model implying that two additional transport equations, partial differential equations, are employed to determine the local turbulent viscosity, $\mu(x, y, z, t)$. Depending on the flow, different transport equations have to be used. Therefore, the k- ϵ model can be divided into the high Reynolds number and the low Reynolds number k- ϵ model. /17/

2.5.1 The high Reynolds number k- ϵ model

In the early 1940s two scholars, Kolmogorov and Prandtl, independently proposed that the turbulent viscosity could be approximated using the proportionality:

$$\nu_t \propto \rho L \sqrt{k}$$

where

L is a reference length scale of turbulence, often referred to as a “turbulence mixing length”, and

k is the turbulent kinetic energy.

Starting from this, the so-called Kolmogorov-Prandtl proportionality, a relationship for the turbulent viscosity can be derived. Here only the result is presented and the interested reader is referred to the literature. Using Favre averaged quantities,

$$\mu_t = C_\mu \bar{\rho} \frac{\tilde{k}^2}{\tilde{\varepsilon}} \quad (\text{Eq. 2.19})$$

where

ε is the viscous dissipation rate of turbulent kinetic energy. The value of ε gives a measure of the irreversible transformation of kinetic energy to heat, thermal energy.

C_μ is an empirical constant with a value of 0.09. /17/

The turbulence kinetic energy and its dissipation rate are obtained from their transport equations. Mathematically these are written:

Turbulent kinetic energy equation

$$\frac{\partial}{\partial t} (\bar{\rho} \tilde{k}) + \tilde{u}_i \frac{\partial}{\partial x_i} (\bar{\rho} \tilde{k}) = \frac{\partial}{\partial x_i} \left[\left(\frac{\mu_t}{\sigma_k} + \mu \right) \frac{\partial \tilde{k}}{\partial x_i} \right] + \mu_t \left(\frac{\partial \tilde{u}_i}{\partial x_j} + \frac{\partial \tilde{u}_j}{\partial x_i} \right) \frac{\partial \tilde{u}_i}{\partial x_j} - \beta g \frac{\mu_t}{\sigma_t} \frac{\partial \tilde{T}}{\partial x_i} - \bar{\rho} \tilde{\varepsilon} \quad (\text{Eq. 2.20})$$

where

σ_k is the turbulent Prandtl number for k , and

$$\beta = -\frac{1}{\bar{\rho}} \frac{\partial \bar{\rho}}{\partial \tilde{T}} \quad \text{is a thermal expansion coefficient.}$$

The above equation describes the transport of turbulent kinetic energy through different processes, including convection, diffusion, viscous dissipation et cetera.

Dissipation rate of turbulent kinetic energy

$$\frac{\partial}{\partial t} (\bar{\rho} \tilde{\varepsilon}) + \tilde{u}_i \frac{\partial}{\partial x_i} (\bar{\rho} \tilde{\varepsilon}) = \frac{\partial}{\partial x_i} \left[\left(\frac{\mu_t}{\sigma_\varepsilon} + \mu \right) \frac{\partial \tilde{\varepsilon}}{\partial x_i} \right] + C_{\varepsilon 1} \frac{\tilde{\varepsilon}}{\tilde{k}} (G_K + G_B) (1 + C_{\varepsilon 3} R_f) - C_{\varepsilon 2} \bar{\rho} \frac{\tilde{\varepsilon}^2}{\tilde{k}}$$

Here

σ_ε is the turbulent Prandtl number for the dissipation of turbulent kinetic energy, ε ,

$C_{\varepsilon 1}$, $C_{\varepsilon 2}$ and $C_{\varepsilon 3}$ are empirical constants,

$$G_K = \mu_t \left(\frac{\partial \tilde{u}_i}{\partial x_j} + \frac{\partial \tilde{u}_j}{\partial x_i} \right) \frac{\partial \tilde{u}_i}{\partial x_j} \quad \text{is a shear stress term,}$$

$$G_B = -\beta g \frac{\mu_t}{\sigma_t} \frac{\partial \tilde{T}}{\partial x_j}$$

is a buoyancy term, and

$$R_f = -\frac{G_B}{G_K}$$

is known as the flux Richardson number.

The standard values of the constants in the k and ε equations are those first proposed by Launder and Spalding in 1974, namely

Table 2.1 Constants employed by the standard k- ε turbulence model

C_μ	0.09
$C_{\varepsilon 1}$	1.44
$C_{\varepsilon 2}$	1.92
$C_{\varepsilon 3}$	0.8
σ_k	1.00
σ_ε	1.30

/11, 12, 16, 17/

2.5.2 The low Reynolds k- ε turbulence model

At low Reynolds number the transport equations used have to be modified in order to take account of the influence of the viscous sublayer in the flow field. This can be done in various ways. Commonly one term is added to the k and ε equation respectively, together with some modifications of the model constants /17/. The low Reynolds k- ε model will be left without further discussion, and therefore the interested reader is again referred to his favourite source.

2.5.3 Documented disadvantages in the k- ε model

Due to its obvious advantages, the two-equation k- ε model is very commonly used in practice. The model is comparatively simple and numerically stable and at the same time computationally rather non-demanding. Therefore, this model can lay claim to be the most extensively validated model in the field. Nevertheless, some major disadvantages have been documented. The major sources of uncertainties are two: the first being the use of Boussinesq's eddy viscosity concept and the second the assumptions made in the derivation of the transport equation for the dissipation of turbulent kinetic energy /19/. Table 2.2 summarises some of the most serious drawbacks of the k- ε model.

Table 2.2 Documented disadvantages of the k- ϵ model.

➤	Using the Boussinesq eddy viscosity concept the assumption concerning local isotropy will inevitably follow. It is no secret though that in a fire this is not the case. /12/
➤	Further, it has been found that the k- ϵ model tends to under-predict the width of the plume. This has an influence on the entrainment of air into the plume and thus the composition of the smoke as well as the temporal smoke spread. /20, 21/
➤	In addition, the model tends to over-predict the entrainment into the ceiling jet, which further exerts influence on the smoke spread. /20, 21/
➤	Comparison between experiments and the two-equation model has shown that the production rate of turbulent kinetic energy by buoyancy in real life is much higher than that predicted by the k- ϵ model./22/

2.6 Summary

The purpose of this chapter has been to give the reader an introduction to turbulence modelling and the problems that have to be dealt with. The reader should also have noted that it is at this point that the field model analysis of a fire ceases to represent an exact science. Approximations and empirical relationships are essential in order to proceed.

A number of turbulence models were named and the k- ϵ approach was further presented. In spite of its obvious disadvantages, the standard k- ϵ method is still the one recommended for practical simulations. Indeed, most new methods are much too time consuming using today's computers.

3. Modelling combustion

Combustion is a transfer process including the transfer of mass and energy. A fuel, the combustible substance, reacts with oxygen in an exothermic reaction, forming products that have lower chemical bond energy than the reactants; chemical bond energy has been transformed to thermal energy, that is heat. Combustion is a chain reaction process involving a large sequence of single, elementary reactions, ultimately ending up with a set of products, for hydrocarbons typically carbon monoxide, carbon dioxide and water. Thus the simplest hydrocarbon, methane, involves over 40 different chemical reactions. At low temperatures, the steps that are able to initiate the chain reaction are very slow. This is fortunate, because otherwise air and fuel, for example air and wood, could not coexist. /23/

While a rather large scientific community seems to be involved and concerned with general Computational Fluid Dynamics, improvements of turbulence models et cetera, the knowledge in combustion modelling, on the other hand, seems to be restricted to a more less numerous assembly of specialists. One logical reason for this is that combustion science is highly interdisciplinary, requiring knowledge in thermodynamics, chemistry, chemical kinetics and fluid mechanics.

Now, why do we have to incorporate a combustion model into our code, what is it good for? There are two major reasons for including the combustion model. Firstly, it allows us to imitate, or simulate, the fuel-oxidiser mixing process. This implies that we do not have to predefine a number of control volumes, that is a certain volume in space, to be the source of heat release. Instead, the heat release can be referred to areas where the appropriate conditions for combustion exists, for example presence of reactants. This way, the combustion model makes it possible to predict and simulate phenomena such as flame lengthening due to under ventilation or because of wind influence. Secondly, submodels for the prediction of chemical species concentration can be incorporated in the combustion model. Thus, for the fire safety engineer, the combustion model is indeed very essential.

In the following sections two combustion models, used in different CFD applications will be presented and shortly discussed. First, probably the most widespread model, the Eddy break up model, is introduced. The second model discussed is the laminar flamelet combustion model.

3.1 The eddy break up model

The Eddy break up model has experienced a world-wide spread and acceptance. It originates from Brian Spaldings (1971) /24/ model for premixed flames and has since been modified to some extent for use with diffusion flames/14/. In the Eddy break up model, all the detailed chemical kinetics have been dropped. Instead, combustion is assumed to be infinitely fast and to follow a single one-step stoichiometric chemical reaction, for a general case written as



where s represents the stoichiometric fuel to oxidant ratio and the *products* are carbon dioxide and water. Note that the general reaction above is written using the masses of fuel, oxidant and product species and not their volumes.

As the chemistry process is assumed to be infinitely fast the reaction rate will be controlled by mass transfer, primarily by the turbulent mixing of reactants which in turn is dependent on the breaking up of eddies in the turbulent flow field. Three subprocesses will then control the reaction rate; these are the turbulent dissipation of fuel, oxidant and products. The model takes the local reaction rate, that is

the rate at which the fuel is consumed at a certain location, to be the slowest of the three mixing processes referred to above. Mathematically this is expressed as

$$R_{fu} = -\bar{\rho} \frac{\varepsilon}{k} \min \left[C_R \bar{Y}_{fu}, C_R \frac{\bar{Y}_{ox}}{s}, C'_R \frac{\bar{Y}_{pr}}{1+s} \right] \quad (Eq. 3.2)$$

where

R_{fu} is the mass rate of fuel consumption, rate of reaction,

$\frac{\varepsilon}{k}$ is the turbulence time scale,

C_R, C'_R are empirically derived factors often expressed by constant values, or some simple relationship including turbulent kinetic energy, k , and its dissipation rate, ε , as variables.

$\bar{Y}_{fu}, \bar{Y}_{ox}, \bar{Y}_{pr}$ are the time averaged mass fractions of fuel, oxidant and hot products respectively.

The model can be made more sophisticated in many ways for example by incorporating soot models and models for NO_x concentration /14/. In addition, equation 3.2 can be extended to include the influence of chemical kinetics. Using the Arrhenius expression for the rate of reaction /10/

$$R_{fu} = A \rho^{-a} Y_{fu}^b Y_{ox}^c \exp(-E_a / RT) \quad (Eq. 3.3)$$

Equation 3.2 then becomes

$$R_{fu} = -\min \left[\bar{\rho} \frac{\varepsilon}{k} C_R \bar{Y}_{fu}, \bar{\rho} \frac{\varepsilon}{k} C_R \frac{\bar{Y}_{ox}}{s}, \bar{\rho} \frac{\varepsilon}{k} C'_R \frac{\bar{Y}_{pr}}{1+s}, -R_{fu,kinetic} \right] \quad (Eq. 3.4)$$

By adopting equation 3.2, the task of the combustion model has been reduced to the solution of the species concentration equations for fuel, oxidant and products. At this point, it is convenient to introduce the mixture fraction, f , which is a dimensionless number defined as

$$f = \frac{\beta - \beta_{ox}}{\beta_{fu} - \beta_{ox}} \quad (Eq. 3.5)$$

where

$$\beta = s Y_{fu} - Y_{ox}$$

The subscripts fu and ox denotes fuel and oxidant streams respectively.

This operation is mathematically convenient because now only the fuel mass fraction and a transport equation for the mixture fraction need to be solved. The oxygen and product concentrations are then given from Equation 3.1 and the chemical species conservation. /25/

The model has proved to give reasonably good predictions, however its reliability depends on a number of factors, perhaps most important the performance of the turbulence model.

3.2 The laminar flamelet combustion model

The laminar flamelet combustion model now experiences an increasing acceptance and interest among CFD users. Its main advantage is based on the fact that it brings the simulation closer to the true nature of combustion, for example when it comes to the prediction of species concentrations.

The principal assumption made is that the turbulent diffusion flame can be described to consist of small, microscopic elements that have a structure similar to an undisturbed laminar flame. The small elements are named flamelets. In addition, the chemical reactions are assumed to be fast. Using these assumptions, chemical species concentrations, relevant thermochemical scalars such as enthalpy, temperature et cetera, can be written in terms of one single conserved scalar, the mixture fraction f with the following limits:

$$\begin{aligned} f=1 & \quad \text{for pure fuel streams and} \\ f=0 & \quad \text{for pure oxidant streams.} \end{aligned}$$

The scalar mixture fraction dependencies can be either calculated theoretically or measured in a laboratory using a stable laminar flame. The relationships are then stored in a flamelet data library.

Statistical information concerning the mixture fraction fluctuation is stored in a probability density function, PDF, usually in the form of a beta function. From the first and second moment of this PDF, that is the favre averaged mixture fraction and the favre averaged mixture fraction variance, the turbulent mixing of scalars can be described using only one assumed probability density function for f . Using this function, the relationships for the relevant thermochemical scalars can be averaged for turbulent flames. This implies that the combustion model has been conveniently separated from the turbulence model, instead the relevant scalars are directly related to the local mixture fraction. If combustion is assumed to take place locally inside the flamelet the sketch in *Figure 3.1* illustrates the flamelet concept. /13, 21, 26/

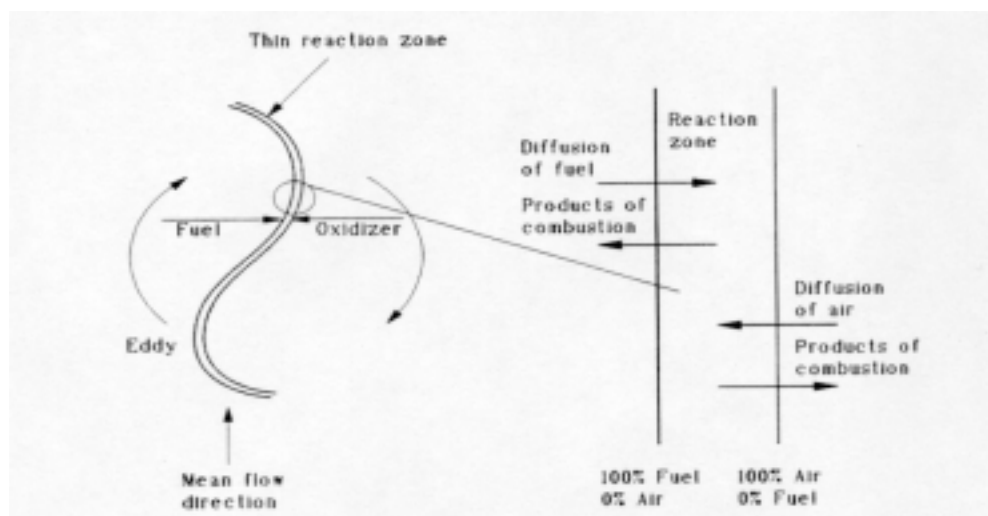


Figure 3.1 Schematic illustration of the flamelet concept. Fuel and oxidant streams meet and react in the reaction zone. /13/

3.3 Summary

Combustion is a complicated process involving several chain reactions. In the combustion model, this complex phenomenon has simplified in order to perform practical simulations. In this chapter, two different combustion models were introduced, the most widespread Eddy Breakup model and the newer Laminar flamelet model. It was concluded that the latter had a larger potential to simulate the nature of combustion. However, it requires more computer power in terms of CPU and memory.

4. Thermal radiation

The purpose of this chapter is to introduce some important aspects concerning thermal radiation, its nature and its modelling. How radiation can be taken account for in CFD applications is discussed in general terms in Section 4.2.

4.1 General

If a body, a fluid or a solid, has a higher temperature than has its environment it will emit heat. Nature strives to adjust and neutralise the differences in temperature. This phenomenon is dealt with in the second law of thermodynamics. The body will lose heat through conduction, convection and through electromagnetic radiation, or thermal radiation. In *Figure 4.1*, one can see that the thermal radiation is confined to include only a limited part of wavelengths in the electromagnetic spectrum.

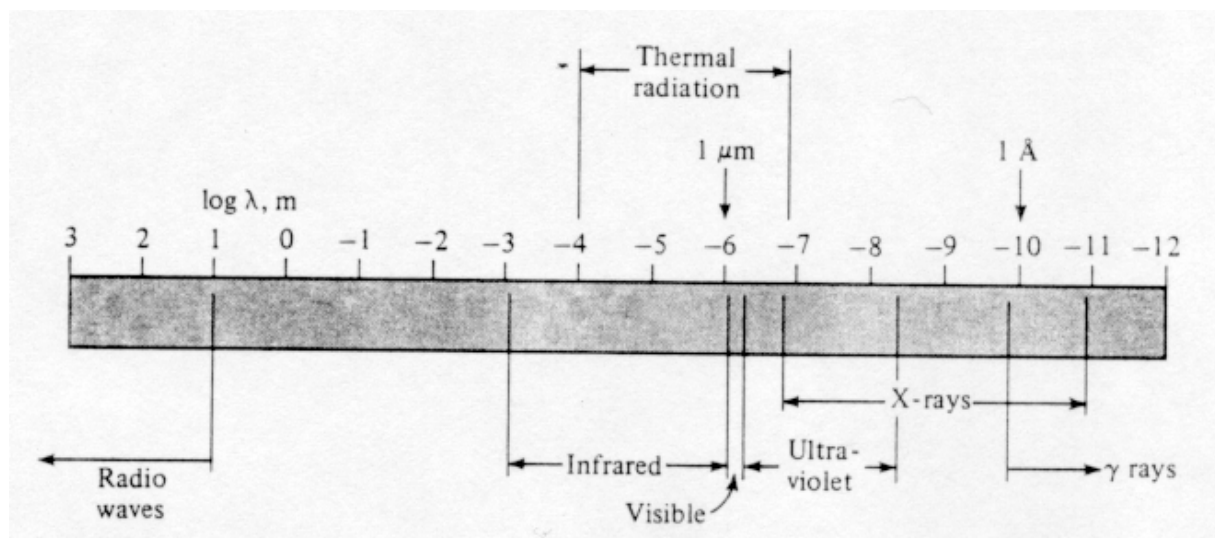


Figure 4.1 Illustration of the electromagnetic spectrum.

The higher the temperature the more intense the radiation. In contrast to conduction and convection, heat transfer through radiation does not require any intermediate medium to propagate. Heat can be transferred over relatively large distances in comparison to these other two modes of heat transfer, which can be considered more local in nature [27].

The fundamental relationship describing heat transfer by thermal radiation relates back to late 19th century and the two Austrian physicists Joseph Stefan who was the first to propose the relationship in 1879 and Ludwig Boltzmann who gave this a theoretical explanation five years later. The equation is known as the *Stefan-Boltzmann equation*.

$$E = \sigma T^4 \quad (\text{Eq. 4.1})$$

E is the energy radiated per unit area and unit time and is called the *total emissive power*,

σ is the Stefan Boltzmann constant, in SI units it has the value $5.669 \cdot 10^{-8} \text{ W}/(\text{m}^2\text{K}^4)$

T is the absolute temperature.

The equation concerns the radiation emitted from an ideal body, a so-called black body, and represents the maximum energy that can be emitted for a given temperature. It is interesting to note that the total radiative energy, or emissive power, is a function of the emitter's temperature alone. /28/

A real body always has an emissive power less than that of the black body. The ratio between the real, actual emissive power and that of a black body, represented by Equation 4.1, is called emissivity, ε .

$$\varepsilon = \frac{E_{real}}{E_{black\ body}} \quad (Eq. 4.2)$$

Implementing this relation into Equation 4.1, the equation for a non-black body emissive power becomes:

$$E_{gray\ body} = \varepsilon \sigma T^4 \quad (Eq. 4.3)$$

Before we begin to discuss the modelling of thermal radiation a few words need to be said concerning the radiation intensity, I . This is defined as the radiation emitted per unit area and unit solid angle, ω , in a certain direction. One differs between total and spectral intensity, where the former is the radiation emitted when all wavelengths are considered and the latter refers to emitted radiation for a single wavelength or a small interval, $d\lambda$, around a single wavelength. /28, 29/ For further material on the fundamentals of thermal radiation, the reader is referred to the literature, for example ref /27/.

4.2 Modelling thermal radiation

The radiation influence has its numerical origin in the energy conservation equation, Equation 1.8, 2.7 and 2.14, where it appears as a source term. In modelling this term, three steps can be distinguished. First, an overall equation to describe radiant transfer, that is, a radiative transfer equation RTE, needs to be found. Second, a way to predict the radiative properties for relevant combustion gases and soot particles has to be found. After these two initial two steps the necessary relationships has been derived and so, a third step will be to find a suitable method to solve them.

Considering a simple set of control volumes, the most fundamental radiative transfer equation implies that the change in intensity in a certain direction equals the energy emitted from matter within the control volume plus energy scattered into it from the outside minus energy losses by absorption inside the control volume and particle scattering out from it. In mathematical terms, this is expressed using an integrodifferential equation, in the Ω direction written as: /11, 30/

$$\frac{dI}{ds} = -(k_a + k_s)I + k_a \frac{E_g}{\pi} + \frac{k_s}{4\pi} \int_{\Omega'=0}^{4\pi} P(\Omega, \Omega') I(\Omega') d\Omega' \quad (Eq. 4.4)$$

I is the radiant intensity in the Ω direction,

s is the relevant distance in the Ω direction,

E_g is the emissive power of gas at the temperature T_g , $E_g = \epsilon \sigma T^4$,

$P(\Omega, \Omega')$ is the probability that incident radiation in the direction Ω' will be scattered into the increment of solid angle $d\Omega$ about Ω , and

$(k_s + k_a)$ represents gas absorption and scattering coefficients. Note that under steady state $k_a = \epsilon$, the so-called Kirchoff's identity, a relationship that can be easily derived using a simple energy balance.

Thus, in Equation 4.4 above:

$-k_a I$ represents radiant loss by absorption

$-k_s I$ represents loss through scattering effects,

$k_a \frac{E_g}{\pi}$ represents gain by emission, and

$\frac{k_s}{4\pi} \int_{\Omega'=0}^{4\pi} P(\Omega, \Omega') I(\Omega') d\Omega'$ represents gain by scattering.

The second step was related to the fact that the radiation emitted depends on the emissivity and absorptivity which in turn are rather complex functions of a number of parameters such as soot and gas concentrations, temperature, pressure, path length et cetera. The crudest approach to take account of the radiative properties of gases and particles, except from ignoring them, is to give a constant value on the absorptivity coefficient. If it is assumed that scattering can be ignored and then integrating, Equation 4.4 will become /25/

$$I_{n+1} = I_n e^{-k_a \Delta s} + \frac{\sigma T^4}{\pi} (1 - e^{-k_a \Delta s}) \quad (\text{Eq. 4.5})$$

In this case, the radiative transfer equation has been simplified to a recurrence equation in which the intensity on exit, I_{n+1} , is expressed in terms of intensity on entry, I_n . But as the accuracy of radiative heat transfer predictions are directly linked to the accuracy of the predictions of radiative properties used, this does not seem to be such a good alternative after all.

Instead of using a constant absorption coefficient, spectral calculations can be performed, in which the thermal electromagnetic spectrum (radiation with wavelengths between 0.1 to 100 μm) is divided into several intervals or bands in order to take account of the variation of the radiative properties with wavelength *Figure 4.2* illustrates the principal reasoning for two models using different degrees of spectral division. These are the wide-band models and the narrow-band models. These two approaches have until recently been considered to be slightly too demanding for general use in CFD modelling of fires. By now, it should not be any secret to the reader that even in CFD applications, some economic measures are of necessity although this inevitably will result in loss of accuracy. However, in reference /30/ a fast narrow-band model is presented, also giving a hint of the possibilities of such a model.

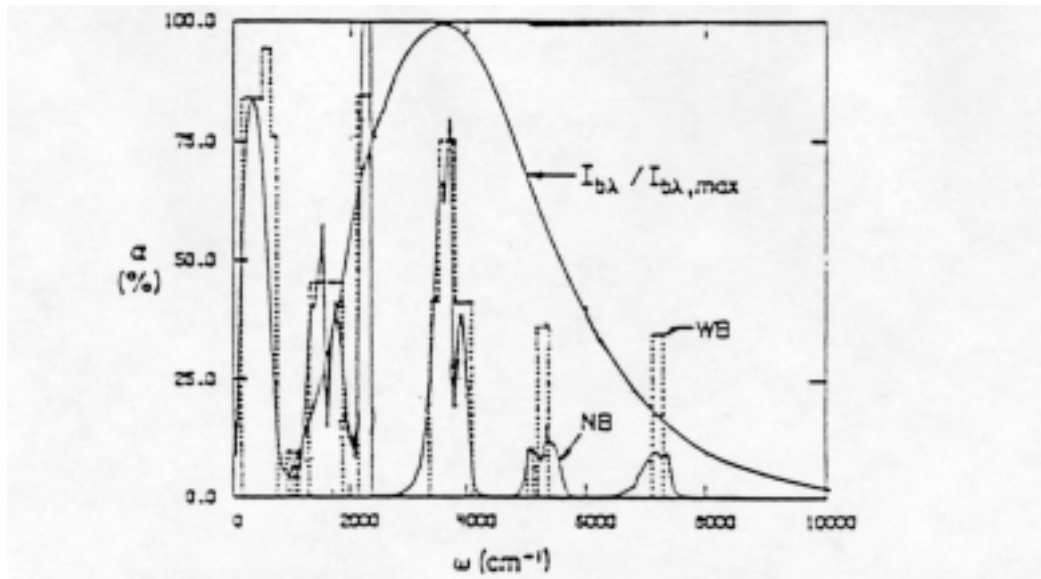


Figure 4.2 Spectral absorptivities of an H₂O-CO₂ air mixture at a temperature of 1000 K, 1 atm and a path length of 1 m. NB denotes Narrow band and WB stands for Wide band.

Another more crude category of models for the prediction of radiative properties is the so-called “Total absorptivity-emission models”. For given temperatures and pressures the band absorptivities are integrated over the total electromagnetic spectrum. This will result in a number of total absorptivity and emissivity curves. Afterwards, one seeks the appropriate polynomials to fit these curves using regression techniques. In some models, the curve-fitted expressions can be arranged so that the resulting expressions would be presented as the sum of all clear and grey gases. These are so-called weighted sum-of-grey-gases, WSGG-models.

Step three in our thermal radiation modelling program was to find a suitable solution procedure for the relationships derived in the previous steps. In the literature, a large number of solution methods are presented and some five families can be distinguished, these are:

- Exact methods
- Statistical methods
- Zonal methods
- Flux methods
- Hybrid methods

As indicated by the name, the hybrid methods can be viewed upon as methods developed by taking advantage of the desirable features of other models. One of these is the discrete transfer radiation model, DTRM in short. Lockwood and Shah /31/ first presented this in 1981. Since then, it has become the most commonly used method for solving the integrodifferential radiative transfer equation (Equation 4.4) when dealing with fire related problems. The general concept of the discrete transfer method is that it solves the radiation equation along a, user defined, number of discrete rays from every element of the boundary surface. The directions of these rays are specified in advance and the intensities in between these rays are assumed constant. /31/

4.3 Summary

In a fire, other than very small fires, thermal radiation is the most dominant mode of heat transfer. It is the major factor of flame spread both in early fire development by heat transfer to nearby combustible objects and in flame spread over solids. Until recently the use of sophisticated radiation models in

general CFD codes has been limited, partly because of its hardware demands. Frequently, the major drawback in today's radiation calculations is related to the use of a too crude model for radiative properties for gases and particles. In addition, when using the discrete transfer radiation model the accuracy will increase with the number of rays chosen.

5. Numerical solution of the governing equations

So far in this report, all attention has been focused on how to describe different physical phenomena in terms of mathematical relationships. The result is a number of complex non-linear partial differential equations. In the following chapter, we are concerned with how to find an appropriate method to solve the set of equations.

5.1 Introduction

Due to the inherent non-linearity of the partial differential equations, they have very few analytical solutions and therefore we will need to discover another kind of solution approach, the science of Computational Fluid Dynamics, CFD. The task includes the transformation of the continuous partial differential equation in both space and time in order to obtain their simultaneous algebraic counterparts. The new set of equations is then to be solved using some suitable solution method. The procedure of transforming a partial differential equation into its algebraic or numerical analogue is called numerical discretisation.

It should be known that a computer is only able to recognise so-called binary data, that is data in the form of zeros and ones. However, given the proper programming they can be instructed to store numbers and to perform simple mathematical operations, such as adding, multiplying and repeating sequences of these operations on stored numbers. Thus, the numerical discretisation makes computer-based calculations of differential equations possible to perform.

Consider the conservation equation below. The discussion above implies that each term within the equation has to be transformed into its algebraic analogue in order to write and use a computer program for its calculation.

$$\frac{\partial}{\partial t}(\rho\phi) + \frac{\partial}{\partial x_i}(\rho u_j \phi) = \frac{\partial}{\partial x_i} \left(\Gamma_{ij} \frac{\partial \phi}{\partial x_j} \right) + S_\phi \quad (\text{Eq. 5.1})$$

Note: In chapter one and two the Cartesian tensor notation was employed in writing the fundamental equations of laminar and turbulent flows. The notation was used in order to make it easier for the reader to obtain a general view of the governing equations as well as the empirically derived. However, throughout this chapter the Cartesian tensor notation will be replaced in favour to a more mathematically straightforward approach using bold types to mark vectors also using *grad* for gradient and *div* for divergence.

Using this new notation equation 5.1 becomes:

$$\frac{\partial}{\partial t}(\rho\phi) + \text{div}(\rho \mathbf{u} \phi) = \text{div}(\Gamma \text{grad} \phi) + S_\phi \quad (\text{Eq. 5.2})$$

There are different techniques used to obtain numerical discretisation, the most common being the finite difference method, the finite element method and the finite volume method.

The finite difference method employs Taylor series expansion to transform the derivatives in equation 5.2 into their algebraic analogues. As an example, consider *Figure 5.1* showing the dependent variable ϕ as a function of the distance x . Two points, one in the negative and one in the positive x -direction, are situated a distance Δx from the midpoint x . Taylor series expansion about x gives in the positive x -direction

$$\phi(x + \Delta x) = \phi(x) + \Delta x \frac{\partial \phi}{\partial x} + \frac{1}{2} (\Delta x)^2 \frac{\partial^2 \phi}{\partial x^2} + \dots \quad (\text{Eq. 5.3})$$

and in the negative x -direction

$$\phi(x - \Delta x) = \phi(x) - \Delta x \frac{\partial \phi}{\partial x} + \frac{1}{2} (\Delta x)^2 \frac{\partial^2 \phi}{\partial x^2} + \dots \quad (\text{Eq. 5.4})$$

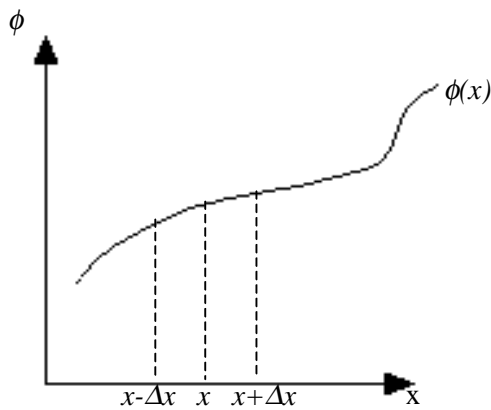


Figure 5.1 Location of points used for Taylor series expansion

The first and second derivatives at point x are found by adding respective subtracting Equation 5.3 and 5.4, ending up with:

$$\frac{\partial^2 \phi}{\partial x^2} = \frac{1}{(\Delta x)^2} (\phi(x + \Delta x) - 2\phi(x) + \phi(x - \Delta x)) \quad (\text{Eq. 5.5})$$

$$\frac{\partial \phi}{\partial x} = \frac{1}{2\Delta x} (\phi(x + \Delta x) - \phi(x - \Delta x)) \quad (\text{Eq. 5.6})$$

Indeed, there are higher order terms to use in the Taylor series and the higher the order used the smaller truncation errors can be expected. However, as Δx is supposed to be small, the higher order terms will become so small that they may be safely ignored. The Equations 5.4 and 5.5 are called

difference formulae as the derivatives are calculated using the differences between the values of the variable in various points.

Using Taylor series expansion in order to describe all the derivatives as the difference between values of the variable in space or time, a library of equations are created which makes it possible to replace the differential equation with a numerical analogue. By placing out points in the computational domain, the derivatives at each of these can be replaced by the difference formula built up of the values in a given point and its neighbours. When this has been done for all points in the domain the resulting set of equations can be solved to acquire the proper numerical solution.

In the **finite element method**, the domain over which the partial differential equation applies is divided into a finite number of pre-defined sub-domains called elements. A variation of the dependent variables are assumed over each of these sub-domains making it possible to create an overall picture of the variation of the dependent variables over the whole domain. A major contrariety to the finite difference method is that equations are produced from data at known points on the element independently of its neighbour elements while in the finite difference method the numerical equations are based on the values of neighbouring points.

The finite element method is most recognised for its use in structural engineering where it has become the most common technique in commercial software packages for the prediction of stress and strain in solid structures.

The finite volume method is probably the most popular and widespread approach for numerical discretisation. The method originates from Patankar /32/ and was specifically developed to solve the equations for heat transfer and fluid flow. The method can be considered to be influenced by both the finite difference and the finite element method, being somewhat like a hybrid between these. In the following section, the finite volume method will be discussed a little further.

5.2 An introduction to the finite volume method

Using the finite volume method the computational space, using today's vocabulary this would probably be called virtual space, is first divided into a number of non-overlapping control volumes. This is done such that every grid point is surrounded by one control volume. The so-called grid points represent the locations where the flow variables are actually computed and stored.

The conservation equations from Chapter 1 are then to be written in integral form. Using for example the generalised conservation equation, Equation 5.2, and integrating over a single control volume Ω gives

$$\frac{\partial}{\partial t} \int_{\Omega} (\rho\phi) d\Omega + \int_{\Omega} \text{div}(\rho\mathbf{u}\phi) d\Omega = \int_{\Omega} \text{div}(\Gamma \text{grad}\phi) d\Omega + \int_{\Omega} S_{\phi} d\Omega \quad (\text{Eq. 5.7})$$

This equation can be somewhat simplified using the well-known Gauss' divergence theorem, which for an arbitrarily vector in space, for example $\mathbf{u}=(u_1, u_2, u_3)$ states that:

$$\iiint_{\Omega} \text{div} \mathbf{u} d\Omega = \iint_S \mathbf{u} \cdot \mathbf{n} dS \quad (\text{Eq. 5.8})$$

where $div \mathbf{u}$ is the divergence of the vector \mathbf{u} mathematically expressed in longhand notation as:

$$div \mathbf{u} = \frac{\partial u_1}{\partial x_1} + \frac{\partial u_2}{\partial x_2} + \frac{\partial u_3}{\partial x_3} ,$$

\mathbf{n} is a vector, $\mathbf{n}=(n_1,n_2,n_3)$, of unity length and normal to the surface of dS , and

S is the sectional area.

Thus, Gauss' divergence theorem simply states that the flow of \mathbf{u} out from a control volume equals the volume integral of $div \mathbf{u}$ over that control volume. The most important and interesting feature of this theorem is that it conveniently reduces two of the volume integrals in Equation 5.7 into surface integrals. These are the convective term, the second on the left-hand side, and the diffusive term, the first term on the right side in Equation 5.7. Implementing this relationship, the integral analogue to the generalised conservation equation applied on the single control volume Ω can be written /10, 32/:

$$\frac{\partial}{\partial t} \int_{\Omega} (\rho\phi) d\Omega + \int_S \mathbf{n} \cdot (\rho\mathbf{u}\phi) dS = \int_S \mathbf{n} \cdot (\Gamma grad\phi) dS + \int_{\Omega} S_{\phi} d\Omega \quad (Eq. 5.9)$$

At this stage, it is convenient to distinguish between transient problems which are time dependent, and steady state problems which does not vary in time. In the steady state problems the rate of change term, the first term on the left hand side in Equation 5.9 will be equal to zero as these involves no time dependencies. The resulting equation then becomes:

$$\int_S \mathbf{n} \cdot (\rho\mathbf{u}\phi) dS = \int_S \mathbf{n} \cdot (\Gamma grad\phi) dS + \int_{\Omega} S_{\phi} d\Omega \quad (Eq. 5.10)$$

In transient problems, on the other hand, Equation 5.9 will also have to be integrated with respect to time, giving the following relationship:

$$\int_{\Delta t} \frac{\partial}{\partial t} \left(\int_{\Omega} (\rho\phi) d\Omega \right) dt + \int_{\Delta t} \int_S \mathbf{n} \cdot (\rho\mathbf{u}\phi) dS dt = \int_{\Delta t} \int_S \mathbf{n} \cdot (\Gamma grad\phi) dS dt + \int_{\Delta t} \int_{\Omega} S_{\phi} d\Omega dt \quad (Eq. 5.11)$$

It is interesting to note that as the above equation is composed of four separate groups, representing different phenomena, each group, or term, may be conveniently treated individually using different numerical algorithms depending on the physical process in question. /19/

5.2.1 An illustrative example

In this section, a simple example will be studied. The purpose is to illustrate the general procedure when using the finite volume discretisation. The example concerns the derivation of the control volume discretisation equation for a steady one dimensional heat conduction through some arbitrarily media and it originates from the excellent book by Patankar, reference /32/ pp 31-39.

The steady one dimensional heat conduction equation can be written in differential form as:

$$\frac{d}{dx} \left(k \frac{dT}{dx} \right) + S = 0 \quad (\text{Eq. 5.12})$$

where

k is the thermal conductivity,

T is the temperature, and

S represents the rate of heat generation per unit volume.

The grid for a one-dimensional problem will have a structure as illustrated in *Figure 5.1*. Assigning a unit length in the y and z directions the control volume will have the volume $\Delta x \times 1 \times 1$.

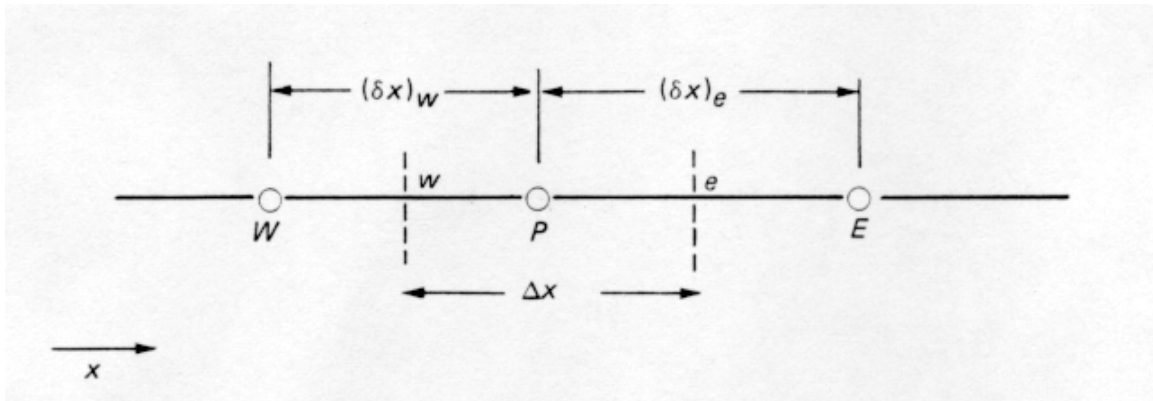


Figure 5.1. Part of a one-dimensional grid. The dashed lines represent the cell wall, W and E denote west and east neighbour grid point, w and e is the west and east cell face respectively. /32/

Focusing on the grid point P and integrating Equation 5.12 over this control volume gives:

$$\left(k \frac{dT}{dx} \right)_e - \left(k \frac{dT}{dx} \right)_w + \int_w^e S dx = 0 \quad (\text{Eq. 5.13})$$

The next task is to render assumptions about and to calculate the variation of the dependent variable between the grid points. This is made using an interpolation formula. In *Figure 5.2*, the two simplest profile assumptions are illustrated.

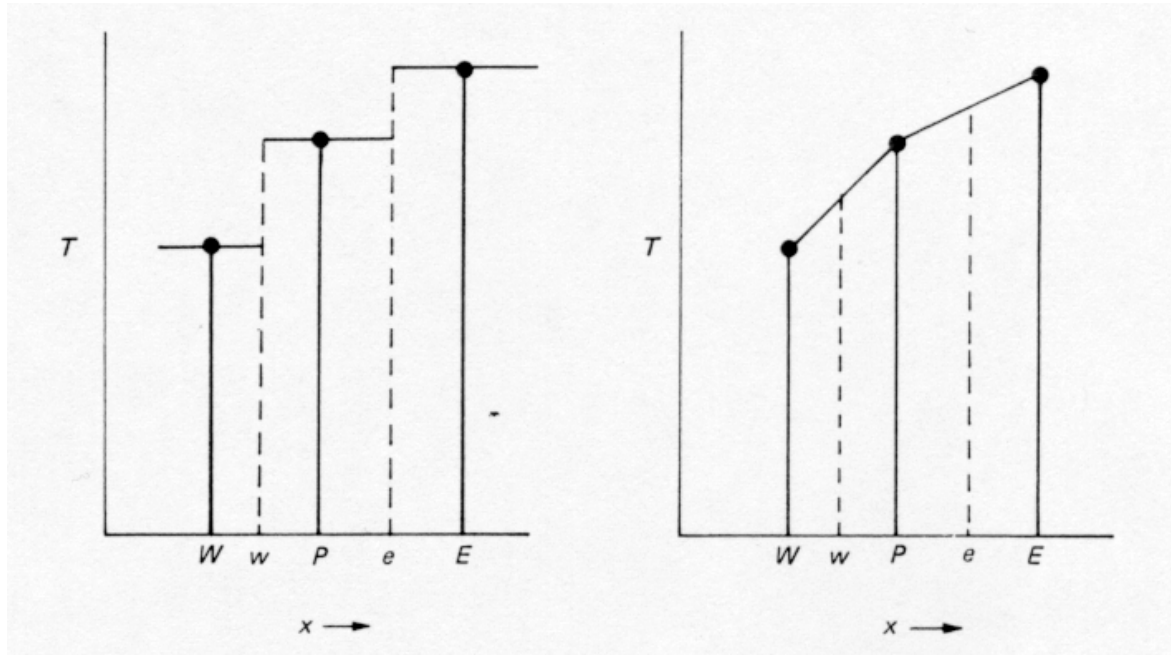


Figure 5.2. The two simplest interpolation functions. (a) Stepwise profile and (b) piecewise-linear profile. /32/

Applying the linear interpolation on the derivatives dT/dx in Equation 5.13 the resulting equation becomes:

$$\frac{k_e(T_E - T_P)}{(\delta x)_e} - \frac{k_w(T_P - T_W)}{(\delta x)_w} + \bar{S} \Delta x = 0 \quad (\text{Eq. 5.14})$$

where

\bar{S} is the average value of S over the control volume.

At this point, when the equation is practically discretised, we will introduce a standard form for writing the discretisation equations. This new form is explained by example in Equation 5.15.

$$a_P \phi_P = \sum a_{Nb} \phi_{Nb} + b \quad (\text{Eq. 5.15})$$

where the subscript Nb is short for neighbour, aiming at the neighbouring grid points, ϕ is an arbitrarily dependent variable and b represents sources within the control volume.

Simplifying and then applying the standard form from above onto equation 5.14 ends up with:

$$a_P T_P = a_E T_E + a_W T_W + b \quad (\text{Eq. 5.16})$$

where

$$a_E = \frac{k_e}{(\delta x)_e} ,$$

$$a_W = \frac{k_w}{(\delta x)_w} ,$$

$$a_P = a_E + a_W , \text{ and}$$

$$b = \bar{S} \Delta x .$$

It should be recognised that the linear interpolation formulation is the simplest formulation that can be used when evaluating the derivative dT/dx . Of course, there are many other interpolation functions that could have been used. In addition, it should be noted that it is not necessary to use the same function for all terms in the equation.

5.2.2 Finite volume method on a steady one-dimensional convection-diffusion problem

In this section, the finite volume method will be applied to a convection diffusion problem. For the sake of simplicity, the problem discussed will involve steady convection and diffusion in one dimension with no sources or sinks. We further assume that the flow field is given that is the density and velocity components are known. How this is achieved in reality is beyond the scope of this text.

Thus, the transport equation that is to be solved is written:

$$\frac{d}{dx}(\rho u \phi) = \frac{d}{dx} \left(\Gamma \frac{d\phi}{dx} \right) \quad (\text{Eq. 5.17})$$

where u represents the velocity of the flow in the x direction.

The continuity equation for the problem described becomes:

$$\frac{d(\rho u)}{dx} = 0 \quad \text{or} \quad \rho u = \text{constant} \quad (\text{Eq. 5.18})$$

The grid in this problem is identical to the one in Section 5.2.1 that was illustrated in *Figure 5.1*. Here, as a simple and straightforward example a uniform grid, such that e is located midway between P and E and w midway between W and P, will be assumed.

Integration of the transport Equation 5.17 over the control volume results in:

$$(\rho u \phi)_e - (\rho u \phi)_w = \left(\Gamma \frac{d\phi}{dx} \right)_e - \left(\Gamma \frac{d\phi}{dx} \right)_w \quad (\text{Eq. 5.19})$$

As a first attempt for interpolation it feels natural to start with a simple approach, as the piecewise linear profile, illustrated in *Figure 5.2 (b)*. This results in:

$$\phi_e = \frac{1}{2}(\phi_E + \phi_P) \quad (\text{Eq. 5.20 a})$$

$$\phi_w = \frac{1}{2}(\phi_P + \phi_W) \quad (\text{Eq. 5.20 b})$$

Note that the factor 1/2 originates from the assumption that the grid is uniform and that the cell faces are located midway between the neighbouring grid points. If the distance had been another these constants would also have had other values.

In connection to this, it is also convenient to introduce two definitions, two symbols that will help to obtain a more compact equation.

$$F \equiv \rho u \quad (\text{Eq. 5.21 a})$$

$$D \equiv \frac{\Gamma}{\partial x} \quad (\text{Eq. 5.21 b})$$

Here F represents the convective mass flux through a unit area and D is the diffusion conductance per unit area. Note that both these two have the same dimensions. However, D will only take positive values while F can have both positive and negative signs depending on the flow direction. Applying these symbols and using the result from the interpolation, Equation 5.20, Equation 5.19 can be written:

$$\frac{F_e}{2}(\phi_E + \phi_P) - \frac{F_w}{2}(\phi_P + \phi_W) = D_e(\phi_E - \phi_P) - D_w(\phi_P - \phi_W) \quad (\text{Eq. 5.22})$$

This equation can further be written on the standard form, Equation 5.15. The resulting discretisation equation then becomes:

$$a_P \phi_P = a_E \phi_E + a_W \phi_W \quad (\text{Eq. 5.23})$$

where

$$a_E = D_E - \frac{F_e}{2}$$

$$a_W = D_w + \frac{F_w}{2}$$

$$a_P = D_e + \frac{F_e}{2} + D_w - \frac{F_w}{2} = a_E + a_W + \underbrace{(F_e - F_w)}_{\text{By continuity } F_e = F_w} = a_E + a_W$$

Equation 5.23 represents the discretisation equation, or the algebraic analogue, for the transport Equation 5.17. The result was obtained using a stepwise linear profile for the interpolation of the dependent variable, this form is also known as the central difference scheme. In order to solve our simple one-dimensional convection diffusion problem, discretisation equations are written for all grid points resulting in a set of algebraic equations. This is then solved to give the distribution of ϕ through the grid.

However, although successful for pure diffusion problems, it turns out that this interpolation scheme has some serious disadvantages. These are seen in problems where Reynolds number increases to an extent where convection dominates diffusion. The example below clearly shows the physically unrealistic results that can turn up. /32/

From given values Equation 5.23 is used to find the value of ϕ_P .

$$D_e = D_w = 1, \text{ and}$$

$$F_e = F_w = 4$$

That is, the convective forces exceed diffusion by a factor four.

Now, if

a) $\phi_E = 200$ and $\phi_W = 100$, then according to Equation 5.23 $\phi_P = 50$.

b) $\phi_E = 200$ and $\phi_W = 100$, then $\phi_P = 250$.

Clearly, the result should be restricted by the values of the ϕ in the neighbouring control volumes. This is an example of a so-called physical unrealistic result. However, this kind of result should not come as a total surprise to the attentive reader as the drawback of the method is quite obvious. Consider a convective flow from west to east in *Figure 5.1*, using the central differencing scheme the value of ϕ at the west face of the control volume will always be influenced by both ϕ_W and ϕ_P , independently of the present flow pattern. It falls under the umbrella of common sense that in such a situation, the value of ϕ at the west cell face will be influenced by ϕ_W more than by ϕ_P . Thus, using a rather non scientific method we have found that the use of the central difference interpolation scheme is limited to low Reynolds number calculations. For higher Re, where convection exceeds diffusion, other interpolation schemes have to be employed. One such is the *upwind scheme*.

5.2.3 The upwind differencing scheme

The upwind scheme is a simple however frequently used interpolation scheme. The fundamental assumption is that the value of variable ϕ at the face of a control volume is depending of the direction of the flow so that the value of ϕ at a cell face equals the value of ϕ at the grid point upwind from the cell face. Mathematically this can be expressed:

$$\phi_e = \phi_P \quad \text{if} \quad F_e > 0 \text{ (the flow is positive i.e. from west to east in } Figure 5.1)$$

$$\phi_e = \phi_W \quad \text{if} \quad F_e < 0 \text{ (the flow is negative i.e. from east to west in } Figure 5.1)$$

Of course, the value of ϕ_w can be treated in a similar manner.

If we let $\max(A, B)$ denote the maximum of A and B and considering the east cell face, the upwind scheme implies that

$$F_e \phi_e = \phi_p \max(F_e, 0) - \phi_E \max(-F_e, 0) \quad (\text{Eq. 5.24})$$

The resulting discretisation equation becomes:

$$a_p \phi_p = a_E \phi_E + a_w \phi_w \quad (\text{Eq. 5.25})$$

where

$$a_E = D_e + \max(-F_e, 0)$$

$$a_w = D_w + \max(F_w, 0)$$

$$a_p = D_e + \max(F_e, 0) + D_w + \max(-F_w, 0) = a_E + a_w + (F_e - F_w)$$

As this interpolation method is particularly attractive when Reynolds number is so high that convection dominates diffusion and the former, central scheme, has advantages when Re is low, these can be combined in order to use the advantages of both methods. This is done in the so-called hybrid scheme. Of course, until today several interpolation schemes with various level of complexity have been proposed. However, it can be interesting to note that for practical problems involving buoyant flow in enclosures, the most successful schemes have been those based on the conventional upwind approximation. /11/

5.3 Solving the equations

In the above sections, a method for discretising a differential equation was introduced. From a general differential equation, the discretisation method produces the algebraic analogue in the form of a set of equations. The next step is to solve these discrete equations and thus acquire values for the different grid points in the domain. One particularly popular solution method is the so-called Thomas algorithm also known as the tri-diagonal matrix algorithm (TDMA). The TDMA is basically a direct method for one-dimensional problems however, it can be successfully applied on two- and three-dimensional problems using an iterative approach scanning line by line and plane by plane and applying standard Gaussian elimination methods to find the solution. One reason for its popularity is that the method is computationally inexpensive, in terms of storage and CPU-time. The interested reader is referred to the literature for more information on the solution of linear algebraic equations. /10, 32, 33/

5.4 Summary

In this chapter different methods for transforming a partial differential equation into an algebraic analogue was introduced. The control volume formulation was used on two simple examples in which the fundamentals of the method were illustrated. For the convection diffusion transport equation, it were noted that the most crucial issue was how to treat the values of the convective term on the faces of the control volumes properly. For simplicity, the calculation of the flow field itself was left for the interested reader to investigate individually.

To close the study the solution of the discretised equations was briefly discussed. It should be recognised that this whole procedure, including both the discretisation procedure and the solution of the resulting equations, is more an issue for the applied mathematician than for the fire safety engineer. Nevertheless, it should be remembered that, using some CFD software requires that the user is familiar with the basics, in some cases even more.

References

- /1/ Birk David M., "An introduction to Mathematical Fire Modeling", Technomic Publishing Company, Pennsylvania, 1991.
- /2/ Stroup David W., "Using Field Models to Simulate Enclosure Fires", The SFPE Handbook 2nd edition, Section 3 / Chapter 8, 1995.
- /3/ Cox Geoffrey, "Compartment Fire Modelling", Combustion Fundamentals of Fire, Academic Press, ISBN 0-12-194-230-9, Watford, 1995.
- /4/ Quintiere J. G., "Compartment Fire Modelling", The SFPE Handbook 2nd edition, Section 3 / Chapter 5, 1995.
- /5/ Forney G. P., Moss W. F., "Analyzing and Exploiting Numerical Characteristics of Zone Fire Models", Fire Science & Technology Vol. 14 No. 1 & No. 2 (49-60), 1994.
- /6/ Lundin Johan, "Uncertainty in smoke transport models", Report 3086, Department of Fire Safety Engineering, Lund University, Lund, 1997.
- /7/ Davis William D., Notarianni Kathy A., McGrattan K. B., "Comparison of fire model predictions with experiments conducted in a hangar with a 15 meter ceiling", Building and Fire Research Laboratory, National Institute of Standards and Technology, Gaithersburg, MD 20899, 1996, (NISTIR 5927).
- /8/ Stenblom Lars-Göran, Karlsson Björn, "Datorsimulering av brandventilation", Rapport räddningstjänstavdelningen R53-147/96, Statens Räddningsverk, Karlstad, 1996.
- /9/ SOFIE homepage, <http://www.cranfield.ac.uk/sme/sofie>
- /10/ Versteeg H. K., Malalasekera W., "An introduction to Computational Fluid Dynamics- The finite Volume Method", Longman Scientific & Technical, Loughborough, ISBN 0-470-23515-5, 1995.
- /11/ Cox Geoffrey, "Combustion Fundamentals of Fire, Chapter 1 pp 1-30 Basic Considerations", Academic Press Limited, London, 1995.
- /12/ Kuo Kenneth Kuan-yun, "Principles of Combustion", John Wiley & Sons, New York, 1986.
- /13/ Tuovinen Heimo, "Simulation of Combustion and Fire-Induced Flows in Enclosures", Phd thesis, Lund University, Lund, 1995.
- /14/ Magnussen Bjørn F., "The Eddy Dissipation Concept", subtask 3.1.C, Presented at Task Leaders Meeting, Lund, 1989.
- /15/ Stanisic, M. M., "The Mathematical Theory of Turbulence", Second Edition, ISBN 0-387-96685-4, Springer-Verlag- New York Berlin Heidelberg, Harrysonburg, Virginia, 1988.
- /16/ Abbott Michael Barry, Basco D.R., "Computational Fluid Dynamics- An Introduction for Engineers", Harlow Longman Science, 1989.
- /17/ Kotake Susumu, Hijikata Kunio, "Numerical Simulation of Heat Transfer and Fluid Flow on a Personal Computer", Elsevier Science Publishers B.V., Amsterdam, 1993.

- /18/ Anderson Dale A., Tannehill John C., Pletcher Richard H., "Computational Fluid Mechanics and Heat Transfer", Hemisphere Publishing Corporation, ISBN 0-89116-471-5, 1984.
- /19/ Rubini, P., "SOFIE- User guide", School of Mechanical Engineering, Cranfield University, England.
- /20/ Holmstedt, Göran, Presentation av kunskapsläget inför ansökan om projektmedel för utveckling av turbulensmodeller till CFD applikation, Dept of Fire Safety Engineering, Lund, 1997.
- /21/ Tuovinen, Heimo, "Application of Flamelet Chemistry Model to Vitiated Methane-Air Diffusion Flames", Lund University, Lund, 1992.
- /22/ Shabbir A., Taulbee D. B., "Evaluation of Turbulence Models for Predicting Buoyant Flows", Journal of Heat Transfer, 112, pp 945-951, 1990.
- /23/ Glassman, Irvin, "Combustion", Third Edition, Academic Press Inc., San Diego, ISBN 0-12-285852-2, 1996.
- /24/ Spalding, D. B., "Mixing and Chemical Reaction in Steady Confined Turbulent Flames", Thirteenth Symposium (International) on Combustion, pp 649-657, The Combustion Institute, Pittsburgh, PA, 1971.
- /25/ Lewis, M.J, Moss, M.B., Rubini, P.A., "CFD Modelling of Combustion and Heat Transfer in Compartment Fires", Fire safety science, Proceedings of the fifth international symposium, pp. 463-474.
- /26/ Libby Paul A., Williams Forman A., "Turbulent Reacting Flows", Academic Press Limited, Padstow, 1994.
- /27/ Blackshear, Perry L. (editor), "Heat Transfer In Fires- thermophysics, social aspects, economic impact", John Wiley & Sons, Washington D.C., 1974.
- /28/ Siegel Robert, Howell John R., "Thermal radiation heat transfer", McGraw-Hill Book Company, 1972.
- /29/ Holman, J. P., "Heat Transfer", Sixth Edition, MacGraw – Hill Book Company, ISBN 0-07-Y66459-5, 1986.
- /30/ Yan Zenghua. Holmstedt Göran, "Fast, narrow-band computermodel for radiation calculations", Numerical Heat Transfer, Part B, 31:61-71, 1997.
- /31/ Lockwood F. C., Shah N. G., "A new radiation solution method for incorporation in general combustion prediction procedures", Eighteenth Symposium (International) on Combustion, pp. 1405-1414, The Combustion Institute, Pittsburgh, PA, 1981.
- /32/ Patankar, Suhas V., "Numerical Heat Transfer and Fluid Flow", Taylor & Francis, ISBN 0-89116-522-3, 1980.
- /33/ Hirsch Charles, "Numerical Computations of Internal and External Flows", Volume 2: Computational Methods for Inviscid and Viscous Flows, John Wiley and Sons, ISBN 0-471-923516-6, Chichester, 1991.

Part 2: Experimental results and Field model simulations

The purpose of this part is twofold. Firstly the experimental series that has been studied in this work will be introduced and discussed. Three different sets of experiments have been studied and among these the experiments executed by the author himself will be presented more thoroughly. As a second objective the numerical results, obtained from field model simulations using the CFD-code SOFIE (Simulation Of Fires In Enclosures) will be compared to the experimental results.

Two small-scale and one large-scale experiment have been used in the study. One of the small-scale tests was executed by the author using a methane fire source, the second was performed by Lasse Bengtsson at the Department of Fire Safety Engineering at Lund University, using heptane as fuel. The large-scale experiment studied in this work is the so-called Cardington experiments performed by FRS in cooperation with Lund University and SP Fire Technology at the Cardington large building test facility, England.

It should be pointed out that none of these experiments can lay claim on representing a real compartment fire but should be regarded as being tools in validating computer codes, making contribution to fire model development and so forth.

It should also be noted that the purpose of the simulations was not meant as validation studies but rather as an evaluation of the utility and accuracy of the present SOFIE-code from a fire safety engineering point of view.

1. The methane small-scale experiments

1.1 The experimental setup

These experiments were executed by the author and his two co-workers /1/ in December 1997. The combustion chamber had an outer shell consisting of 0.02 meters thick fibre insulated concrete slabs. In order to preserve the walls of the combustion chamber the walls and ceiling were covered by 0.05 meters thick mineral wool insulation.

The internal dimensions of the chamber were

Width	0.70 m
Depth	1.10 m
Height	0.75 m

The dimensions of the opening were adjusted using pieces of mineral wool. The temperature was measured in the front corner of the combustion chamber using a thermocouple tree, the temperature was also measured between the mineral wool and the concrete slabs in the walls and in the ceiling. The presence of combustion gases; CO, CO₂ and O₂ was monitored using a probe placed at different locations inside the combustion chamber. The combustion gases were also collected and analysed outside the chamber using a hood located above the small test room. One of the major purposes when measuring the concentration of these combustion gases above the combustion chamber is that the rate of heat release, RHR, easily can be estimated from the composition of combustion gases together with a given pressure difference and temperature. *Figure 1.1* illustrates the general configuration of the methane experiments.



Figure 1.1 The experimental rig used in the Methane experiments. Photo by Anders Edstam

Mass flow control. The mass flow of methane fuel was controlled by placing the methane container on a load cell. The weight of the gas bottle was then monitored manually every 15 th second. This procedure yields the rate of fuel consumption as a mean over 15 seconds. The burner used was made

of a box, 0.3×0.3 meters, filled with sand increasing the combustion area and also decreasing the momentum of the gas released from the bottom of the sandbox, thus producing a more natural flame.

Measuring temperature. A number of thermocouples were used to measure the temperature inside the combustion chamber and in the walls. A total of 12 thermocouples were used and of these the thermocouple tree, located in the right front corner approximately 0.05 meters from the walls, consisted of eight evenly positioned in a vertical row. The other four was used to monitor the temperature on the back of the mineral wool, between the insulation and the fibre-insulated slabs.

Measuring the concentration of combustion gases inside the combustion chamber. The presence and concentration of combustion gases inside the combustion chamber was measured by placing a probe, see *Figure 1.2*, at different locations in the chamber. Using a vacuum-pump gas samples were continuously collected by the probe. The gas was cooled, dried and filtered before entering the gas-analyser.



Figure 1.2 A photograph of the probe placed inside the test room. Photo by Anders Edstam

When monitoring the CO concentration in the combustion chamber it was noted that in some of the experiments, the concentration of CO in the chamber exceeded the calibrated range of the gas analysis equipment, 1 vol%. Although the error from this may be expected to be small this implies that in those cases the CO concentration exceed 1 vol% the values should be used with care.

Measuring the concentration of combustion gases outside the combustion chamber. The combustion chamber was placed beneath a collecting hood connected to a thermally insulated exhaust duct and a fan. The apparatus is illustrated in *Figure 1.3*.

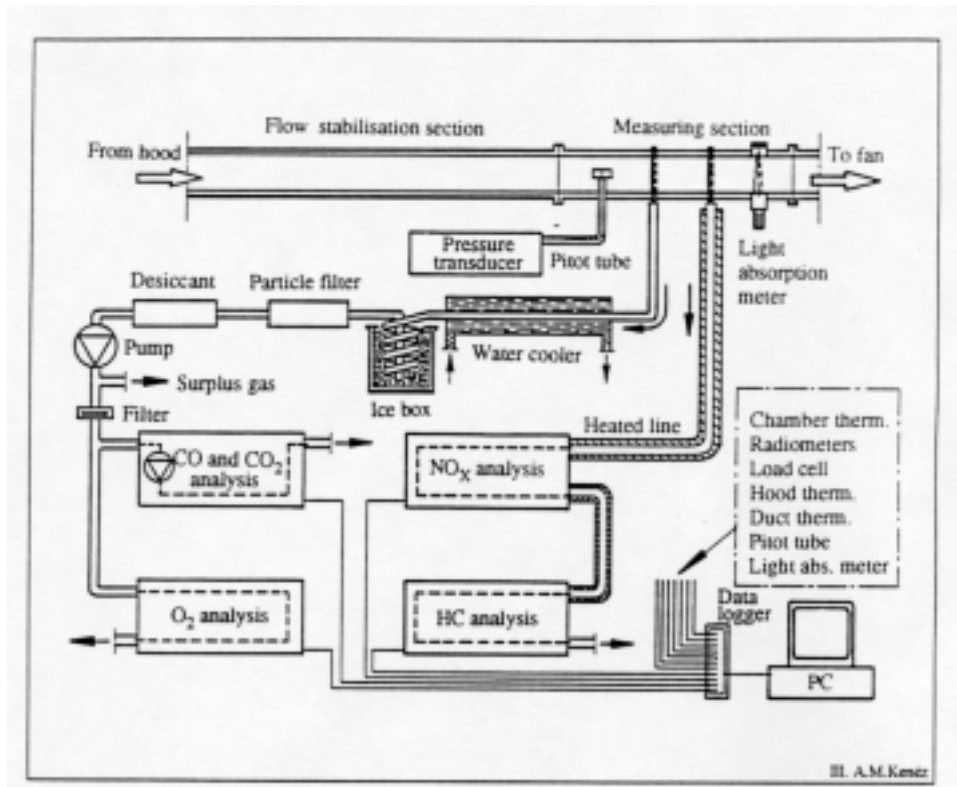


Figure 1.3 Sketch of the experimental set-up. /2/

Note that in the methane experiments only CO, CO₂ and O₂ concentrations were measured. The principal purpose of measuring the concentration of combustion gases outside the chamber was to obtain a value for the rate of heat release, RHR, in the experiments. The procedure for this is outlined in short in Appendix A.

2. The heptane small-scale experiments

2.1 Short description of the experimental set-up

In 1997, Lasse Bengtsson, PhD student at the Department of Fire Safety Engineering at Lund University, performed a series of experiments using heptane as fuel. The experimental set-up has many similarities to the methane experiments described in Chapter 1. Thus, the purpose of this chapter will be to elucidate the major differences. For details the reader is referred to Bengtsson /3/.

The combustion chamber used was made up by a box of stainless steel placed inside a furnace of firebrick. In order to allow different degrees of ventilation the opening dimensions were adjustable using mineral wool slabs. The internal dimensions of the test chamber was as follows:

Width	0.75 m
Depth	1.10 m
Height	0.80 m

A schematic illustration of the combustion chamber is presented in *Figure 2.1*.

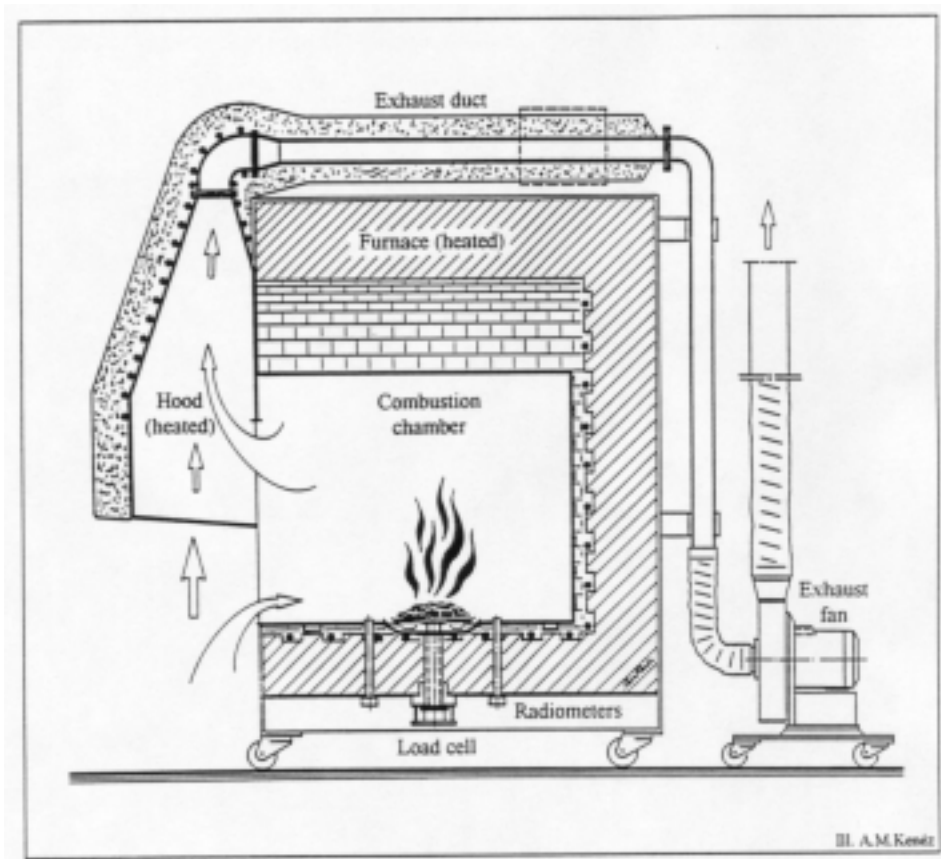


Figure 2.1 Sketch of the combustion chamber used in the heptane experiments. /4/

Mass flow control. In the experiments, a heptane pool fire was used as fire source. The containers used were circular with a diameter 0.20 or 0.30 meters. The rate of gasification was monitored by connecting the heptane container inside the combustion chamber to a load cell. The load cell was in

turn connected to the data-logger. In order to adjust for fluctuations, created by the turbulent flow of gases, the fuel mass loss were calculated as a mean over 72 seconds.

Measuring temperature. A total of 21 thermocouples was used in the experiments. Eight of these were placed on a thermocouple tree located approximately 0.05 meters from the front corner of the test chamber. In order to measure the temperature in the flow of gases in the opening seven thermocouples were positioned in a vertical row in the opening. Another three thermocouples were placed onto the walls and the final three was located in the ceiling.

The measuring of **combustion gases**, both inside and outside the combustion chamber, was performed in a similar way as in the methane experiments.

3. The Cardington large-scale experiments

These experiments were performed at the Cardington large building test facility in 1997, see *Figure 3.1*. The experiments were initiated by the Fire Research Station, England, and were carried out in co-operation with a Swedish team from the Department of Fire Safety Engineering at Lund University and SP Fire Technology, Borås. The pronounced objective of the experiments were twofold:

- To develop a protocol for use in evaluation of fire models.
- To carry out limited development of fire models, especially to adapt them for large fires that are dominated by radiation and soot production, and to carry out systematic evaluation of fire models, with particular attention to the requirements of the end user.



Figure 3.1 The Cardington hangars. Photo by S-I Granemark

This chapter will give a short summary of the experiments, how they were carried out and what type of measurements that were made. A more thorough description of the experiments can be found in the referred literature /5/. It should be pointed out that the data used in this report are the results from the measurements carried out by the Swedish team.

3.1 Short description of the experimental setup

The experimental series were performed in a section of the eight-storey large-scale test facility in the Cardington hangar, *Figure 3.2*. The section included an atrium connected to a separate compartment at the first floor level.

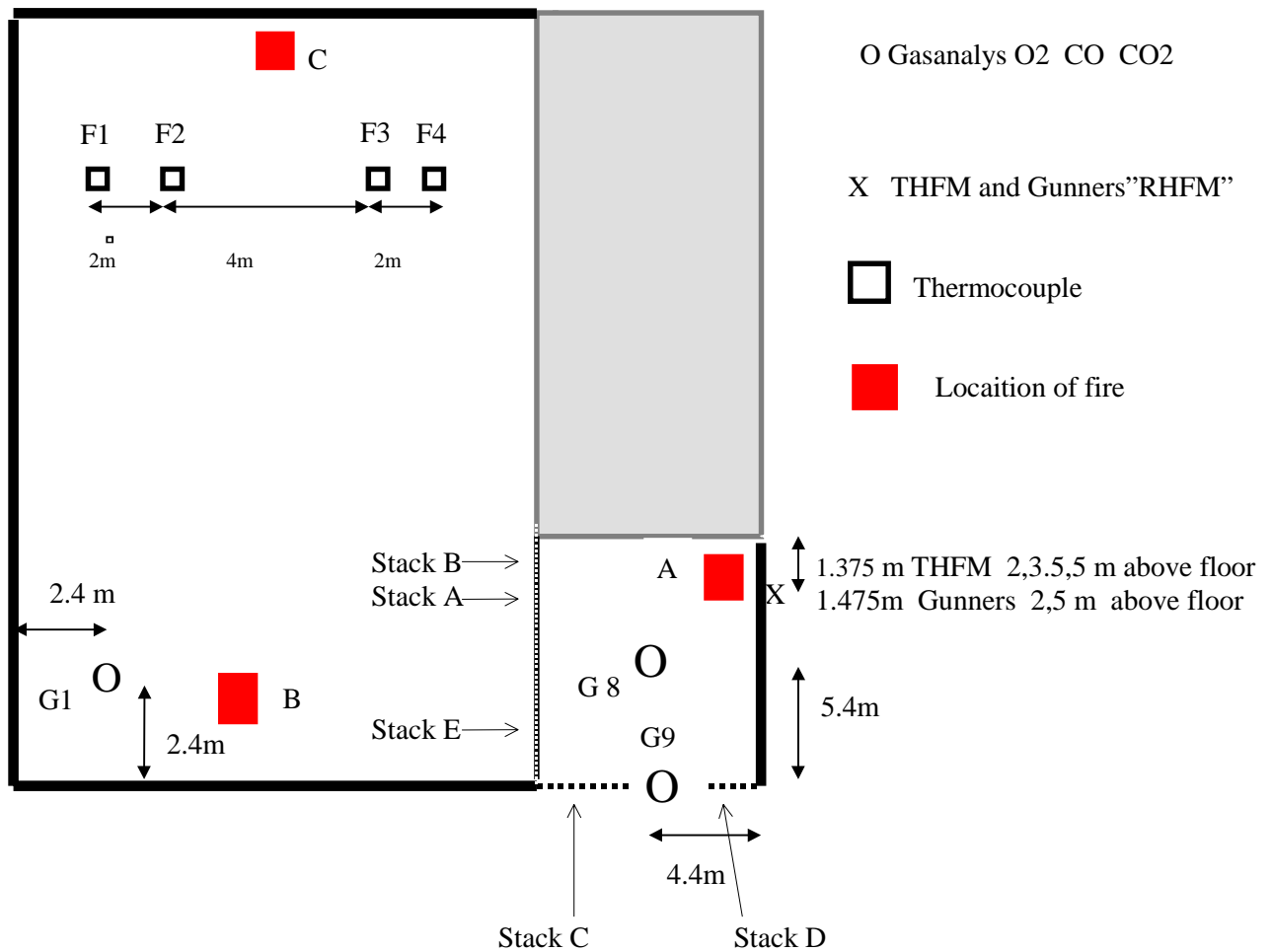


Figure 3.2 Plan-views of the Cardington test-room. /6/

The internal dimensions of the sections were

	Atria [m]	Compartment [m]
Width	8.78	13.3
Depth	10.8	20.9
Height	8.39	4.12

The ceiling was made by corrugated steel with a concrete slab on top; 0.30-meter steel beams supported the construction. The outer walls were made of concrete and the partitioning walls, separating the section from the rest of the test facility were made of plasterboard and non-combustible sheets. The test section is illustrated in Figure 3.2. Figure 3.3 shows the external opening of the atria.



Figure 3.3 Photo from one of the experiment showing the external opening. Photo by S-I. Granemark

Mass flow control. The fire source was a pool fire using kerosene and IMS as fuel. In this report, only the kerosene experiments are considered. In order to facilitate ignition and fast fire growth heptane was added as an accelerant. The rate of gasification was measured and monitored during the experiment using load cells that were located beneath the fuel tray.

Measuring temperature. The gas temperature was measured using 18 thermocouple columns giving the temperature at 210 different locations in the test section. In addition, surface temperatures were measured at 50 locations

Measuring the concentration of combustion gases. The concentrations of oxygen, carbon monoxide and carbon dioxide were measured using a 0.3 meters long perforated probe of stainless steel. These were placed at nine different locations in the test section.

Measuring gas velocity. The gas velocity was measured in the internal and the external opening. In the internal opening, the gas velocity was measured in four columns, using bi-directional probes. In the external opening three columns were used, two containing pitot tubes and one containing bi-directional probes.

It should be noted that the pitot tubes are very sensitive to the direction of the flow. If the flow arrives from behind or at an angle more than 45° from the direction of the flow the data obtained will be questionable. In addition, the pitot tubes are less reliable at low velocities, that is where the pressure differences are small, typically less than 1 Pa. This implies that in locations where the gas velocity can be expected to be low, for example near the neutral plane, again the data obtained might be questionable.

4. The field-model SOFIE

The simulations in this work have been carried out using the field model SOFIE, Simulation Of Fire In Enclosures. SOFIE was developed, and is still being developed, under the umbrella of a consortium including several European fire research laboratories and Universities, Cranfield University where the SOFIE project was initiated, Lund University, Fire Research Station, Swedish National Testing and Research Institute, Technical Research Centre of Finland, CSTB (France), Home Office Fire Safety Engineering Group, Health & Safety Laboratory. The principal objectives in developing this CFD code are three:

- To develop a field model specifically for the prediction of fires in buildings, that incorporates the core features of current commercially available, general-purpose fluid dynamic computer codes.
- To develop within the code a range of fire specific features to enable prediction of more complex fire phenomena not normally accessible in general purpose codes. For example, fire growth and spread, toxic emissions and dispersion, fire and water spray interaction.
- To make available to the fire science community a robust field model that may be used for both fire safety assessment and as a well-validated common benchmark for comparison with other codes. /7/

It is without questions that field modelling has gained recognition in several fire safety applications. A major strength in the SOFIE concept is the development of fire specific models such as soot production, flame spread etc. Nevertheless, the development of different models should not be allowed to conceal the problems of the existing models. For example, the radiation models and the turbulence model are far from perfection in the present code.

This chapter will outline the most fundamental features of SOFIE, beginning with how to set up a problem and ending with a discussion on how to examine and present the results obtained from a performed calculation. The version of the code that was used in this work (mainly PC version 2.7.1) has no graphical pre- or post processor, but uses a text only interface.

4.1 Pre-processor

SOFIE uses a text interface pre-processor. There are two approaches in setting up a problem: to follow the text menus systematically or to write a text file in which all commands are written in the proper order. In reality the text file method is the only practical way, however, this implies that all relevant commands and the order in which these are to be given to SOFIE have to be known by the user.

When setting up a case the location of the relevant databases has to be checked and if necessary specified. These databases contain information on material and species properties that are required in order to solve the problem.

The required type of solution is then specified. This includes options concerning radiation, combustion and combustion models, and turbulence and turbulence models. The DTRM is the default radiation model using either a constant absorption coefficient or a WSGG property model. However, a narrow-band model is under development. A heat source can be modelled by simply defining an enthalpy source, in $W \cdot m^{-3}$ where the local cell volume is used to calculate the actual heat source, or by using a combustion model. The combustion models available are the Eddy break-up model, which in fact is Magnussens extended Eddy Break-up model, better known as the Eddy Dissipation Concept of Magnussen, EDC, and the laminar flamelet combustion model. At this moment, the laminar flamelet model is restricted to include only some simple hydrocarbon fuels, such as methane and PMMA. However, more are to be expected in a near future. When combustion has been chosen, turbulence will

automatically follow; SOFIE has a standard k- ϵ turbulence model, the options connected to this is high- or low Re k- ϵ model and whether to include buoyancy correction terms or not. In the case of fire, the choice is not too difficult.

When the user has specified the desired type of solution methods that are to be used, the geometrical foundation is to be identified. This is done by defining a two or three-dimensional grid in space. At present, the most common way of doing this is to determine a length and the number of zones that this length should be divided into for each dimension. Making this choice for all directions, a grid containing a number of non-overlapping control volumes can be generated in the domain. In fact, SOFIE is capable of handling any general curvilinear grid but as the built-in grid generator is for Cartesian and cylindrical polar grids only, present use is confined to these types of grid.

The actual geometry that is to be simulated is constructed by applying different kinds of blockages on the control volumes. Blockages are used in order to create floor, ceiling and walls. Once applied, the control volumes in question are excluded from the fluid flow calculations. There are two kinds of blockages, known as “active” and “inactive”. If the active blockage is chosen this implies that the control volume will participate in the enthalpy equation, while an inactive blockage is taken out of all calculations. If the active blockages are used a building material has to be chosen in order to give SOFIE access to relevant data properties. The database used for this is an ordinary text-file and the user can easily contribute to this by defining his own material.

At this stage, the geometry of the simulation object has been specified however; nothing has been said about its environment. Thus, the next step is to define relevant boundary conditions. This is done by setting the type of conditions existing at the faces of relevant control volumes. The two major classes of boundary types are “thermal” and “fluid” boundaries. Under the umbrella of these a number of boundary types are defined. As the names imply the boundary types are intended to specify the environmental conditions such as the conditions for heat transfer but the boundary types also include the boundary between the domain and the computational “infinity” and determination of the fuel inlet. Assigning relevant boundary values completes the boundary types. The interested reader is further referred to the SOFIE manual /8/ for detailed information.

4.1.1 Special models under development

In agreement with the objective of SOFIE to include a range of fire specific features into the code, a number of research programmes have been launched to develop models on subjects such as fire growth and spread, toxic emission and dispersion, soot formation and two phase flow, such as water sprinkler fire interaction. In the present code both soot models and fire spread models are included. However, these should not be used other than for educational or laboratory purposes. In addition, further improvements of existing models are scheduled or ready to be implemented into the base code, this includes for example the turbulence and radiation models. To speed up the simulations, some measures have been scheduled for example a code written for parallel processors.

4.2 Solver

The simulation can be run in steady state or in (first order implicit) transient mode. Using the steady state mode the solution obtained will represent the appearance after what is effectively an infinite amount of time. When running a transient simulation the number of calculation steps per unit time are set by the user. The transient solution approach will of course use much more CPU time than will the steady state, but indeed, the use of steady state simulation may sometimes be questionable, particularly in cases of under-ventilation.

The base code includes several different optional solvers such as Line by line Gauss-Seidal, Bi-linear-, ILC-, IC pre-conditioned conjugate gradient solver (biccg, iluccg, iccg) and Stones strongly implicit procedure (sip3d).

The interpolation schemes available for relating the nodal value of the dependent variable to the cell face include upwind, hybrid, powerlaw, TVD, QUICK, UQUICK, SOUP and central. /8/

4.3 Output and post-processor possibilities

The present version of SOFIE (version 2.7.1 for PC, 2.4.3 for UNIX) has a simple text interface. Results from simulations can be printed in text form on the screen or be exported in different data formats to be viewed using other computer software. An easily available approach is to export a variable profile as a text file and use for example Microsoft Excel or similar to prepare the results. Another approach is to make use of some of the commercially available CFD visualisation packages. SOFIE is at present capable to export data in either plot3d, a format that is recognised by most available visualisation software, or fieldview format, a separate format for use in the commercially available Fieldview software package. Using these programs to present results from a simulation in a colourful manner has become an art performed by the members of the CFD community. However, it is an unfortunate fact that this procedure is somewhat time consuming.

5. Results from simulations

In this chapter, results from CFD simulations are compared with experimental measurements. The CFD code SOFIE, version 2.7.1 for Windows and version 2.4.3 for UNIX, has been used. It should be pointed out that this work is not a validation work but rather an investigation on the application of field modelling in fire safety engineering. The reader should feel free to make his (or hers) own conclusions from the material presented in this chapter.

Using a field model, the engineer is offered a vast number of parameters to evaluate and display. In this work the gas-temperature and species concentration (oxygen and carbon dioxide) are presented and compared with experimental results. Also, for the Cardington experiments, gas-velocity is presented and compared with experiments.

5.1 General remarks

As this work has been carried out for almost a year and a half it is indeed very remarkable that so few simulations has been successful such that the computational result has been physically relevant. Simulations have failed although the input files have been, seemingly, free of errors. In addition, it is not satisfactory that no explanation yet has been found.

A decisive factor in today's CFD modelling of fires is the lack of adequate computer power. In the later half of this work, the author used computer with one Pentium II 300 MHz processor. Using this computer to simulate the Cardington experiments required more than one month (four weeks) time to finish simulating an approximately 13 minutes long scenario. Of course, the actual time of a simulation depends upon the input given by the user, such as the lengths of time steps and number of control volumes in the scenario etc. However, it gives a hint on the time-factor involved in these kinds of simulations. The solution to this problem is solely to rely on future; faster processors and a SOFIE code rewritten to work using several processors.

It should also be pointed out that the two small-scale experiments were both somewhat under-ventilated. This may be decisive, as SOFIE has not yet been sufficiently validated against these kinds of fires.

5.2 The methane experiments

The simulations from the methane experiments involve experiment number 9, 10 and 11, which were performed under identical conditions. The purpose with making three identical experiments was to obtain measurements on gas concentration in different locations in the test room. The concentration of combustion gases was measured in three different locations, as illustrated in *Figure 5.1*. The door opening had the dimensions 0.085 meters in width and 0.42 meters in height. The methane gas-flow was set to 1.3 g/s.

5.2.1 Input fundamentals

These experimental series has been extensively simulated. In the following two scenarios will be presented. These are basically identical however, the first is based on steady state while the second is simulated in a transient mode. The input file for these simulations can be found in Appendix C.

Combustion was modelled using Magnussen's dissipation concept and the distribution of species concentration was accounted for using a simple HC combustion model. Also, radiative exchange was

taken account for by using the default discrete transfer radiation model. The calculation domain was divided into 61065 control volumes: 59, 45 and 23 in the x, y and z dimension respectively.

It was assumed that the thermal properties of the wall material would not remain throughout the experiments made (18 experiments were made during three days) and therefore thermocouples was used to measure the temperature behind the walls and the ceiling. In this way the thermal properties of wall and ceiling material, $k\rho c$, could be subsequently calculated and used in simulations. A simulation using original values on $k\rho c$, obtained from Rockwool, resulted in an overestimation of the gas-temperature with several hundred degrees. On the outer boundaries of the wall, a convective heat transfer coefficient was set to 10 J/mK. On the outer domain, static pressure boundaries were used.

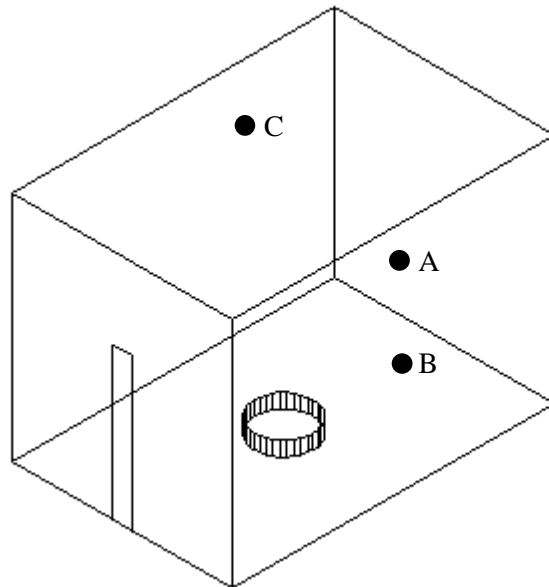


Figure 5.1 Three-dimensional illustration of the test room. The different locations of the probe are marked with a large dot.

5.2.2 Steady state mode

Only temperature can be presented here. The simulation was performed using SOFIE version 2.4.3 for UNIX. The SOFIE-curve presented is the “thermocouple temperature” curve from SOFIE and the Experiment-curve is taken as a mean over 60 seconds. The simulation required approximately 10 hours to reach this convergence using a Pentium processor 300MHz. As can be seen in *Figure 5.2* the agreement is rather good. However, it should be noticed that the simulation could not be reproduced using version 2.7.1 in Windows environment.

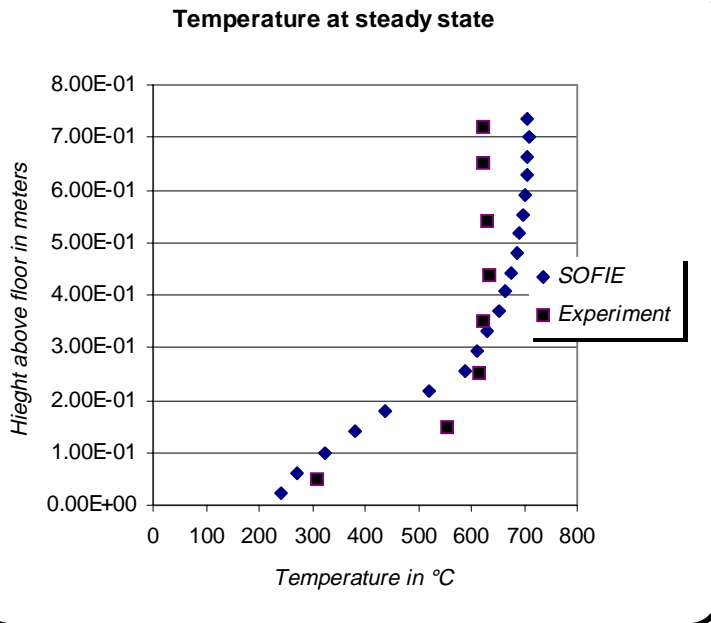


Figure 5.2 Temperature-Height profile at the end of the experiment, steady state mode was used in the simulation.

5.2.3 Transient mode

Nevertheless, using SOFIE version 2.7.1 in the Windows NT system, a transient solution was found. To obtain this solution a rather advanced “transient run”-scriptfile was added to the original scriptfile.

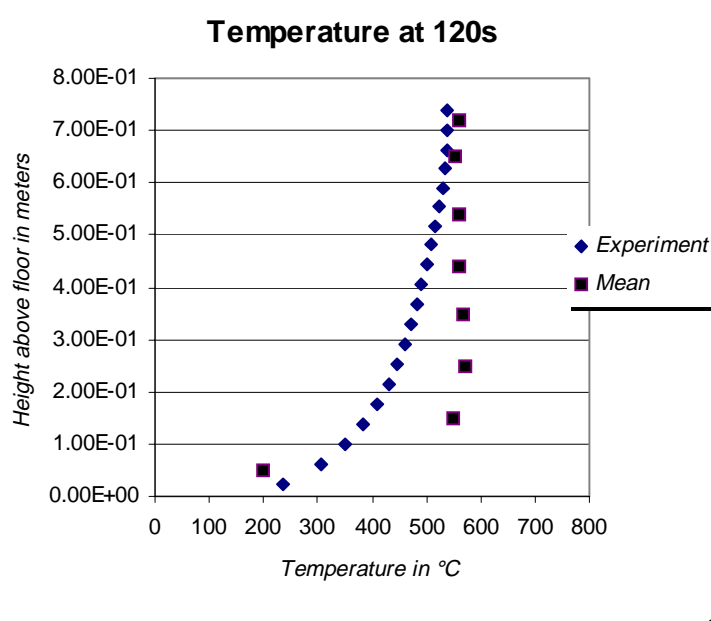


Figure 5.3 Temperature-Height profile at 120 seconds.

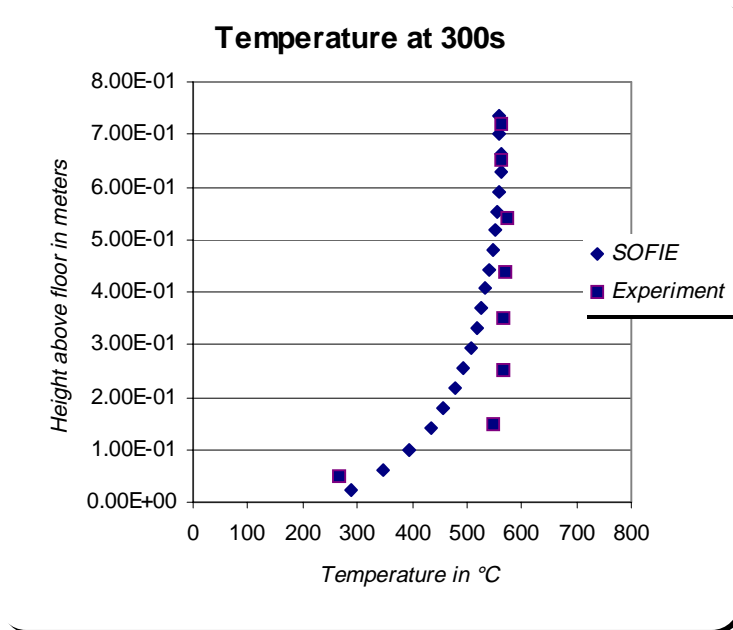


Figure 5.4 Temperature-Height profile after 300 seconds (5 minutes).

Comments on Figures 5.2-4.

Generally speaking, SOFIE have estimated the temperature in a satisfying way. The results are not exact, especially in the lower parts the error is perceptible. This is partly due to the radiative effects on the thermocouples which results in increased measuring errors.

Table 5.1 Comparison of oxygen concentration from experiment and CFD simulation.

Position	A		B		C	
	Experiment vol%	Simulation vol%	Experiment vol%	Simulation vol%	Experiment vol%	Simulation vol%
30 s	1.7	0.4	12.2	13.5	1.5	0.3
60 s	0.0	0.0	-	- ¹	0.1	0.0

¹ Value not available

Table 5.2 Comparison of concentration of carbon dioxide (CO₂) from experiment and CFD simulation.

Position	A		B		C	
	Experiment vol%	Simulation vol%	Experiment vol%	Simulation vol%	Experiment vol%	Simulation vol%
30 s	3.1	5.2	1.5	2.8	3.7	5.5
60 s	6.0	8.5	3.3	7.9	6.3	8.7
300 s	10.1	8.7	10.0	8.7	10.0	8.7

Comments on Tables 5.1-2.

As the gradients are very large in the beginnings of the experiments, it is very difficult to make accurate readings from the experimental results. The results presented above are basically within the margin of error. The experimental gas-concentrations presented above have not been evaluated theoretically in a physical point of view. The inertia factor in the measuring instruments was taken into account by adding the instruments “time of reaction”.

5.3 The heptane experiments

The experiment simulated in this work is heptane-experiment number 9. The ventilation area in this experiment was 0.07 meters in width and 0.52 meters in height. The rate of heat release peaked at approximately 40 kW.

5.3.1 Input fundamentals

The input file to this simulation was originally based on the one made for the methane experiments. However, of some curious reason this did not fall out that good and no convergence could be found that resulted in physically relevant values. The final scriptfile used is presented in its full length in Appendix D.

The Magnussen dissipation concept was used to simulate combustion and the radiation exchange is taken account for using the DTRM. The calculation domain was divided into 46000 control volumes: 50, 40 and 23 in the x, y and z dimension respectively. As the exact location of the probe was not known at the time when the results was displayed, no values of the presence of combustion gases is presented in this text.

The walls of the test room used were made of a thin stainless steal container inside a furnace of firebrick. In the simulation the steal container was neglected in terms of heat transfer, also as the firebrick is old and utilised enough to have experienced all possible phase transformation this had to be counted for when assigning thermal property values for the walls. A convective heat transfer coefficient of 10 J/mK was used on the outside of the walls. Static pressure boundaries were assigned on the outer domain boundaries.

5.3.2 Results from transient simulation

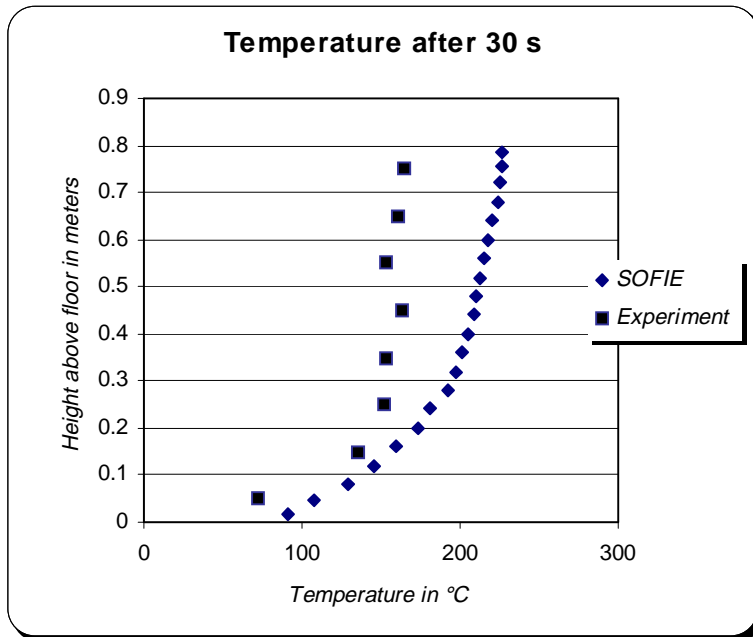


Figure 5.5 Temperature-Height profile after 30 seconds (0.5 minutes).

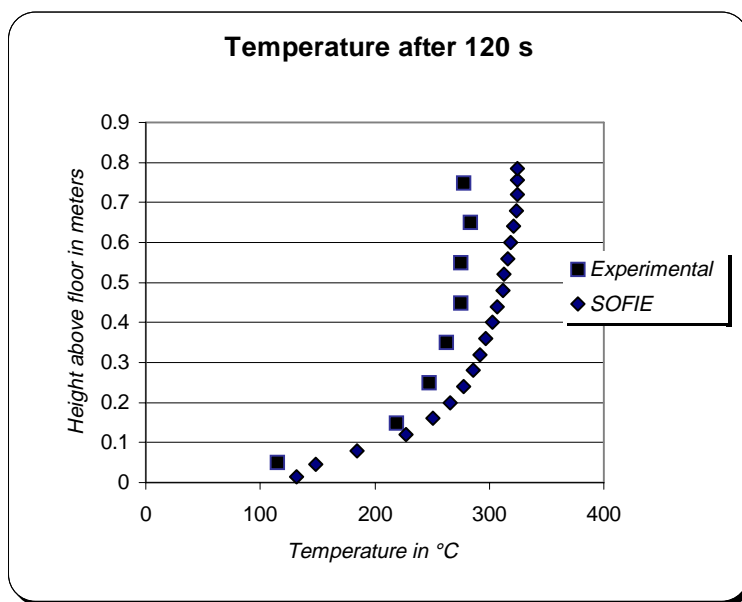


Figure 5.6 Temperature-Height profile after 120 seconds (2 minutes).

Comments on Figures 5.5-6.

Again, the temperature agreement is satisfying; the results are not exact nevertheless, the discrepancies are well within the margin of error.

5.4 The Cardington experiments

These experiments were all fuel controlled, in contradiction to the experiments simulated above. This may be one explanation to why SOFIE did not have any particular problems with the scenario simulated. The simulation made in this work is experiment number 11 and 12 in which the fire was located in the back corner of the atria and the rate of heat release was 4.8 MW.

5.4.1 Input fundamentals

The results presented in this work were archived using the scriptfile presented in Appendix E. The experiment was simulated using other input files giving approximately the same result. The problem associated with this simulation was the time needed for simulating a transient mode, which in turn was due to the large amount of control volumes used.

The computational domain was divided into 355300 control volumes, 76×55×85 in the x, y and z dimensions respectively. This corresponded to a cell side of approximately 0.30 meters which turned out to be something like a limit for what was possible to simulate on the computer used. The combustion process was modelled using Magnussen's eddy dissipation concept. The fuel, kerosene, was modelled as a simple hydrocarbon compound, $C_{12}H_{23}$. Radiative losses were accounted for by reducing the rate of heat release by 30 %. It should be pointed out that this affects the accuracy of the simulation for all parameters displayed below; gas-temperature, gas-velocity and species concentration.

Heat losses through walls were accounted for by assigning non-adiabatic concrete properties. The convective heat transfer coefficient was set to 8 J/mK on the outside of the walls. The boundaries on the outer domain were set as static pressure boundaries.

5.4.2 Results from transient simulation; 270 seconds

Location A (Internal opening)

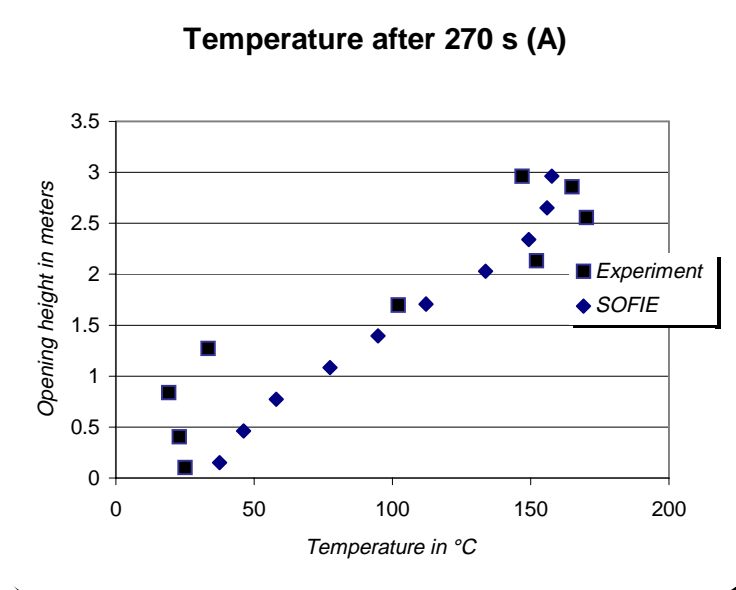


Figure 5.7 Temperature-Height profile at A-location after 270 seconds (4.5 minutes).

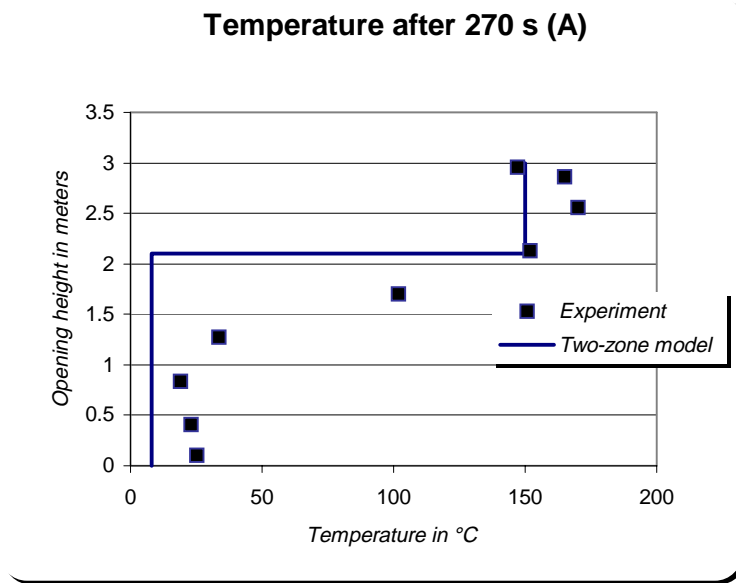


Figure 5.8 Temperature-Height profile at A-location after 270 seconds (4.5 minutes). Comparison between experimental and two-zone model results.

Location B (Internal opening)

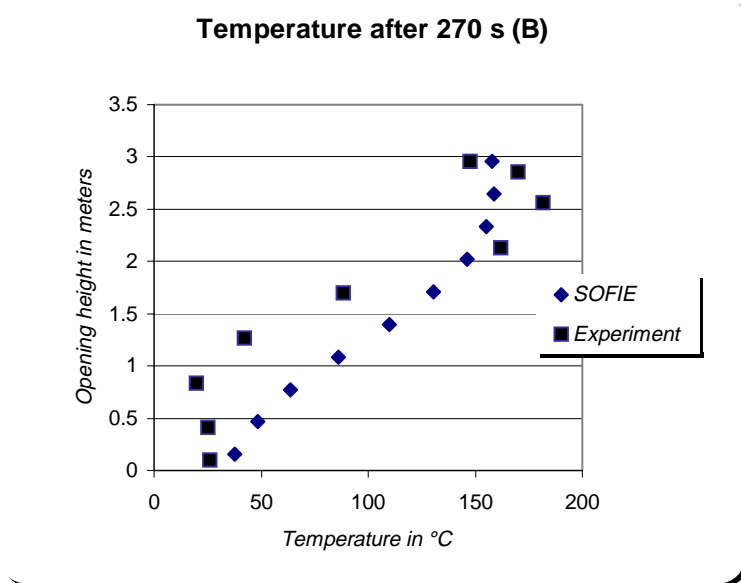


Figure 5.8 Temperature-Height profile at B-location after 270 seconds (4.5 minutes).

Location E (Internal opening)

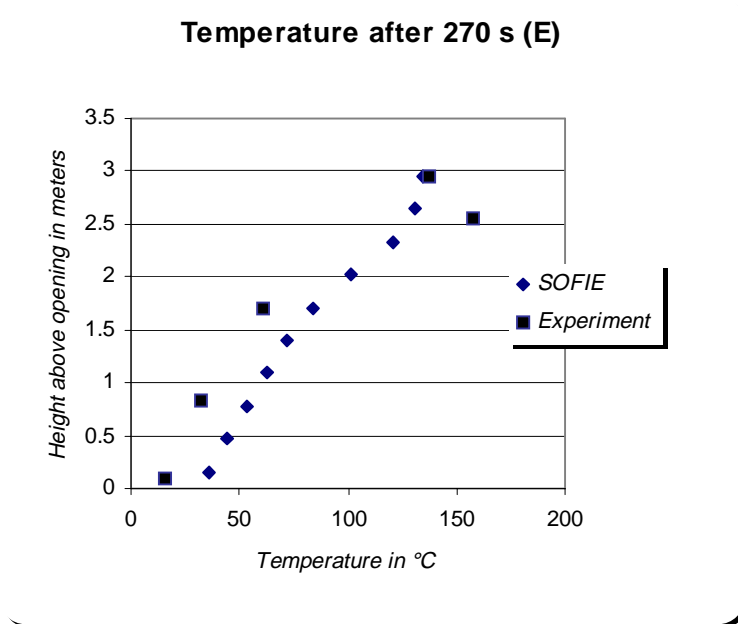


Figure 5.9 Temperature-Height profile at E-stack after 270 seconds (4.5 minutes).

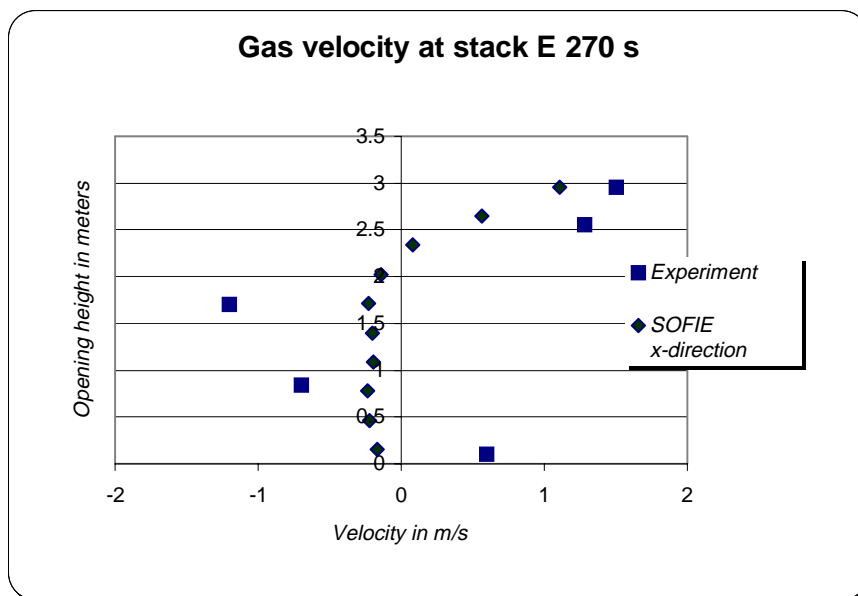


Figure 5.10 Velocity-Height profile at E-stack after 270 seconds (4.5 minutes). The SOFIE-values originates from velocity in the x-direction. This may not be entirely true and therefore a source of discrepancy. Notice that the neutral plane is very well estimated.

Location D (External opening)

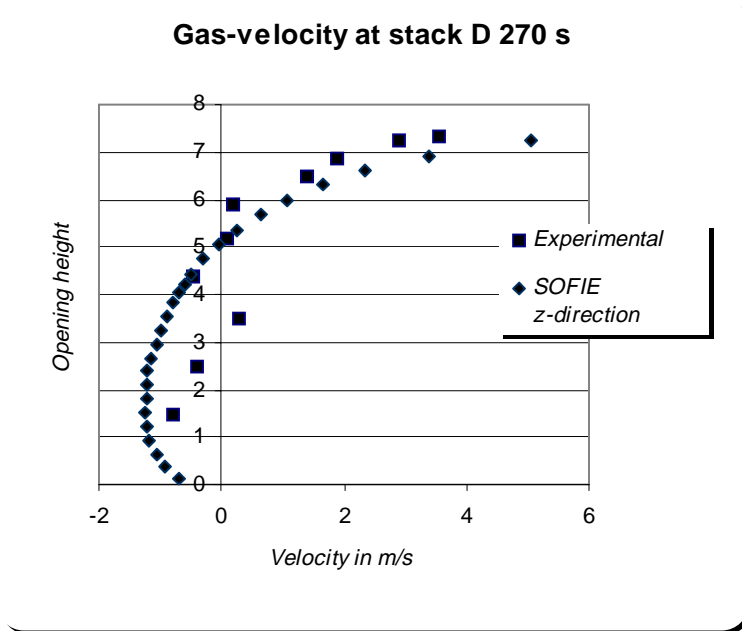


Figure 5.11 Velocity-Height profile at D-stack after 270 seconds (4.5 minutes). Again, note that the neutral plane are predicted correctly

5.4.3 Results from transient simulation; 750 seconds

Location A (Internal opening)

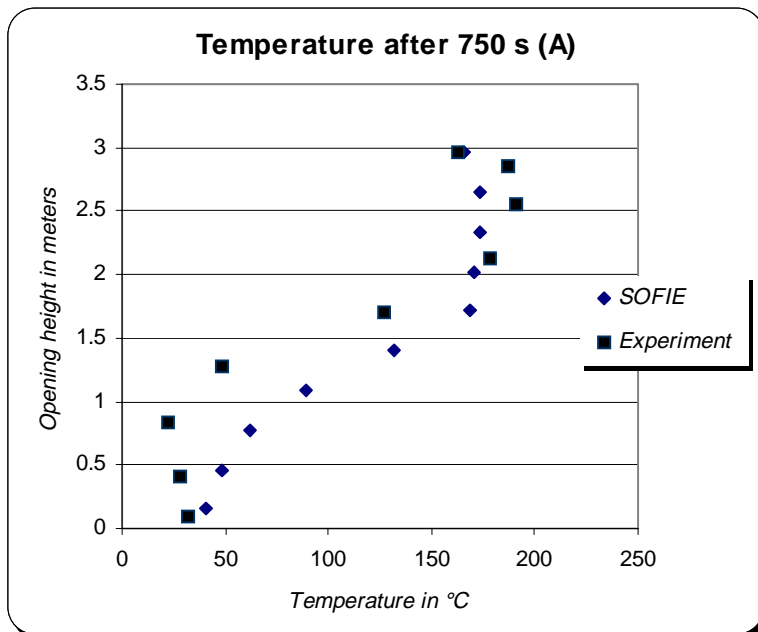


Figure 5.12 Temperature-Height profile at A-stack after 750 seconds (12.5 minutes).

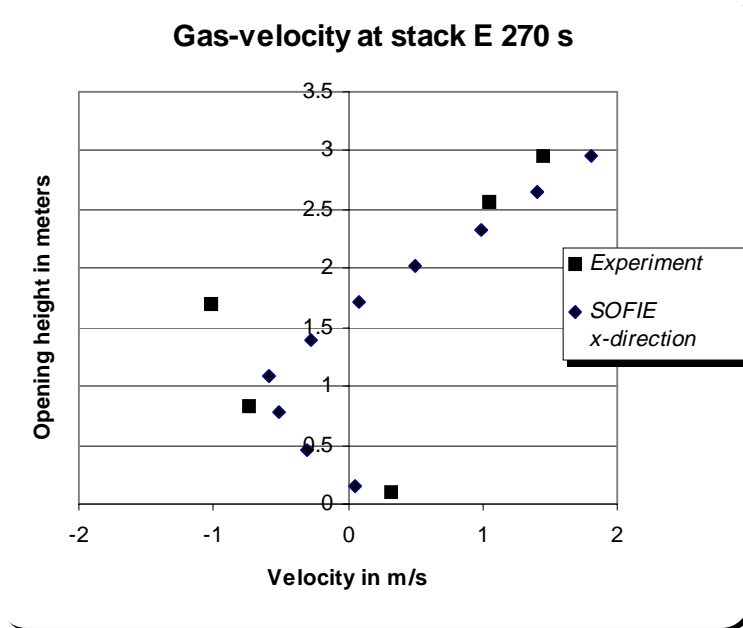


Figure 5.11 Velocity-Height profile at E-stack after 750 seconds (12.5 minutes).

References

- /1/ Edstam, Anders, Söderström, Peter, "Beräkningsmodeller för övertändning och förbränningsprodukter- en utvärdering", Brandingenjörslinjen, Lunds Tekniska Högskola, 1998.
- /2/ Andersson, Petra, Holmstedt, Göran, "CFD modelling applied to fire detection – Validation studies and influence of background heating", Department of Fire Safety Engineering, Lund University.
- /3/ Bengtsson, Lars-Göran, "Övertändning, backdraft och brandgasexplosion sett ur räddningstjänstens perspektiv", Räddningsverket, FOU rapport, Best. nr. P21-250/98, ISBN 91-88891-66-6, Karlstad, 1998.
- /4/ Andersson, Berit et al, "Combustion of chemical substances and impact of the environment of the fire products", Department of Fire Safety Engineering, Institute of Technology, Lund University, 1994.
- /5/ Bengtsson, Lars-Göran et al, "Experiment at the Cardington Large Building Test Facility", Brandforsk project no 746-961, SP Technical Notes 1997:15, Borås, 1997.
- /6/ Cardington experimental results FOA Cd-ROM.
- /7/ SOFIE homepage, www.cranfield.ac.uk/sme/sofie
- /8/ Rubini, P., "SOFIE- User guide", School of Mechanical Engineering, Cranfield University, England.

APPENDIX

Appendix A Method for calculating the rate of heat release

The rate of heat release was calculated using the oxygen consumption method. It has been argued that the significance of carbon monoxide and carbon dioxide formation can be safely ignored in this procedure. /1, 2/ The difference from using only the O_2 concentration in the calculation can be expected to be small, typically of a magnitude 1 to 5 %. Nevertheless, when calculating the RHR in these experiments, the measurements of O_2 together with CO and CO_2 concentrations have been used.

The key assumption when using the oxygen consumption method is that the heat release of a fuel per unit mass of oxygen that is consumed during combustion is constant. This assumption has been found true for a large number of organic materials, gases as well as liquid and solid organic fuels, with an average value of $13.1 \text{ MJ}\cdot\text{kg}^{-1}$ and an interval $\pm 5\%$. /4/ The influence from the combustion gases on the RHR calculation is due to depletion and additional combustion of the CO formed from combustion of the primary fuel.

The resulting equation for RHR calculation that was used in this study is presented below, Equation 1.1

$$\dot{Q} = \left[E\phi - (E_{CO} - E) \frac{1-\phi}{2} \frac{X_{CO}^{A^e}}{X_{O_2}^{A^e}} \right] \cdot \frac{\dot{m}_e}{1 + \phi(\alpha - 1)} \frac{M_{O_2}}{M_a} (1 - X_{H_2O}^a) X_{O_2}^{A^a} \quad (\text{Eq. 1.1})$$

where

E heat release per unit mass of oxygen consumed in the primary combustion, a constant value of 13.1 MJ/kg has been used,

E_{CO} heat release per unit mass of oxygen consumed in the secondary combustion of formed CO to CO_2 , a constant value of 17.6 MJ/kg has been used,

$X_{CO}^{A^e}$ measured mole fraction of carbon monoxide in the exhaust flow.

$X_{O_2}^{A^e}$ measured mole fraction of oxygen in the exhaust flow,

$X_{H_2O}^{A^a}$ actual mole fraction of water vapour in the combustion air,

$X_{O_2}^{A^a}$ actual mole fraction of oxygen in the combustion air,

M_{O_2} molecular weight of oxygen, 32 kg/kmole

M_a molecular weight of the combustion air, 29 kg/kmole

α volumetric expansion factor a constant value of 1.1 was used in the study.

The variable ϕ is the so-called oxygen depletion factor representing the fraction of incoming air that is fully depleted from oxygen. Using the mole fractions of O_2 , CO_2 and CO , it can be calculated from Equation 1.2.

$$\phi = \frac{X_{O_2}^{A^a} (1 - X_{CO_2}^{A^e} - X_{CO}^{A^e}) - X_{O_2}^{A^e} (1 - X_{CO_2}^{A^a})}{(1 - X_{O_2}^{A^e} - X_{CO_2}^{A^e} - X_{CO}^{A^e}) X_{O_2}^{A^a}} \quad (Eq. 1.2)$$

$X_{CO_2}^{A^e}$ measured mole fraction of carbon dioxide in the exhaust flow.

$X_{CO_2}^{A^a}$ actual mole fraction of carbon dioxide in the air (approximately 330 ppm),

The mass flow of gas in the exhaust duct is calculated from the sectional area of the duct, the pressure difference measured and the temperature of the flow in the duct using Equation 1.3 and 1.4. /3/

$$\dot{m}_e = \rho_e \dot{V}_e \quad (Eq. 1.3)$$

where

ρ_e is the density of the exhaust gases, and

$$\dot{V}_e = A \frac{k_1}{k_2} \frac{1}{\rho_{298}} \sqrt{\frac{2\Delta p T_0 \rho_0}{T_e}} \quad \text{volumetric gas flow in the duct} \quad (Eq. 1.4)$$

A the sectional area of the exhaust duct,

k_1 ratio of the average mass flow per unit area to the mass flow per unit area in the centre of the duct, a constant value of 0.9 was used in the study,

k_2 a calibration constant for the bi-directional pitot tube, a value 1.08 was used,

ρ_{298} the density of air at 298 degrees Kelvin,

Δp measured pressure difference in the exhaust duct,

T_0 ambient temperature,

ρ_0 density of air at ambient temperature, and

T_e gas temperature in the duct

References

- /1/ Drysdale, Dougal, "An introduction to fire dynamics", John Wiley & Sons Ltd, ISBN 0-471-90613-1, 1985.
- /2/ Janssens, Mark, "Calorimetry", SFPE Handbook of Fire Protection Engineering, Second Edition 1995.
- /3/ Andersson, Berit et al, "Combustion of chemical substances and impact of the environment of the fire products", Department of Fire Safety Engineering, Institute of Technology, Lund University, 1994.

Appendix B Methane simulation scriptfile

```

%*****
file
  options
    physical data path
    c:\sofie97n\sofie\database\data2.4
  end
  problem path
  c:\sofie97n\metan101
  end
%*****
%
%-----
setup
%-----
  solution type
%-----
  radiation
    combustion
      eddy breakup
        high-Re k-e
        options
          buoyancy corrections
        end
      end
    fuel type
    CH4
  end
end
%-----
% extra derived
% thermocouple temperature
% end
%-----
  solids
    add min-ull
    add concrete
  end
%-----
  buoyancy
%-----
  transient
  end
%=====
% Physical dimensions
%-----
@set walld 0.05 ;
@set floor 0.03 ;
%-----
% x direction
%-----
@set roomdx 1.1 ;
@set firedx 0.3 ;
@set ambientx 2.0 ;
%
@set roomdx1 0.4 ;
@set roomdx2 0.4 ;
%-----
% y direction

```



```

%-----
@set roomdy 0.75 ;
@set doordy 0.42 ;
@set ambienty 2.5 ;
@set firedy 0.15 ;
%
@set roomdym 0.33 ;      %roomdy doordy -
%-----
% z direction
%-----
@set roomdz 0.70 ;
@set firedz1 0.1075 ;      %must be checked before every new simulation
@set firedz2 0.1075 ;      %must be checked before every new simulation
@set doordz 0.085 ;      %must be checked before every new simulation
%
@set roomdz1 0.2 ; %must be checked before every new simulation
@set roomdz2 0.2 ; %must be checked before every new simulation
%-----
% Grid dimensions, number of regions
%-----
@set nwall 2 ;
@set nfloor 2 ;
%-----
% x direction
%-----
@set nroomdx1 10 ;
@set nroomdx2 10 ;
@set nfiredx 10 ;
@set nambientx 25 ;
%-----
% y direction
%-----
@set ndoordy 11 ;
@set nroomdym 9 ;
@set nambienty 30 ;
@set nfiredy 4 ;
%-----
% z direction
%-----
@set nroomdz1 5 ;
@set nfiredz1 3 ;
@set nfiredz2 3 ;
@set nroomdz2 5 ;
@set ndoordz 3 ;
%-----
% Region locations
%-----
% x direction
%-----
@set wall1xs = 2 ;
@set wall1xe = 1 nwall sum ;
@set firexs = 2 nwall nroomdx1 sum ;
@set firexe = 1 nwall nroomdx1 nfiredx sum ;
@set wall2xs = 2 nwall nroomdx1 nfiredx nroomdx2 sum ;
@set wall2xe = 1 nwall nroomdx1 nfiredx nroomdx2 nwall sum ;
%-----
% y direction
%-----
@set floors = 2 ;
@set floore = 1 nfloor sum ;
@set fireys = 2 nfloor nfiredy sum ;

```

```

@set burnerye = 1 nfloor nfiredy sum ;
@set doorys   = 2 nfloor sum ;
@set doorye   = 1 nfloor ndoordy sum ;
@set ceils    = 2 nfloor ndoordy nroomdym sum ;
@set ceile    = 1 nfloor ndoordy nroomdym nwall sum ;
%-----
% z direction
%-----
@set wall1zs  = 2 ;
@set wall1ze  = 1 nwall sum ;
@set firezs   = 2 nwall nroomdz1 sum ;
@set fireze   = 1 nwall nroomdz1 nfiredz1 ndoordz nfiredz2 sum ;
@set doorzs   = 2 nwall nroomdz1 nfiredz1 sum ;
@set doorze   = 1 nwall nroomdz1 nfiredz1 ndoordz sum ;
@set wall2zs  = 2 nwall nroomdz1 nfiredz1 ndoordz nfiredz2 nroomdz2 sum ;
@set wall2ze  = 1 nwall nroomdz1 nfiredz1 ndoordz nfiredz2 nroomdz2 nwall
sum ;
%=====
    generate grid
    cartesian
        x      0.0  6  [nwall]    [walld]    0.0 0.0
                [nroomdx1] [roomdx1]  0.0 0.0
                [nfiredx]  [firedx]   0.0 0.0
                [nroomdx2] [roomdx2]  0.0 0.0
                [nwall]    [walld]    0.0 0.0
                [nambientx] [ambientx] 1.0 1.15
        y      0.0  5  [nfloor]   [floor]    0.0 0.0
                [ndoordy]  [doordy]   0.0 0.0
                [nroomdym] [roomdym]  0.0 0.0
                [nwall]    [walld]    0.0 0.0
                [nambienty] [ambienty] 1.0 1.15
        z      0.0  7  [nwall]    [walld]    0.0 0.0
                [nroomdz1] [roomdz1]  0.0 0.0
                [nfiredz1] [firedz1]  0.0 0.0
                [ndoordz]  [doorz]    0.0 0.0
                [nfiredz2] [firedz2]  0.0 0.0
                [nroomdz2] [roomdz2]  0.0 0.0
                [nwall]    [walld]    0.0 0.0
    generate
    end
end
end
%-----
assign blockages
%-----
solid type
concrete
%-----
active   i    f+1      [wall2xe]
         j    [floors]  [floore]
         k    f+1      l-1      ok  %Floor
%-----
solid type
min-ull
%-----
inactive i    [firexs --] [firexe ++]
         j    f+1      [burnerye]
         k    [firezs --] [fireze ++]      ok
% active  i    [wall2xe --] [wall2xe]
%         j    [ceile ++]  l-1
%         k    f+1      l-1      ok
active   i    [wall1xs] [wall1xe]

```

```

        j    f+1      [ceile]
        k    f+1      l-1      ok
    active  i    [wall2xs] [wall2xe]
        j    f+1      [ceile]
        k    f+1      l-1      ok
    active  i    f+1      [wall2xe]
        j    f+1      [ceile]
        k    [wall1zs] [wall1ze]      ok
    active  i    f+1      [wall2xe]
        j    f+1      [ceile]
        k    [wall2zs] [wall2ze]      ok
    active  i    f+1      [wall2xe]
        j    [ceils]   [ceile]
        k    f+1      l-1      ok
    delete i    [wall2xs] [wall2xe]
        j    [doorys]  [doorye]
        k    [doorzs]  [doorze]      ok      %Door opening
    end
%-----
% boundary types
%-----
fluid    inflow    south    i    [firexs] [firexe]
        j    [fireys] [fireys]
        k    [firezs] [fireze]      ok
fluid    staticp   north    i    f l-4
        j    l-1      l-1
        k    f+1      l-1      ok
fluid    staticp   east     i    l-1      l-1
        j    f+1      l-1
        k    f+1      l-1      ok
thermal  htcoef    west     i    [wall1xs] [wall1xs]
        j    f+1      [ceile]
        k    f+1      l-1      ok
thermal  htcoef    bottom   i    f+1      [wall2xe]
        j    f+1      [ceile]
        k    [wall1zs] [wall1zs] ok
thermal  htcoef    top      i    f+1      [wall2xe]
        j    f+1      [ceile]
        k    [wall2ze] [wall2ze] ok
thermal  htcoef    south    i    f+1      [wall2xe]
        j    [floors] [floors]
        k    f+1      l-1      ok
%thermal htcoef    north    i    f+1      [wall2xe]
%
%        j    [ceile] [ceile]
%        k    f+1      l-1      ok
%thermal htcoef    north    i    [wall2xe --] [wall2xe]
%
%        j    l-1      l-1
%        k    f        l        ok
end
%-----
% boundary values
%-----
% Fire
%-----
    v_f    south    i    [firexs] [firexe]
        j    [fireys] [fireys]
        k    [firezs] [fireze]      ok      0.005
    t_f    south    ok      293
    tke_f  south    ok      1e-5
    ted_f  south    ok      1e-6
    mfrac_f south    ok      1.0

```

```

mfuel_f south ok 1.0
%-----
% static pressure
%-----
t_f east i l-1 l-1
j f+1 l-1
k f+1 l-1 ok 293
tke_f east ok 1.0
ted_f east ok 0.1
t_f north i f l-4
j l-1 l-1
k f+1 l-1 ok 293
tke_f north ok 1.0
ted_f north ok 0.1
%-----
% emissivity
%-----
eps_f all_faces all ok 0.90
%-----
% external heat transfer
%-----
htcoef_f west i [wall1xs] [wall1xs]
j f+1 [ceile]
k f+1 l-1 ok 10.0
htcoef_f bottom i f+1 [wall2xe]
j f+1 [ceile]
k [wall1zs] [wall1zs] ok 10.0
htcoef_f top i f+1 [wall2xe]
j f+1 [ceile]
k [wall2ze] [wall2ze] ok 10.0
htcoef_f south i f+1 [wall2xe]
j [floors] [floors]
k f+1 l-1 ok 10.0
htcoef_f north i f+1 [wall2xe]
j [ceile] [ceile]
k f+1 l-1 ok 10.0
% htcoef_f north i [wall2xe --] [wall2xe]
% j l-1 l-1
% k f 1 ok 10.0
end
%-----
interior values
%-----
solution u fluid range f+1 l-1 f [ceils --] f+1 l-1 ok 0.01
solution v fluid range f+1 l-1 f+1 [ceils --] f+1 l-1 ok 0.01
solution v fluid range [firexs] [firexe] [fireys] [ceils --] [firezs]
[fireze] ok 0.5
solution tke fluid range f+1 37 f+1 [ceils --] f+1 l-1 ok 1e-3
solution ted fluid range f+1 37 f+1 [ceils --] f+1 l-1 ok 1e-2
derived t fluid range f+1 37 f+1 [ceils --] f+1 l-1 ok 500
end
%-----
control
%-----
solved variables
relax
u 0.3
v 0.3
w 0.3
enth 1.0
mfuel 0.5

```

```
        mfrac 0.5
    end
%-----
    solver
    enth
        sip3d
    end
%-----
    cycle
        enth 10
    end
end
%-----
    derived variables
        relax
            p 0.5
            rho 0.5
            t 1.0
        end
    end
%-----
    solver control
%-----
        pressure correction solver sip3d
        pressure correction cycles 30
        minimum residual 1e-2
        minimum timestep iterations 50
    end
%-----
    physical models
%-----
    % ambient temp 293
    % reference temp 273.15
    end
end
%-----
end
%-----
```

Appendix C Heptane simulation scriptfile

```

%*****
file
  options
    physical data path
    c:\sofie97n\sofie\database\data2.4
  end
  %problem path
  % c:\sofie97n\heptan91
  end
%*****
%
%-----
setup
%-----
  solution type
%-----
  radiation
    combustion
      eddy breakup
      high-Re k-e
      options
        buoyancy corrections
      end
    end
    fuel type
    C7H16
  end
end
%-----
  solids
  add Fireclay_brick
  end
%-----
  buoyancy
%-----
  transient
  end
%=====
% Physical dimensions
%-----
@set walld 0.1 ;
@set ceild 0.15 ;
%-----
% x direction
%-----
@set roomdx 1.1 ;
@set firedx 0.177 ;
@set ambientx 2.0 ;
%
@set roomdx1 0.4615 ;
@set roomdx2 0.4615 ;
%-----
% y direction
%-----
@set roomdy 0.8 ;
@set doordy 0.52 ;
@set ambiency 2.0 ;
%

```

```

@set roomdym 0.28 ; %roomdy doordy - ;
%-----
% z direction
%-----
@set roomdz 0.75 ;
@set firedz1 0.0535 ;
@set firedz2 0.0535 ;
@set doordz 0.07 ;
%
@set roomdz1 0.2865 ;
@set roomdz2 0.2865 ;
%-----
% Grid dimensions, number of regions
%-----
@set nwall 2 ;
%-----
% x direction
%-----
@set nroomdx1 10 ;
@set nroomdx2 10 ;
@set nfiredx 6 ;
@set nambientx 20 ;
%-----
% y direction
%-----
@set ndoordy 13 ;
@set nroomdym 7 ;
@set nceil 3 ;
@set nambienty 15 ;
%-----
% z direction
%-----
@set nroomdz1 6 ;
@set nfiredz1 2 ;
@set nfiredz2 2 ;
@set nroomdz2 6 ;
@set ndoordz 3 ;
%-----
% Region locations
%-----
% x direction
%-----
@set wall1xs = 2 ;
@set wall1xe = 1 nwall sum ;
@set firexs = 2 nwall nroomdx1 sum ;
@set firexe = 1 nwall nroomdx1 nfiredx sum ;
@set wall2xs = 2 nwall nroomdx1 nfiredx nroomdx2 sum ;
@set wall2xe = 1 nwall nroomdx1 nfiredx nroomdx2 nwall sum ;
%-----
% y direction
%-----
@set floors = 2 ;
@set floore = 1 nwall sum ;
@set firey = 2 nwall sum ;
@set doorys = 2 nwall sum ;
@set doorye = 1 nwall ndoordy sum ;
@set ceils = 2 nwall ndoordy nroomdym sum ;
@set ceile = 1 nwall ndoordy nroomdym nceil sum ;
%-----
% z direction
%-----

```

```

@set wall1zs = 2 ;
@set wall1ze = 1 nwall sum ;
@set firezs = 2 nwall nroomdz1 sum ;
@set fireze = 1 nwall nroomdz1 nfiredz1 ndoordz nfiredz2 sum ;
@set doorzs = 2 nwall nroomdz1 nfiredz1 sum ;
@set doorze = 1 nwall nroomdz1 nfiredz1 ndoordz sum ;
@set wall2zs = 2 nwall nroomdz1 nfiredz1 ndoordz nfiredz2 nroomdz2 sum ;
@set wall2ze = 1 nwall nroomdz1 nfiredz1 ndoordz nfiredz2 nroomdz2 nwall
sum ;
%=====
generate grid
cartesian
  x      0.0  6  [nwall]    [walld]    0.0 0.0
          [nroomdx1] [roomdx1] 0.0 0.0
          [nfiredx]  [firedx]  0.0 0.0
          [nroomdx2] [roomdx2] 0.0 0.0
          [nwall]    [walld]    0.0 0.0
          [nambientx] [ambientx] 1.0 1.15
  y      0.0  5  [nwall]    [walld]    0.0 0.0
          [ndoordy]  [doordy]  0.0 0.0
          [nroomdym] [roomdym] 0.0 0.0
          [nceil]    [ceild]    0.0 0.0
          [nambienty] [ambienty] 1.0 1.15
  z      0.0  7  [nwall]    [walld]    0.0 0.0
          [nroomdz1] [roomdz1] 0.0 0.0
          [nfiredz1] [firedz1] 0.0 0.0
          [ndoordz]  [doordz]  0.0 0.0
          [nfiredz2] [firedz2] 0.0 0.0
          [nroomdz2] [roomdz2] 0.0 0.0
          [nwall]    [walld]    0.0 0.0

generate
end
end
%-----
assign blockages
%-----
solid type
  Fireclay_brick
%-----
active  i  f  [wall2xe]
        j  [floors] [floore]
        k  f  l  ok
inactive i  [firexs --] [firexe ++]
        j  [floors] [floore]
        k  [firezs --] [fireze ++] ok
% inactive i  f  [wall2xe]
%          j  [ceile ++] l
%          k  f  l  ok
active  i  [wall1xs] [wall1xe]
        j  f  [ceile]
        k  f  l  ok
active  i  [wall2xs] [wall2xe]
        j  f  [ceile]
        k  f  l  ok
active  i  f  [wall2xe]
        j  f  [ceile]
        k  [wall1zs] [wall1ze] ok
active  i  f  [wall2xe]
        j  f  [ceile]
        k  [wall2zs] [wall2ze] ok
active  i  f  [wall2xe]

```



```

        j    [ceils]    [ceile]
        k    f          l      ok
delete   i    [wall2xs] [wall2xe]
        j    [doorys]  [doorye]
        k    [doorzs]  [doorze]    ok    %Door opening
end
%-----
boundary types
%-----
fluid    inflow    south    i    [firexs] [firexe]
        j    [firey] [firey]
        k    [firezs] [fireze]    ok
fluid    staticp   north    i    f 1-3
        j    l-1      l-1
        k    f        l-1      ok
fluid    staticp   east     i    l-1      l-1
        j    f        l-3
        k    f        l        ok
thermal  htcoef    west     i    [wall1xs] [wall1xs]
        j    f        [ceile]
        k    f        l        ok
thermal  htcoef    bottom   i    f        [wall2xe]
        j    f        [ceile]
        k    [wall1zs] [wall1zs] ok
thermal  htcoef    top      i    f        [wall2xe]
        j    f        [ceile]
        k    [wall2ze] [wall2ze] ok
thermal  htcoef    south    i    f        [wall2xe]
        j    [floors] [floore]
        k    f        l        ok
%thermal htcoef    north    i    f        [wall2xe]
%        j    [ceile] [ceile]
%        k    f        l        ok
end
%-----
boundary values
%-----
% Fire
%-----
v_f      south    i    [firexs] [firexe]
        j    [firey] [firey]
        k    [firezs] [fireze]    ok    0.001
t_f      south    ok    371    %kokp C7H16
tke_f    south    ok    1e-5
ted_f    south    ok    1e-6
mfrac_f  south    ok    1.0
mfuel_f  south    ok    1.0
%-----
% static pressure
%-----
t_f      east     i    l-1    l-3
        j    f      l-1
        k    f      l        ok    298.15
tke_f    east     ok    1.0
ted_f    east     ok    0.1
t_f      north    i    f      l
        j    l-1    l-3
        k    f      l-1      ok    298.15
tke_f    north    ok    1.0
ted_f    north    ok    0.1
%-----

```

```

% emissivity
%-----
eps_f    all_faces    all                ok  0.90
%-----
% external heat transfer
%-----
htcoef_f west        i  [wall1xs] [wall1xs]
           j  f      [ceile]
           k  f      l      ok 10.0
htcoef_f bottom     i  f      [wall2xe]
           j  f      [ceile]
           k  [wall1zs] [wall1zs] ok 10.0
htcoef_f top        i  f      [wall2xe]
           j  f      [ceile]
           k  [wall2ze] [wall2ze] ok 10.0
htcoef_f south      i  f      [wall2xe]
           j  [floors] [floore]
           k  f      l      ok 10.0
%htcoef_f north     i  f      [wall2xe]
%                   j  [ceile] [ceile]
%                   k  f      l      ok 10.0
end
%-----
interior values
%-----
solution  u  fluid    interior  ok  0.01
solution  v  fluid    interior  ok  0.01
solution  w  fluid    interior  ok  0.01
%solution tke fluid    interior  ok  1e-3
%solution ted fluid    interior  ok  1e-2
%derived  t  fluid    interior  ok  450
end
%-----
control
%-----
solved variables
  relax
  u 0.3
  v 0.3
  w 0.3
  enth 1.0
  mfuel 0.7
  mfrac 0.7
end
%-----
cycle
  enth 10
end
end
%-----
derived variables
  relax
  p 0.5
  rho 0.5
end
end
%-----
solver control
%-----
pressure correction solver sip3d
pressure correction cycles 30

```

```
        minimum residual 1e-2
        minimum timestep iterations 50
    end
%-----
    physical models
%-----
        % ambient temp 293
        end
    end
%-----
end
%-----
```

Appendix D Cardington simulation scriptfile

```

%*****
file
  options
    phys data path
      c:\sofie97n\sofie\database\data2.4
    end
  end
%*****
%
%-----
setup
%-----
  solution type
%-----
  % radiation
    combustion
      eddy breakup
        high-Re k-e
          options
            buoyancy corrections
          end
        end
      fuel type
        C12H23
      end
    %end
species
HC combustion
flamesheet
end
%-----
  solids
    add concrete_sl
  end
%-----
  buoyancy
  transient
  %extra derived
  % therm temp
  %end
%-----
  transient
  end
%=====
%=====
% Physical dimensions
%-----
@set walld 0.3 ;
%-----
% x direction
%-----
@set roomdx1 13.3 ;
@set atriadx 8.78 ;
@set firedx 1.5 ;
%
@set atriadx1 6.63 ;
@set atriadx2 0.75 ;
%-----

```

```

% y direction
%-----
@set atria      8.39 ;
@set exopen    7.39 ; %opening atria-ambient
@set upperwy   1.0  ; %top atria between int. and ext. openings
@set burnery   0.5  ; %height, burner body
@set floor0    3.47 ; %ground floor minus burner height corr for cardlr
@set floor1    4.12 ; %first floor
@set inopeny   3.12 ; %opening atria-floor1
@set ambienty 12.0  ; %ambient atmosphere in y dir
%-----
% z direction
%-----
@set roomdz1   10.1 ;
@set opside    3.2  ; %side of opening atria-floor1 JFR bild; verkar mkt
@set opendz    7.33 ; %opening atria-floor1
@set ambientz 10.0  ; %ambient atmosphere in z dir
%-----
% Grid dimensions, number of regions
%-----
@set nwall 2 ;
%-----
% x direction
%-----
@set nroomdx1  40 ;
@set natriadx1 22 ;
@set natriadx2 3  ;
@set nfiredx   5  ;
%-----
% y direction
%-----
@set nburnery  2 ;
@set nfloor0   12 ;
@set ninopeny  10 ;
@set nupperwy  3 ;
@set nambienty 18 ;
%-----
% z direction
%-----
@set nroomdz1  30 ;
@set nopside   10 ;
@set nopendz   24 ;
@set nambientz 15 ;
%-----
% Region locations
%-----
% x direction
%-----
@set wallx1s   = 2 ;
@set wallx1e   = 1 nwall sum ;
@set inopenxs  = 2 nwall nroomdx1 sum ;
@set inopenxe  = 1 nwall nroomdx1 nwall sum ;
@set exopenxs  = 2 nwall nroomdx1 nwall sum ;
@set exopenxe  = 1 nwall nroomdx1 nwall natriadx1 nfiredx natriadx2 sum ;
@set burnerxs  = 2 nwall nroomdx1 nwall natriadx1 sum ;
@set burnerxe  = 1 nwall nroomdx1 nwall natriadx1 nfiredx sum ;
@set wallx3s   = 2 nwall nroomdx1 nwall natriadx1 nfiredx natriadx2 sum ;
@set wallx3e   = 1 nwall nroomdx1 nwall natriadx1 nfiredx natriadx2 nwall
sum ;
%-----
% y direction

```

```

%-----
@set flooras = 2 ;
@set floorae = 1 nwall sum ;
@set floor0s = 2 nwall sum ;
@set floor0e = 1 nwall nburnery nfloor0 nwall sum ;
@set floor = 2 nwall nburnery nfloor0 sum ;
@set burnerys = 2 ;
@set burnerye = 1 nwall nburnery sum ;
@set fireys = 2 nwall nburnery sum ;
@set inopenys = 2 nwall nburnery nfloor0 nwall sum ;
@set inopenye = 1 nwall nburnery nfloor0 nwall ninopeny sum ;
@set exopenys = 2 nwall sum ;
@set exopenye = 1 nwall nburnery nfloor0 nwall ninopeny sum ;
@set ceils = 2 nwall nburnery nfloor0 nwall ninopeny nupperwy sum ;
@set ceile = 1 nwall nburnery nfloor0 nwall ninopeny nupperwy nwall sum ;
;
%-----
% z direction
%-----
@set wallz1s = 2 ;
@set wallz1e = 1 nwall sum ;
@set wallz2s = 2 nwall nroomdz1 sum ;
@set wallz2e = 1 nwall nroomdz1 nwall sum ;
@set atriass = 2 nwall nroomdz1 nwall sum ;
@set atriase = 1 nwall nroomdz1 nwall nopside nopendz nwall sum ;
@set burnerzs = 2 nwall nroomdz1 nwall 2 sum ;
@set burnerze = 1 nwall nroomdz1 nwall 7 sum ;
@set opsides = 2 nwall nroomdz1 nwall sum ;
@set opsidae = 1 nwall nroomdz1 nwall nopside sum ;
@set inopenzs = 2 nwall nroomdz1 nwall nopside sum ;
@set inopenze = 1 nwall nroomdz1 nwall nopside nopendz sum ;
@set wallz3s = 2 nwall nroomdz1 nwall nopside nopendz sum ;
@set soffitzs = 2 nwall nroomdz1 nwall nopside nopendz sum ;
@set soffitze = 1 nwall nroomdz1 nwall nopside nopendz nwall sum ;
%=====
generate grid
cartesian
x      0.0  7  [nwall]      [walld]      0.0 0.0
          [nroomdx1]    [roomdx1]    0.0 0.0
          [nwall]      [walld]      0.0 0.0
          [natriadx1]   [atriadx1]   0.0 0.0
          [nfiredx]    [firedx]    0.0 0.0
          [natriadx2]   [atriadx2]   0.0 0.0
          [nwall]      [walld]      0.0 0.0
y      0.0  8  [nwall]      [walld]      0.0 0.0
          [nburnery]   [burnery]    0.0 0.0
          [nfloor0]    [floor0]     0.0 0.0
          [nwall]      [walld]      0.0 0.0
          [ninopeny]   [inopendy]   0.0 0.0
          [nupperwy]   [upperwy]    0.0 0.0
          [nwall]      [walld]      0.0 0.0
          [nambienty]  [ambienty]   1.0 1.15
z      0.0  7  [nwall]      [walld]      0.0 0.0
          [nroomdz1]   [roomdz1]    0.0 0.0
          [nwall]      [walld]      0.0 0.0
          [nopside]    [opside]     0.0 0.0
          [nopendz]    [opendz]     0.0 0.0
          [nwall]      [walld]      0.0 0.0
          [nambientz]  [ambientz]   1.0 1.15
generate
end

```

```

end
%-----
assign blockages
%-----
solid type
concrete_sl
%-----
active i [inopenxe ++] [wallx3s --]
      j [flooras] [floorae]
      k [atriazs] [atriaze] ok %floor in atria
active i [wallx1s] [wallx1e]
      j [floor0e] [ceile]
      k f [wallz3s] ok %east wall in comp
inactive i f [inopenxe]
      j f [floor --]
      k f [atriaze] ok %ground floor
active i f+1 [inopenxe]
      j [floor] [floor0e]
      k f+1 [atriaze] ok %floor in comp
inactive i f+1 [inopenxe]
      j f l
      k [inopenze ++] l ok %atm in front (z)
active i f+1 [inopenxe]
      j [floor0e] [ceile]
      k [wallz3s] [soffitze] ok %top wall in comp
inactive i f l
      j [ceile ++] l
      k f [atriaze] ok %space above building
active i f l
      j [ceil] [ceile]
      k f [atriaze] ok %ceiling
inactive i [inopenxs] l
      j f [ceil]
      k f [atriazs --] ok %control room
active i [inopenxs] [inopenxe]
      j [floor0e] [ceile]
      k f [atriazs] ok %west wall in comp
active i [inopenxe ++] l
      j f [ceile]
      k [wallz2s] [wallz2e] ok %bottom atria wall
active i [inopenxe ++] l-1
      j f [ceil]
      k [soffitzs] [soffitze] ok %soffit ext opening
delete i [inopenxe ++] [wallx3s --]
      j [exopenys] [exopenye]
      k [soffitzs] [soffitze] ok %external opening
active i [inopenxs] [inopenxe]
      j [inopenys] [ceil]
      k [atriazs] [wallz3s] ok %soffit int opening
delete i [inopenxs] [inopenxe]
      j [inopenys] [inopenye]
      k [inopenzs] [inopenze] ok %internal opening
inactive i [burnerxs] [burnerxe]
      j [burnerys] [burnerye]
      k [burnerzs] [burnerze] ok %burner body
active i [wallx3s] [wallx3e]
      j [floorae] [ceile]
      k [atriazs] [soffitze] ok %west wall atria
active i f [inopenxs]
      j [floor0e] [ceile]
      k [wallz1s] [wallz1e] ok %bottom wall comp

```

```

    active i [inopenxs] [inopenxe]
           j [floorae] [floor0e]
           k [atriazs] [soffitze] ok %east wall atria
end
%-----
boundary types
%-----
fluid inflow south i [burnerxs] [burnerxe]
           j [fireys] [fireys]
           k [burnerzs] [burnerze] ok
%-----
fluid staticp top i [exopenxs] [exopenxe]
           j f+5 1-5
           k 1-1 1-1 ok
fluid staticp north i [exopenxs] [exopenxe]
           j 1-1 1-1
           k [atriaze ++] 1-8 ok
%-----
thermal htcoef south i [inopenxe ++] [wallx3s --]
           j [flooras] [flooras]
           k [atriazs] [atriaze] ok %floor in
atria
thermal htcoef west i [wallx1s] [wallx1s]
           j [floor0e] [ceile]
           k f [wallz3s] ok %west wall
in comp
thermal htcoef south i f+1 [inopenxe]
           j [floor] [floor]
           k f+1 [atriaze] ok %floor in
comp
thermal htcoef top i f+1 [inopenxe]
           j f [ceile]
           k [soffitze] [soffitze] ok %top wall
in comp
thermal htcoef north i f 1
           j [ceile] [ceile]
           k f [atriaze] ok %ceiling
thermal htcoef east i [inopenxe] [inopenxe]
           j [floor0e] [ceile]
           k f [atriazs] ok %east wall
in comp
thermal htcoef bottom i [inopenxe ++] 1
           j f [ceile]
           k [wallz2s] [wallz2s] ok %bottom
atria wall
% thermal htcoef top i [inopenxe ++] 1-1
% j f [ceils]
% k [soffitzs] [soffitze] ok %soffit
ext opening
% thermal htcoef i [inopenxs] [inopenxe]
% j [inopenys] [ceils]
% k [atriazs] [wallz3s] ok %soffit
int opening
thermal htcoef west i [wallx3e] [wallx3e]
           j [floorae] [ceile]
           k [atriazs] [soffitze] ok %west
wall atria
thermal htcoef bottom i f [inopenxs]
           j [floor0e] [ceile]
           k [wallz1s] [wallz1s] ok %bottom
wall comp

```



```

thermal   htcoef   west      i   [inopenxs]   [inopenxs]
                                                j   [floorae]   [floor0e]
                                                k   [atriazs]   [soffitze]   ok   %west wall
atria
end
%-----
% boundary values
%-----
% Fire
%-----
v_f       south    i   [burnerxs]   [burnerxe]
                                                j   [fireys]   [fireys]
                                                k   [burnerzs]   [burnerze]   ok   0.001 %0.00917
t_f       south    ok   543 %kokpkt!
tke_f     south    ok   1e-4
ted_f     south    ok   1e-2 %exp=0.5exp tke
mfrac_f   south    ok   1.0
mfuel_f   south    ok   1.0
%-----
% static pressure
%-----
t_f       top      i   [exopenxs]   [exopenxe]
                                                j   f+5        1-5
                                                k   1-1        1-1           ok   280
tke_f     top      ok   1.0
ted_f     top      ok   0.1
t_f       north   i   [exopenxs]   [exopenxe]
                                                j   1-1        1-1
                                                k   [atriaze ++] 1-8           ok   280
tke_f     north   ok   1.0
ted_f     north   ok   0.1
% end
%-----
% emissivity
%-----
% eps_f   all_faces   all           ok   0.80
%-----
% external heat tranfer
%-----
htcoef_f  south    i   [inopenxe ++] [wallx3s --]
                                                j   [flooras]   [flooras]
                                                k   [atriazs]   [atriaze]   ok 8.0 %floor in atria
htcoef_f  west    i   [wallx1s]   [wallx1s]
                                                j   [floor0e]   [ceile]
                                                k   f          [wallz3s]   ok 8.0 %west wall in
comp
htcoef_f  south    i   f+1        [inopenxe]
                                                j   [floor]     [floor]
                                                k   f+1        [atriaze]   ok 8.0 %floor in comp
htcoef_f  top      i   f+1        [inopenxe]
                                                j   f          [ceile]
                                                k   [soffitze] [soffitze] ok 8.0 %top wall in
comp
htcoef_f  north   i   f          1
                                                j   [ceile]    [ceile]
                                                k   f          [atriaze]   ok 8.0 %ceiling
htcoef_f  east    i   [inopenxe] [inopenxe]
                                                j   [floor0e]   [ceile]
                                                k   f          [atriazs]   ok 8.0 %east wall in
comp
htcoef_f  bottom  i   [inopenxe ++] 1

```

```

j f [ceile]
k [wallz2s] [wallz2s] ok 8.0 %bottom atria
wall
% htcoef_f top i [inopenxe ++] l-1
% j f [ceils]
% k [soffitzs] [soffitze] ok 8.0 %soffit ext
opening
% htcoef_f i [inopenxs] [inopenxe]
% j [inopenys] [ceils]
% k [atriazs] [wallz3s] ok 8.0 %soffit int
opening
htcoef_f east i [wallx3e] [wallx3e]
j [floorae] [ceile]
k [atriazs] [soffitze] ok 8.0 %east wall
atria
htcoef_f bottom i f [inopenxs]
j [floor0e] [ceile]
k [wallz1s] [wallz1s] ok 8.0 %bottom wall
comp
htcoef_f west i [inopenxs] [inopenxs]
j [floorae] [floor0e]
k [atriazs] [soffitze] ok 8.0 %west wall
atria
end
%-----
interior values
%-----
solution u fluid interior ok 0.01
solution v fluid interior ok 0.01
solution w fluid interior ok 0.01
solution tke fluid interior ok 1e-4
solution ted fluid interior ok 1e-2
derived t fluid interior ok 280
end
%-----
control
%-----
solved variables
relax
u 0.5
v 0.5
w 0.5
enth 1.0
mfuel 0.5
mfrac 0.5
end
solver
enth
sip3d
end
%-----
cycle
enth 10
end
end
%-----
derived variables
relax
p 0.5
rho 0.5
end

```

```
end
%-----
solver control
%-----
    pressure correction solver sip3d
    pressure correction cycles 30
    minimum residual 5e-2
    minimum timestep iterations 50
end
%-----
physical models
%-----
    ambient temp 280
    referen temp 280
    time step 0.125
end
end
%-----
end
%-----
```